Power and particle exhaust in tokamaks

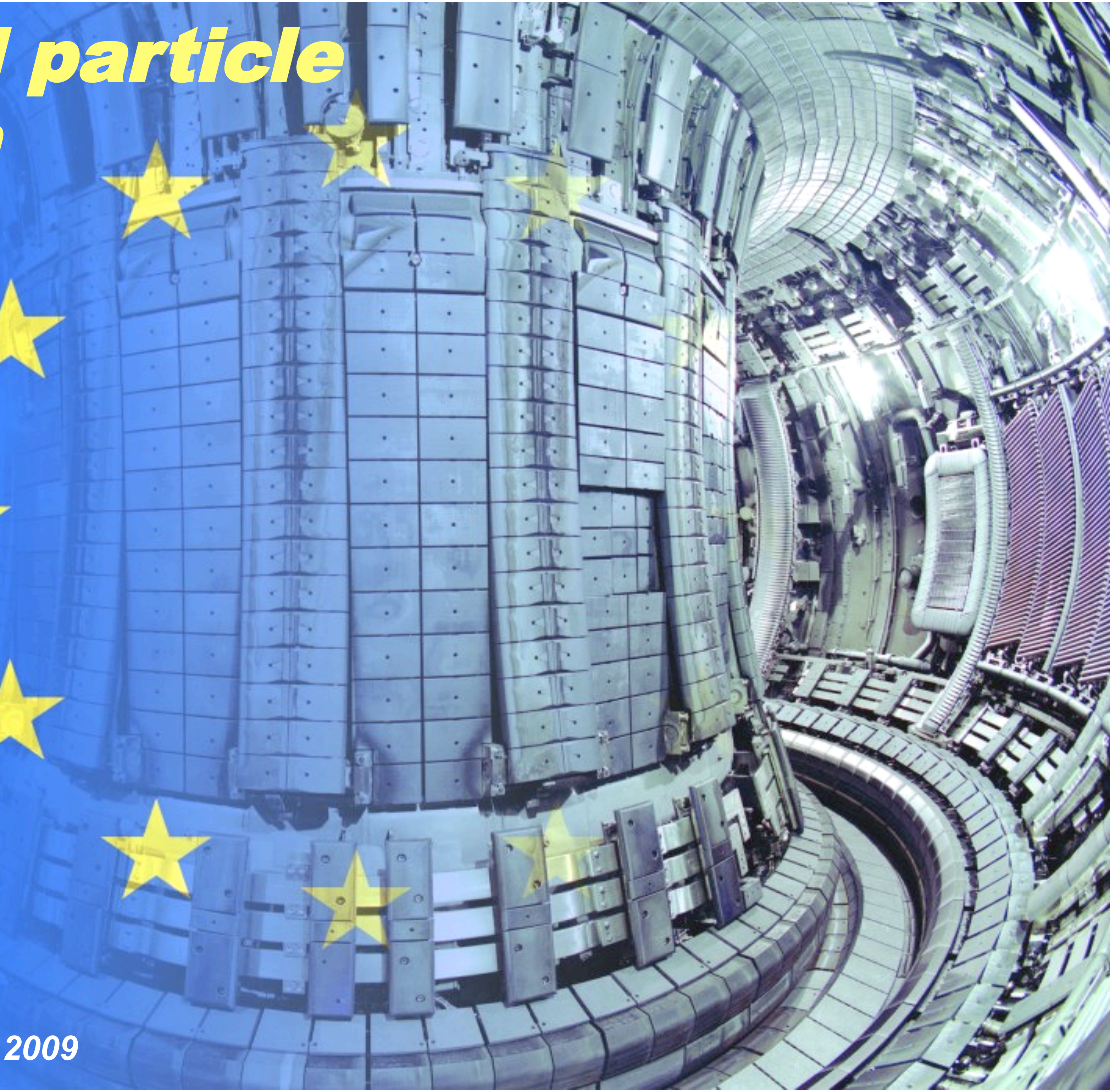

W.Fundamenski
UKAEA, EFDA-JET

ITER Summer School
Aix-en-Provence, 23 June 2009

with thanks to many contributors

A. Alonso[1], P. Andrew[2], G. Arnoux[3], S. Brezinsek[4], R. Dux, T. Eich[6], T.Evans, M.Fenstermacher, A. Huber[4], S. Jachmich[9], M. Jakubowski[10], E.Joffrin, A. Kirk, T. Loarer[3], B. LaBombard, P.Lang, Y.Liang, B. Lipschultz, A. Loarte[12], G. F. Matthews[5], D. Moulton, V. Naulin, R. Neu, V. Philipps[4], R.A. Pitts[8], J.Rapp[4], D. Tskhakaya[15] M. Wischmeier and JET EFDA Contributors*

[1]Associacion Euratom/CIEMAT para Fusion, Madrid, Spain
[2]ITER Organization, Cadarache, France,
[3]Association EURATOM-CEA, DSM-DRFC, CEA Cadarache, 13108 Saint Paul lez Durance, France
[4]Institut für Plasmaphysik, Forschungszentrum Jülich GmbH, EURATOM Association, Trilateral Euregio Cluster, D-52425 Jülich, Germany
[5]Euratom/UKAEA Fusion Association, Culham Science Centre, Abingdon, OX14 3DB, UK
[6]Max-Planck-Institut für Plasmaphysik, IPP-EURATOM Association, D-85748 Garching, Germany
[7]FZ Karlsruhe, Postfach 3640, D-76021 Karlsruhe, Germany
[8]CRPP-EPFL, Switzerland, Association EURATOM-Swiss Confederation
[9]LPP, ERM/KMS, Association Euratom-Belgian State, B-1000, Brussels, Belgium
[10]Max-Planck-Institut für Plasmaphysik, Teilinstitut Greifswald, Germany
[11]VTT Technical research Centre of Finland, Association EURATOM-Tekes, Finland
[12]EFDA-Close Support Unit, Garching, Boltzmannstrasse 2, D-85748 Garching bei München, Germany
[13]Association EURATOM-VR, Fusion Plasma Physics, Stockholm, Sweden
[14]PPPL Princeton University, Princeton, NJ 0854, USA
[15]University of Innsbruck, Institute for Theoretical Physics, Association EURATOM-ÖAW, A-6020 Innsbruck, Austria
**See appendix of M. Watkins et al., Fusion Energy 2006 (Proc. 21st Int. Conf. Chengdu, 2006) IAEA Vienna (2006)*

Outline

- **Compatibility between the plasma scenarios and PFCs**
  - Ignition vs. exhaust criteria
  - Impact of PFCs on fusion gain
  - Power balance on ITER
- **Steady-state particle and power exhaust**
  - Limiter vs Divertor exhaust
  - Steady plasma loads
    - on main chamber PFCs
    - on divertor PFCs
  - Divertor plasma detachment
- **Transient particle and power exhaust**
  - Edge localised modes (ELMs)
  - Plasma loads associated with ELMs
    - on divertor PFCs
    - on main chamber PFCs
  - ELM mitigations techniques
    - Magnetic perturbations
    - Pellet pacing
    - Impurity injection
- **Conclusions**

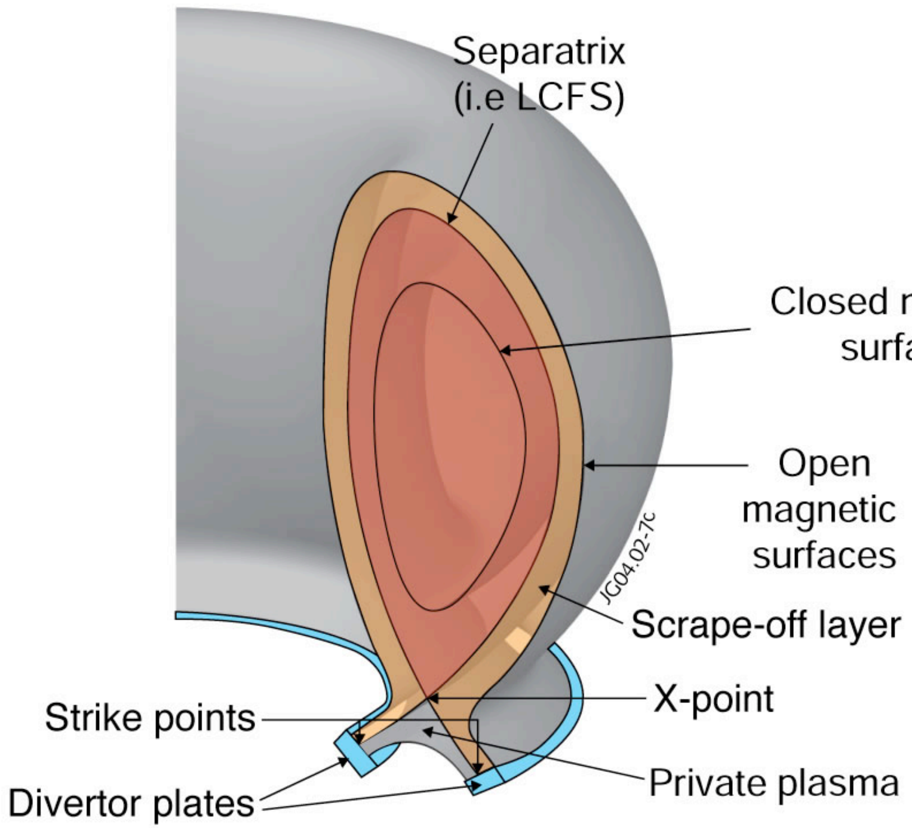

Ignition vs. Exhaust criteria

$Q_{DT} = P_{fus} / P_{heat} \sim 10$

achieve

- **Fuelling**
  - gas
  - pellets
  - beams
- **Heating**
  - RF
  - NBI
  - alpha
- **Confinement**
  - equilibrium
  - stability
  - transport

maintain

- **Particle exhaust**
  - He ash
  - Intrinsic Z
  - Extrinsic Z
- **Power exhaust**
  - neutron
  - photon
  - plasma
- **First wall design**
  - mechanical
  - thermal
  - nuclear

+ current drive,

disruptions, tritium, dust, …

max Q_{DT} = function(reactor design)

‘Ignition’ systems

Fuelling syste

Heating systems

Fu

Heatin

Current profile

Confinement

Core plasma conditions

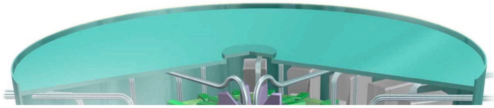

‘Exhaust’ systems

ntrol system

ooling circuit

e exhaust

ower exhaust

PFC loads

Impurity influx

Edge plasma conditions

$Q_{DT} = P_{fus} / P_{heat} \sim p_{DT}\, \tau_E\, f(Z_{eff})$

Maximum achievable Q_{DT} determined by the reactor design, including PFC limits

Impact of a given PFC limit = $\Delta Q / Q_0 = 1 - Q(PFC) / Q_0$

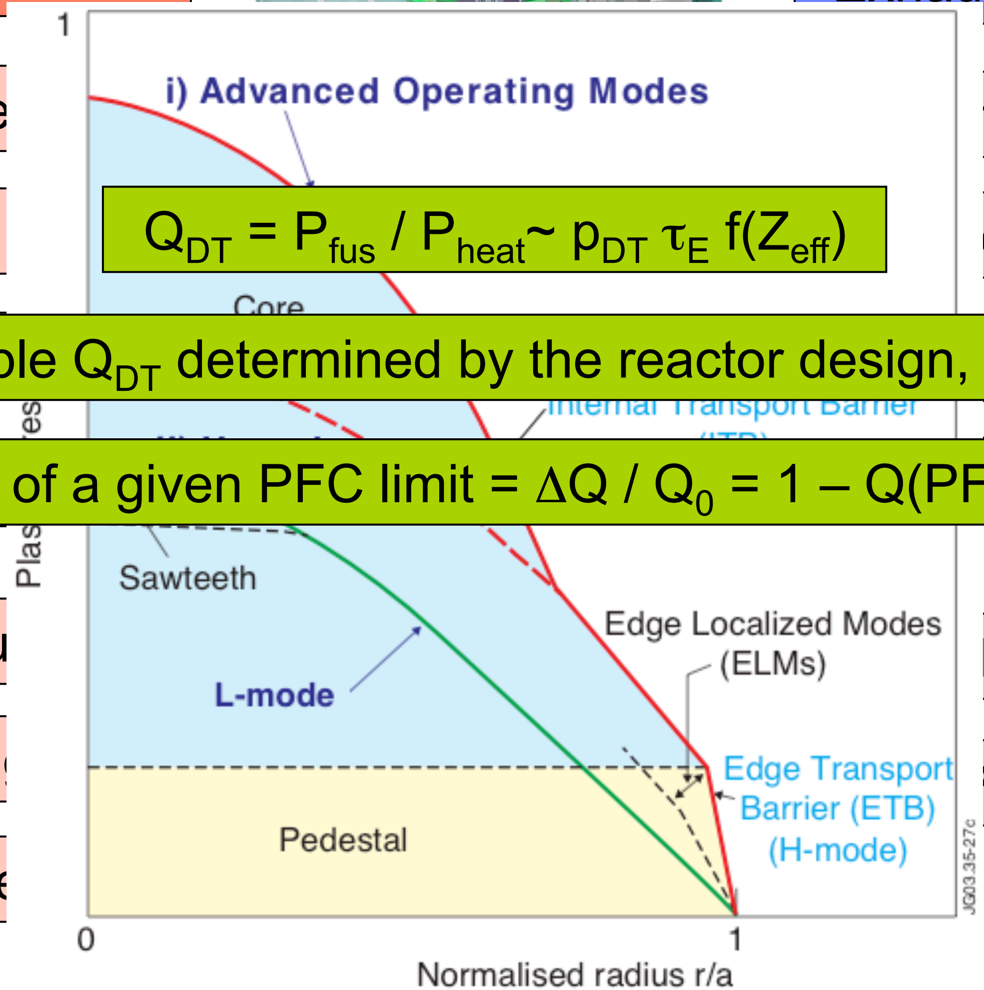

Impact of PFCs on fusion gain

$Q_{DT} = P_{fus} / P_{heat} \sim p_{DT} \tau_E f(Z_{eff})$

Profile stiffness: T(0) / T(a) ~ const

Critical temperat gradier

Turbuler transpo

on

l

DT fuel dilution with Z_{eff}

need cool, dense edge plasma

or active size cont pellets, RI

need cool, dense edge plasma

ELM size decreases with edge collisionality

Edge mode

Trans or

partially detached divertor operation

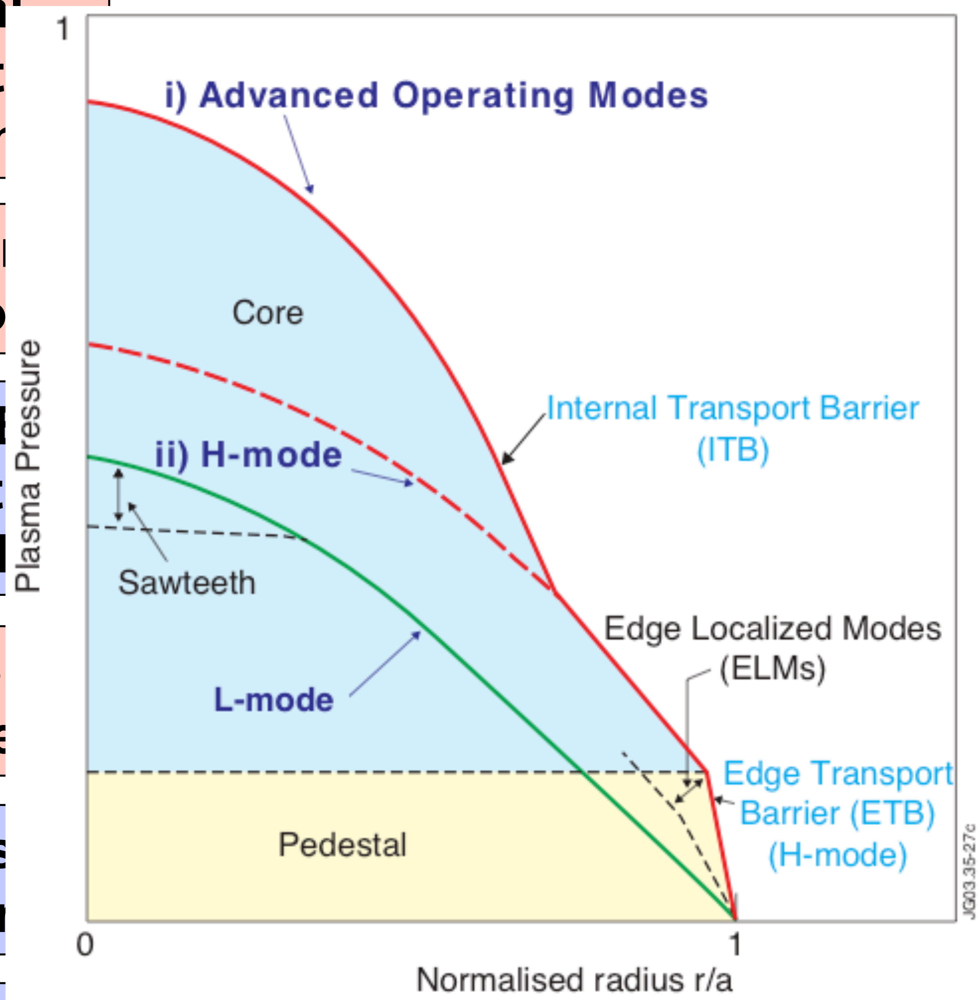

must not exceed: ~ 0.5 MJ/m2 in 250 us

Erosion, ablation, melting, cracking

must not exceed: ~10 MW/m2; ~10 eV

Transient heat load limits in ITER

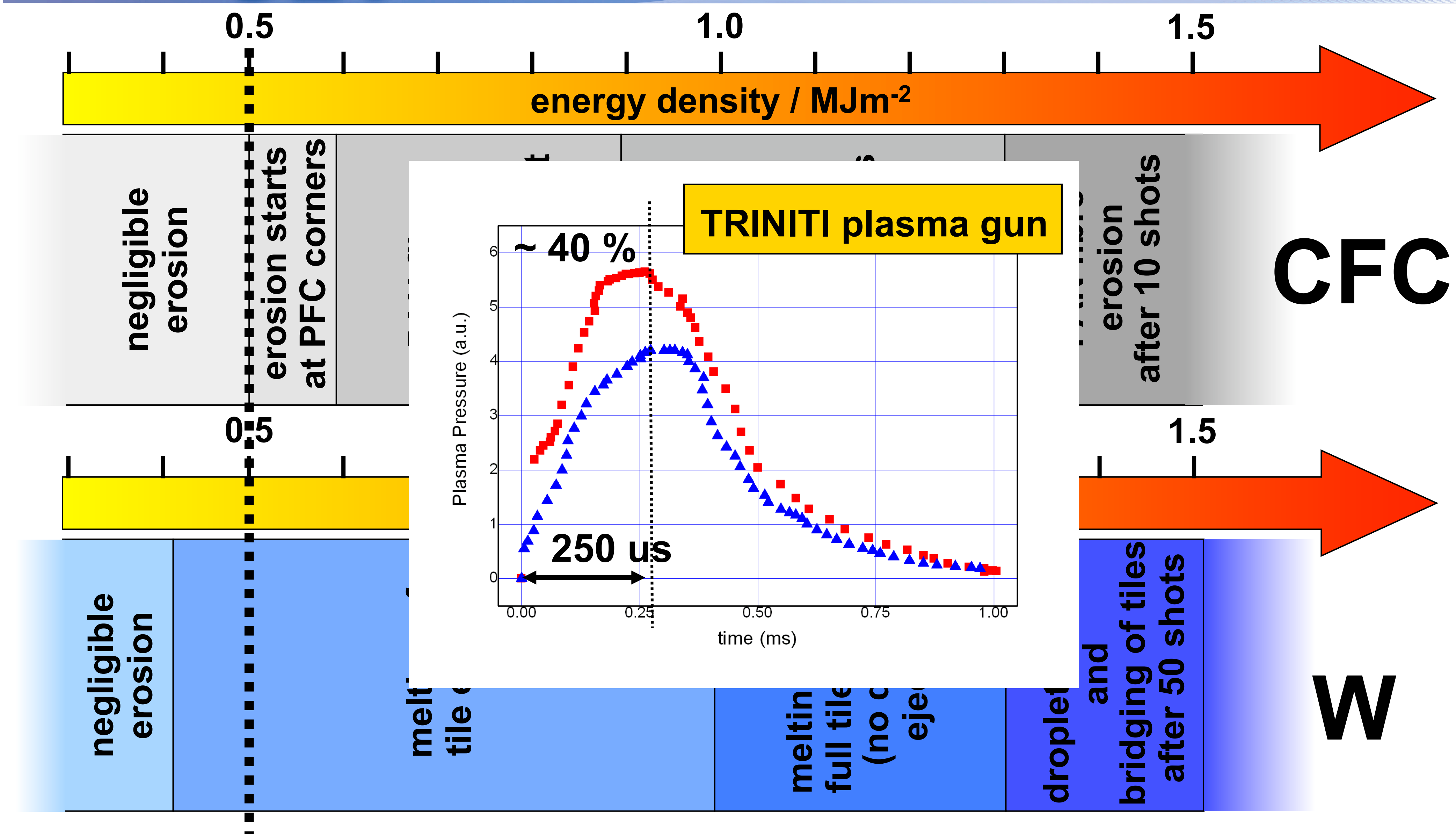

ITER adopted **0.5 MJ/m²** for the maximum allowed ELM energy load in 250 us

Power balance on ITER

Heating $P_h = 40$ MW

Fusion $P_{fus} = 400$ MW $Q_{DT} = 10$

Wall area

Alphas $P_\alpha = 80$ MW

$P_n = 320$ MW Neutrons ~ 800 m^2

Plasma $P_{SOL} \sim 60$ MW ? $P_{rad}^{core} \sim 60$ MW Photons (50%) ~ 800 m^2

ELMs $P_{ELM} \sim 20$ MW ? $P_{inter\text{-}ELM} \sim 40$ MW Inter-ELM

inner ~ 14 MW ? ~ 6 MW inner 2π x 5 m x 4 mm x 10 ~ 1.2 m^2

outer ~ 6 MW ? ~ 34 MW outer ? 2π x 6 m x 4 mm x 10 ~ 1.5 m^2

Outer divertor losses (CX, ES, radiation) ~ 25 MW ~ 15 MW Total plasma (outer) ~ 1.5 m^2

Steady-state design limit ~ 10 MW/m^2

In reality, must repeat backwards to find maximum achievable Q_{DT} for given PFC limits

Plasma purity ($Z_{eff} \sim 1.7$) requires high density ($f_{GW} \sim 0.85$) and cold divertor (< 5 eV)

Need ~ 85 MW total radiation (70 % total = 50% in core + 20% in SOL), and ELM frequency above ~ 20 Hz (ELM size ~ 1 MJ or ~ 1% of W_{ped})

Ignition vs. Exhaust beta limits

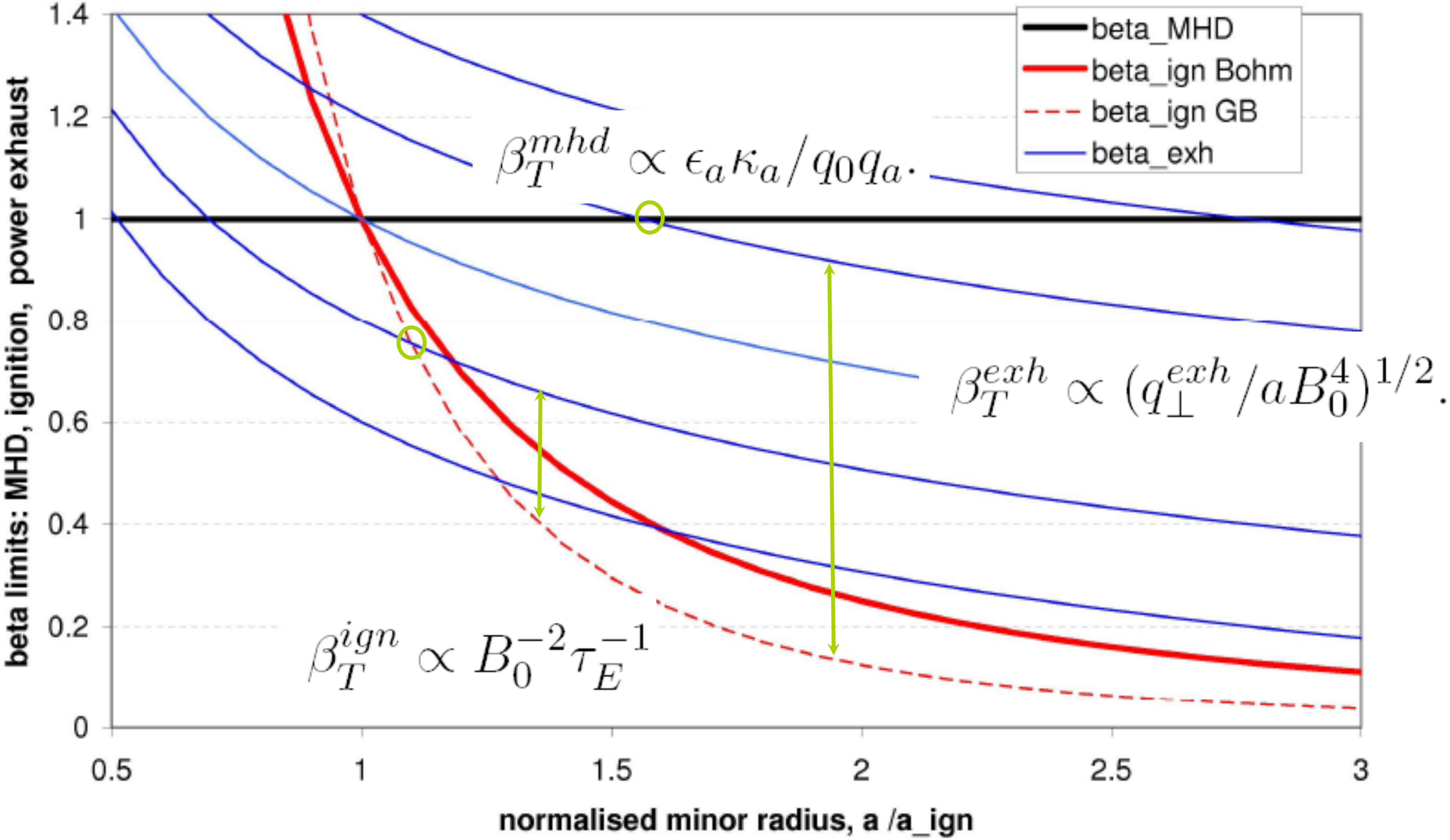

Steady-state exhaust

- **Compatibility between the plasma scenarios and PFCs**
  - Ignition vs. exhaust criteria
  - Impact of PFCs on fusion gain
  - Power balance on ITER
- **Steady-state particle and power exhaust**
  - Limiter vs Divertor exhaust
  - Steady-state plasma loads
    - on main chamber PFCs
    - on divertor PFCs
  - Divertor plasma detachment
- **Transient particle and power exhaust**
  - Edge localised modes (ELMs)
  - Plasma loads associated with ELMs
    - on divertor PFCs
    - on main chamber PFCs
  - ELM mitigations techniques
    - Magnetic perturbations
    - Pellet pacing
    - Impurity injection
- **Conclusions**

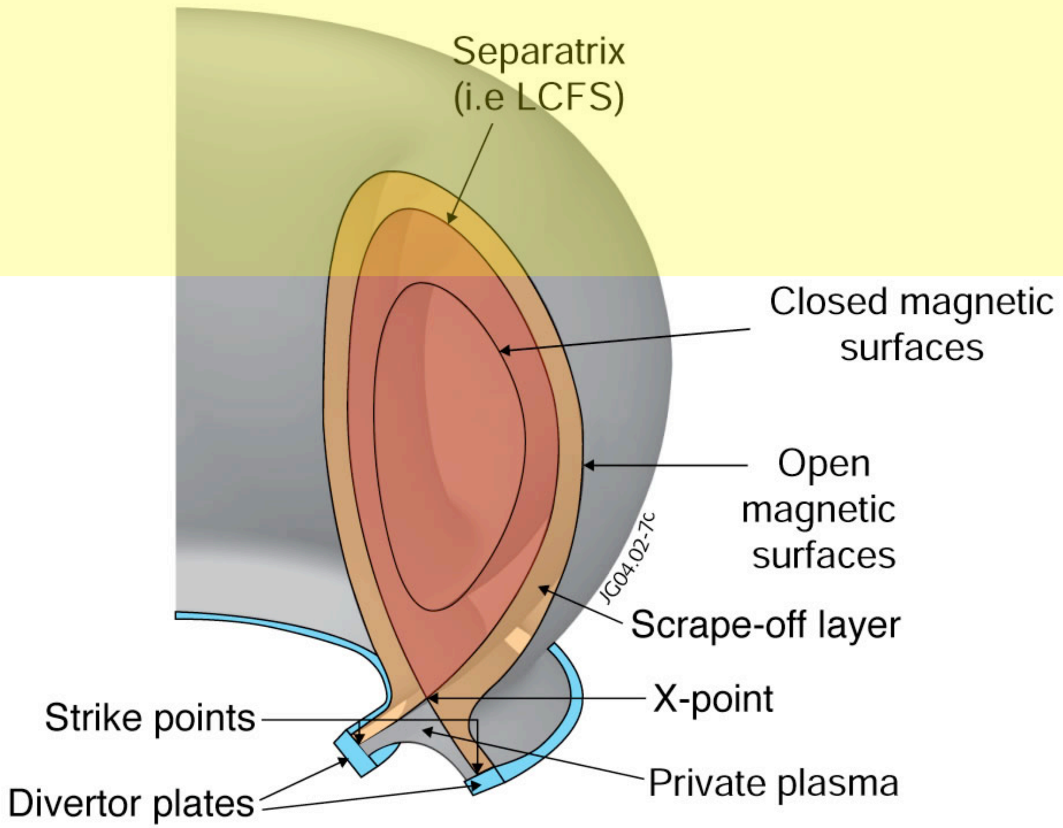

Physical vs chemical erosion

Physical sputtering yield…

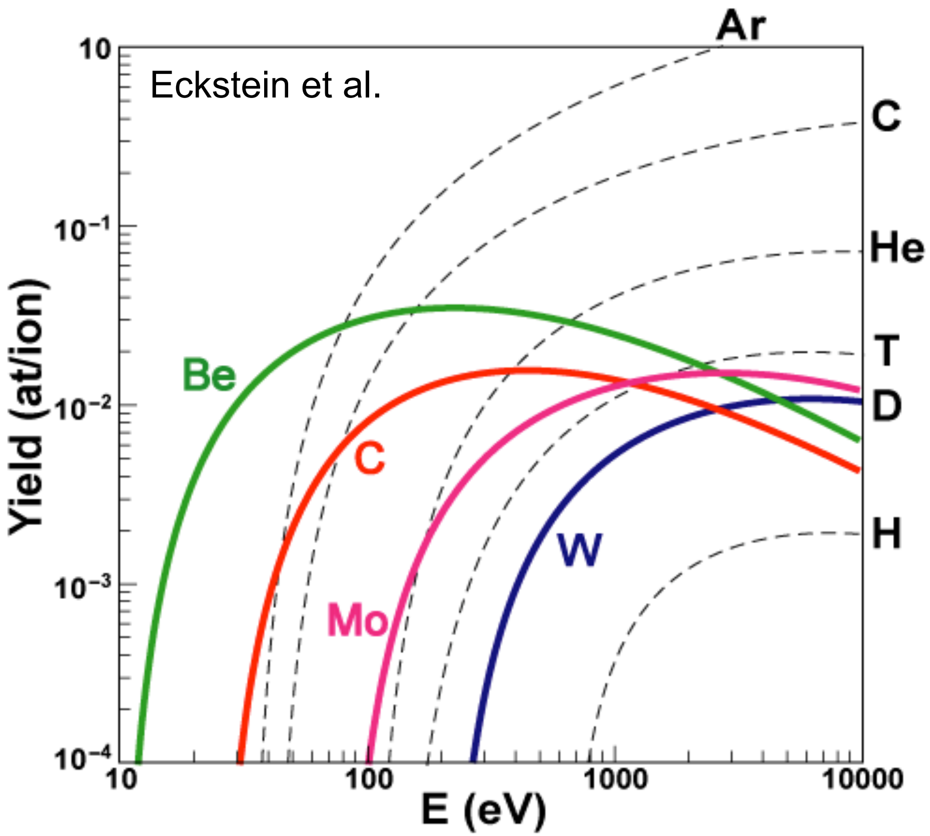

increases with projectile energy and mass, while decreasing with target (PFC) material atomic mass

Chemical erosion yield (D on C)…

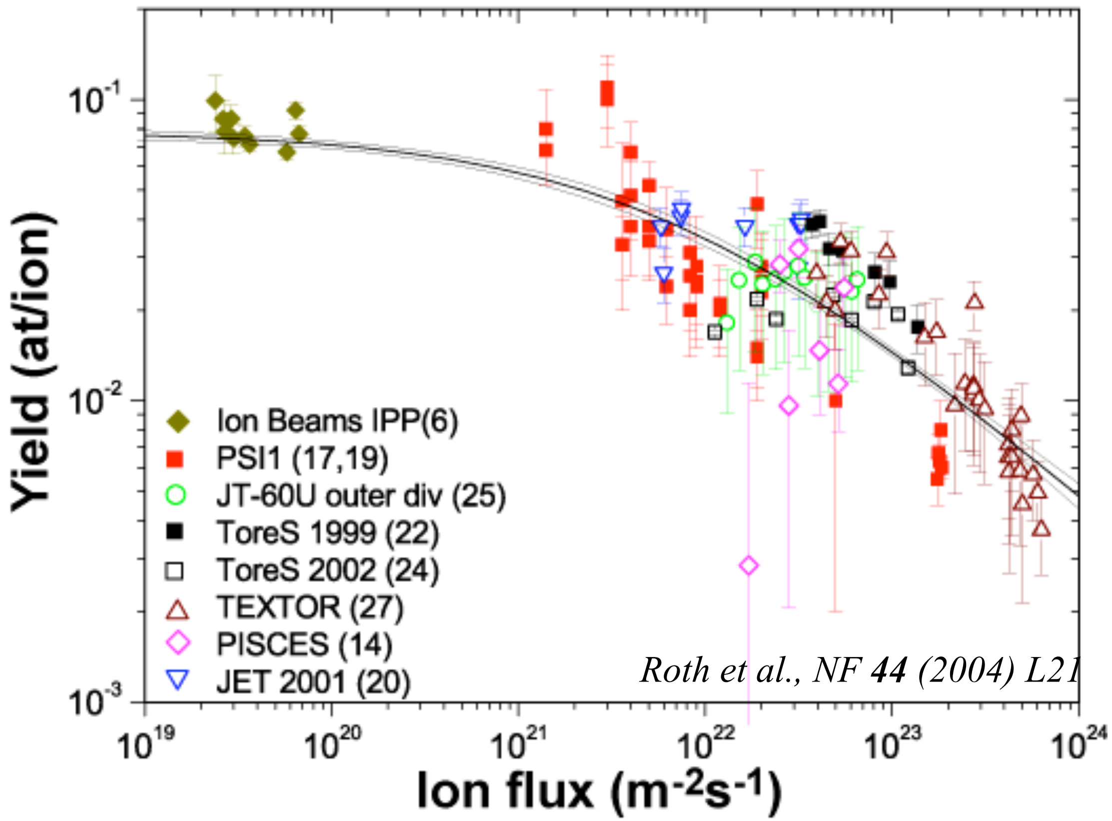

decreases with D ion flux and is sensitive to C target temperature

Limiter vs divertor recycling

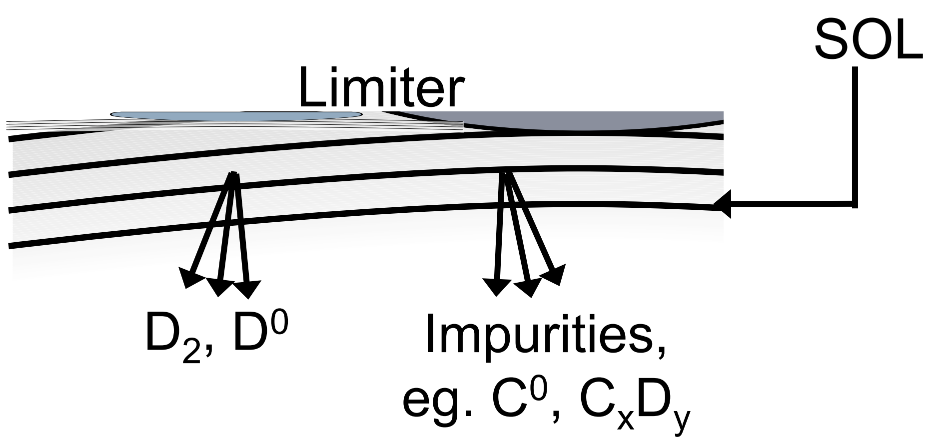

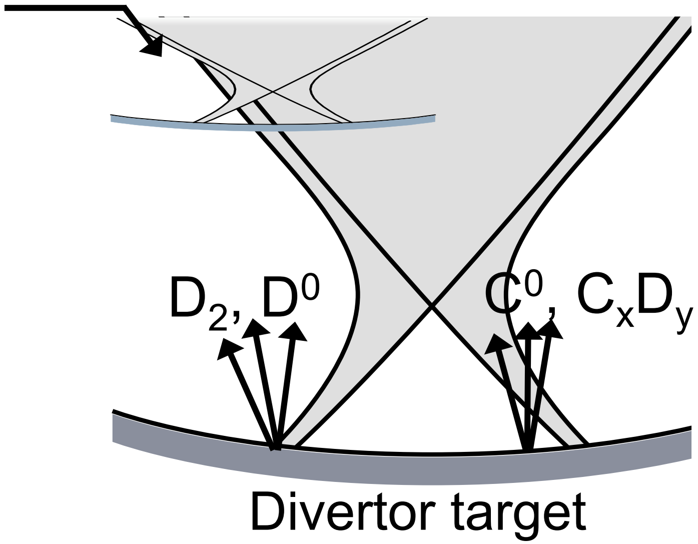

λ_{D0} ~ few cm, λ_{C0} ~ 1 cm, λ_{CxDy} ~ few mm

Limiter	Divertor
Intimate contact with edge plasma	PFCs removed from edge plasma
Little recycling/cooling in the SOL results in a hot, tenous SOL plasma	Colder, denser SOL plasma, due to local recycling / cooling
High erosion yields, poor pumping	Lower erosion yields, improved pumping
Strong influx of both fuel and impurity neutrals into the edge	Fuel and impurity sources screened from the edge by the divertor plasma
Impure edge & core, i.e. high Z_{eff}	Improved plasma purity, i.e. lower Z_{eff}

Limiter vs divertor exhaust

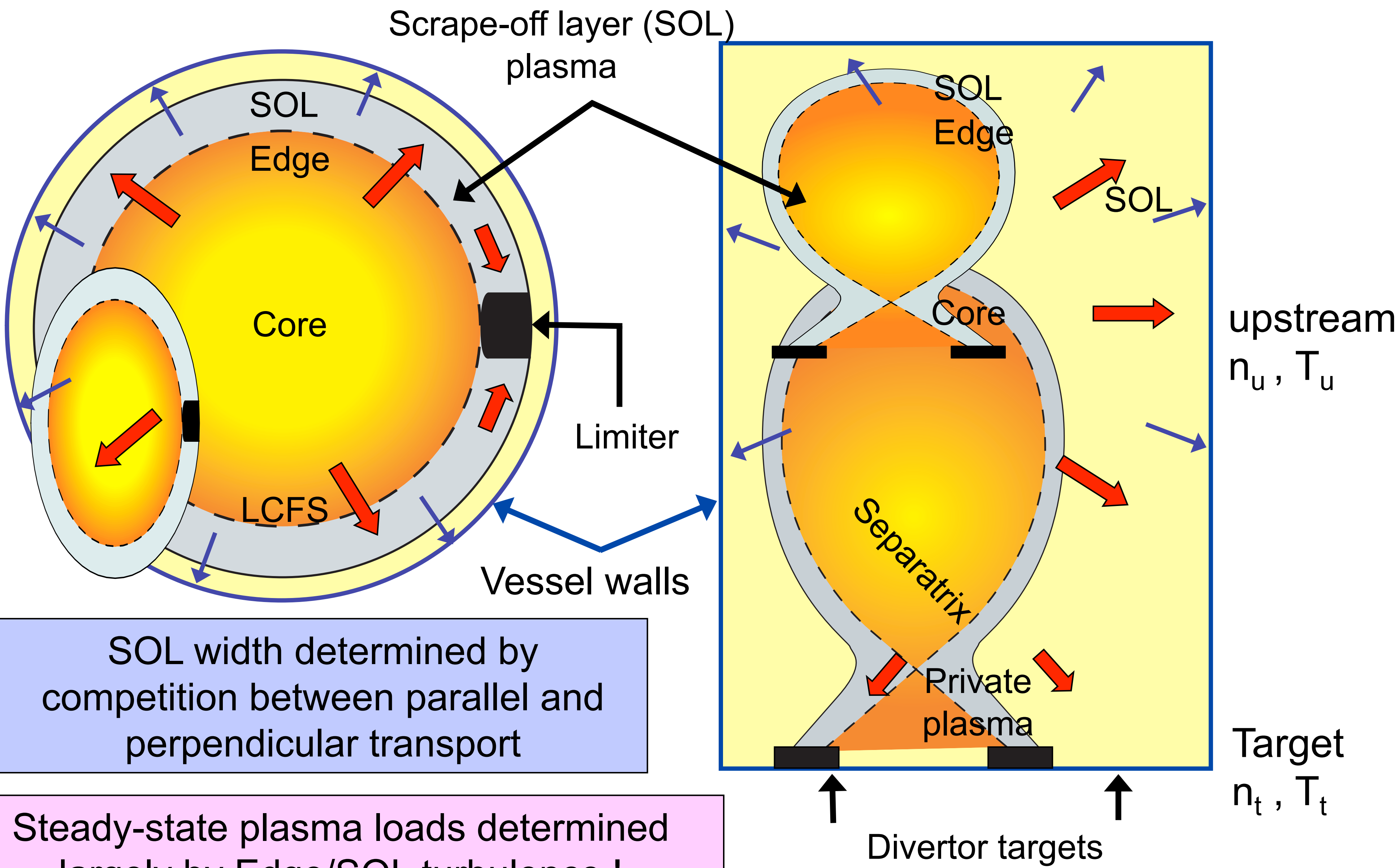

SOL width determined by competition between parallel and perpendicular transport

Steady-state plasma loads determined largely by Edge/SOL turbulence !

Limiter SOL profiles

As expected, limiter SOL width decreases with increasing plasma current

Physical mechanism not understood at the time !

$$\lambda_{\Gamma}^{\Omega} \approx 30 I_p^{-1}, \qquad \lambda_{T_e}^{\Omega} \approx 3 \times 10^{-18} \bar{n}_e I_p^{-1.3},$$

*J.A.Tagle et al, 14th EPS **11C** (1987) 662*
*S.K.Erents et al, NF **28** (1988) 1209*

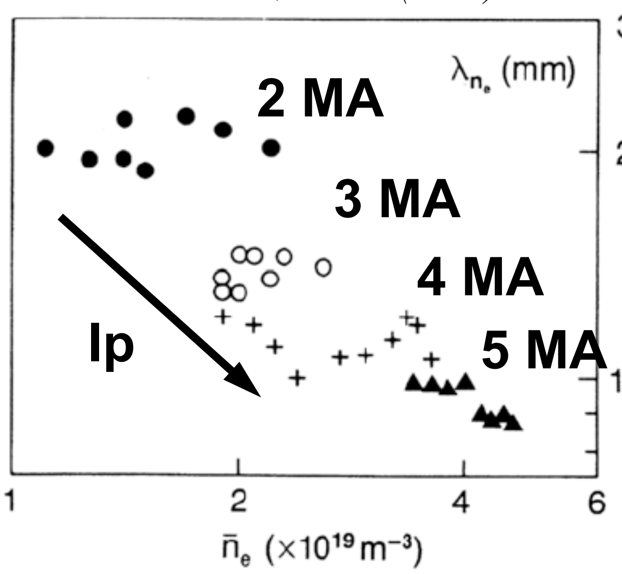

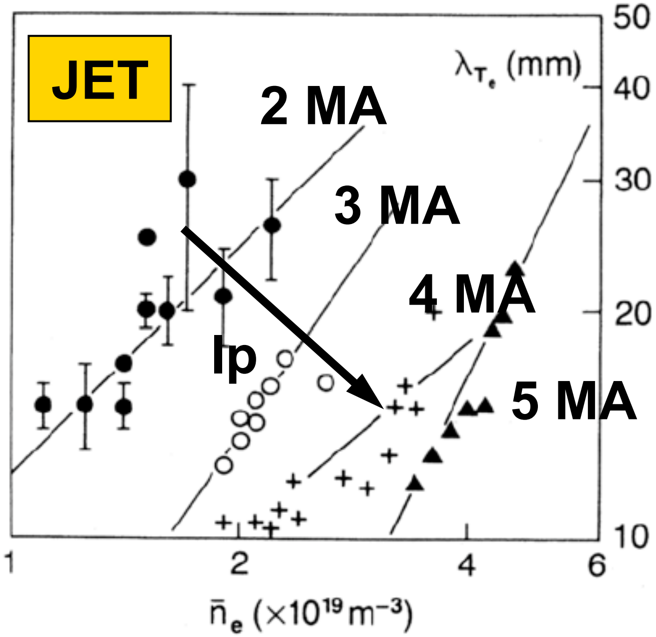

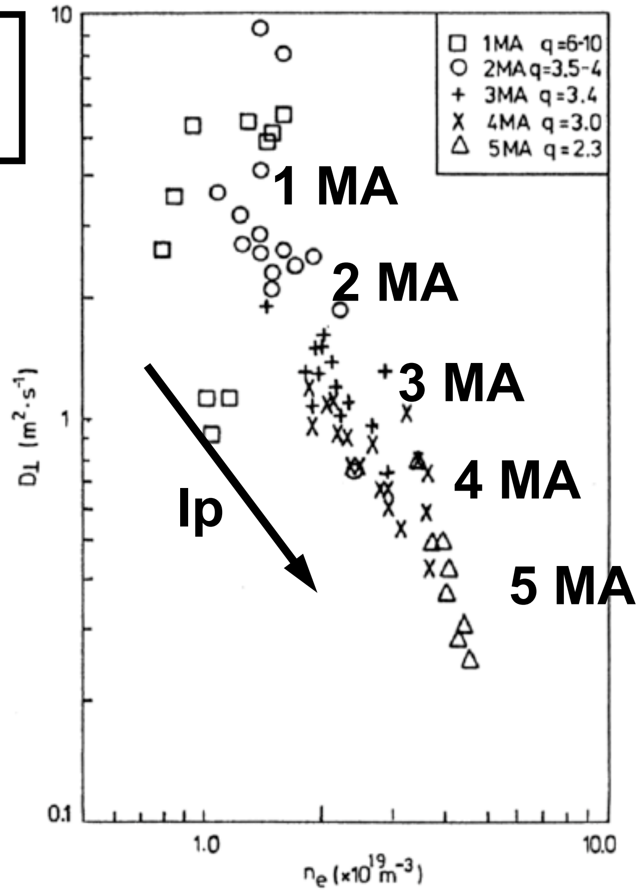

Limiter heat loads in ITER

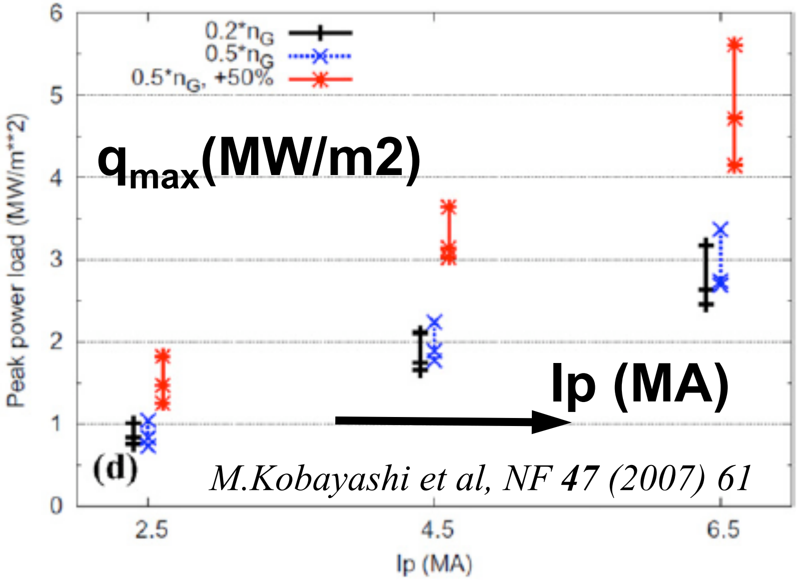

JET diffusivities combined with a 3D fluid-neutral code (EMC3/EIRENE)

Calculated limiter heat loads of several MW/m2, increasing with I_p

MC simulation of impurity transport (DIVIMP) suggest W-limiter a problem

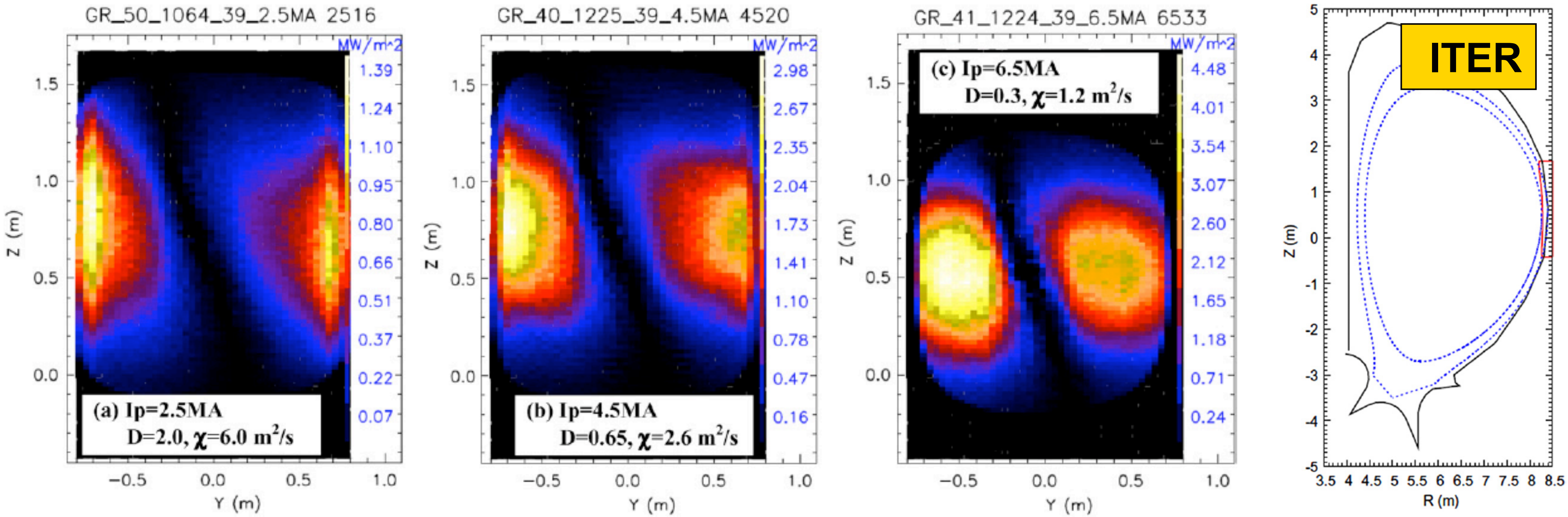

Effective radial velocity ~ const

Describing SOL transport by standard parallel-perpendicular transport competition relations, reveals a roughly constant radial Mach number

$$\mathrm{v}_{\perp n} = \Gamma_\perp / n \text{ and } \mathrm{v}_{\perp T} = q_\perp / \tfrac{5}{2} nT$$

$$D_\perp = \Gamma_\perp / \nabla n \text{ and } \chi_\perp = q_\perp / n \nabla T,$$

$$\lambda_\Gamma \approx \mathrm{v}_{\perp n} \tau_{\|n}, \qquad \lambda_n \lambda_\Gamma \approx D_\perp \tau_{\|n}, \qquad \tau_{\|n} \approx \frac{L_\|}{c_s},$$

$$\lambda_q \approx \mathrm{v}_{\perp T} \tau_{\|T}, \qquad \lambda_T \lambda_q \approx \chi_\perp \tau_{\|T}, \qquad \tau_{\|T} \approx \frac{L_\|^2}{\chi_{\|e}},$$

$$\lambda_n \sim \lambda_\Gamma \sim \sqrt{\tau_{\|n} D_\perp}, \qquad \lambda_T \sim \lambda_q \sim \sqrt{\tau_{\|T} \chi_\perp}.$$

$$I_p \propto B_\theta \propto q_{95}^{-1} \propto L_\|^{-1} \propto P_\Omega^{0.85} \propto (p_e^{LCFS})^{0.85}.$$

$$c_s = [(T_e + T_i)/m_i]^{1/2}$$

Effective radial velocity

$$\mathrm{v}_{\perp n} / c_s^{LCFS} \propto const$$

Effective radial diffusivity

$$D_\perp^\Omega \propto L_\| c_s^{LCFS}$$

Physical mechanism not understood for a long time…

but great progress made in the last few years !!!

Plasma turbulence in the Edge-SOL

Density scan

Pulse number	$\bar{n}_e$ (10^{19} m^{-3}
24530	11
26092	8.4
26060	6.5
26084	4.8
24530	4.4
ESEL	

Current scan

m)	$\nu^*_{ei}(\rho = 0.25)$	Symbol
	160	▲
	130	■
	105	●
	85	◆
	75	▼

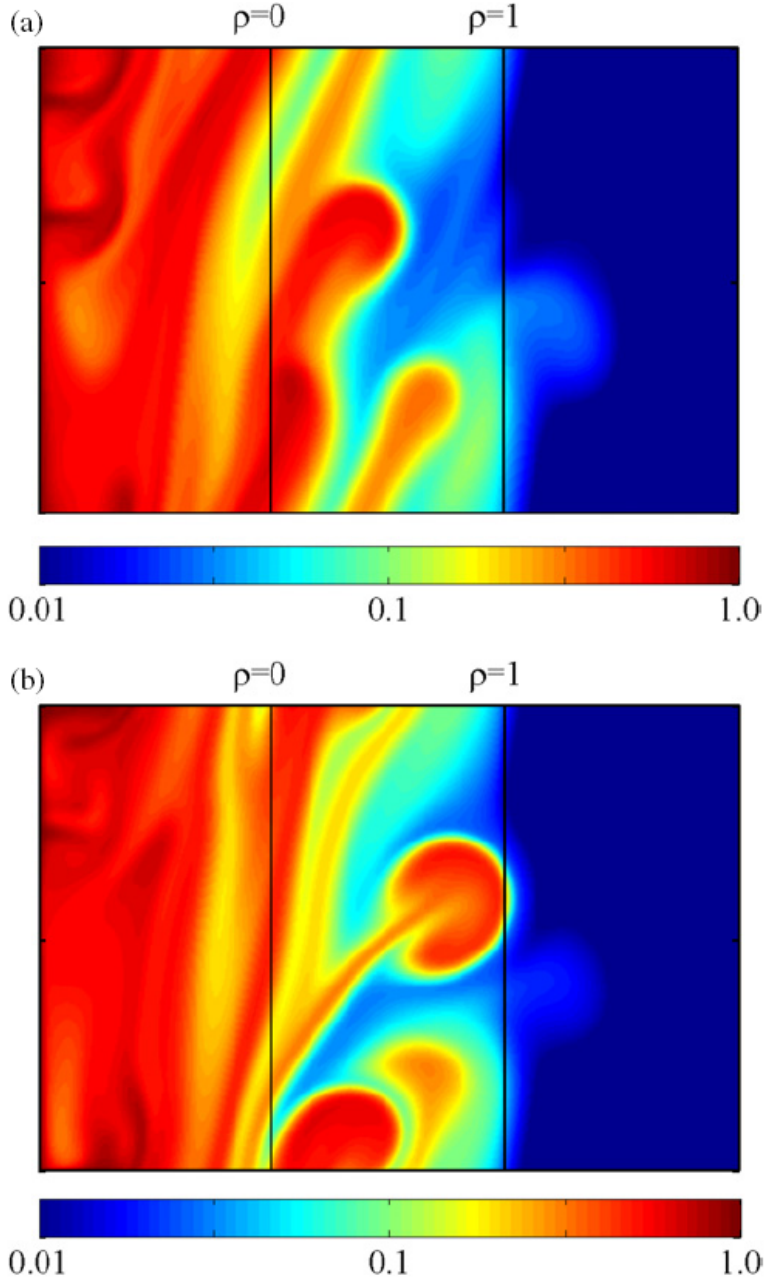

Wall flux ~ density^2

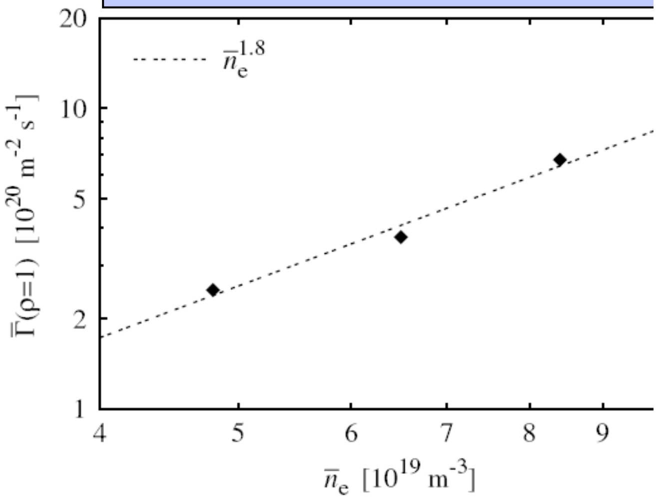

Wall flux ~ 1/current

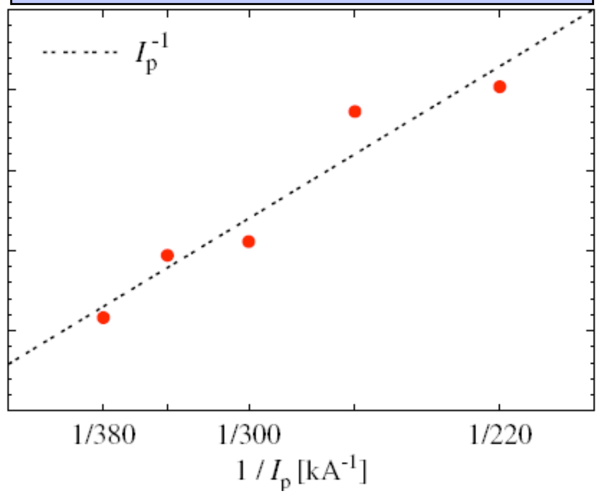

*O.E.Garcia et al, PPCF **48** (2006) L1*

Density profiles in the Edge-SOL

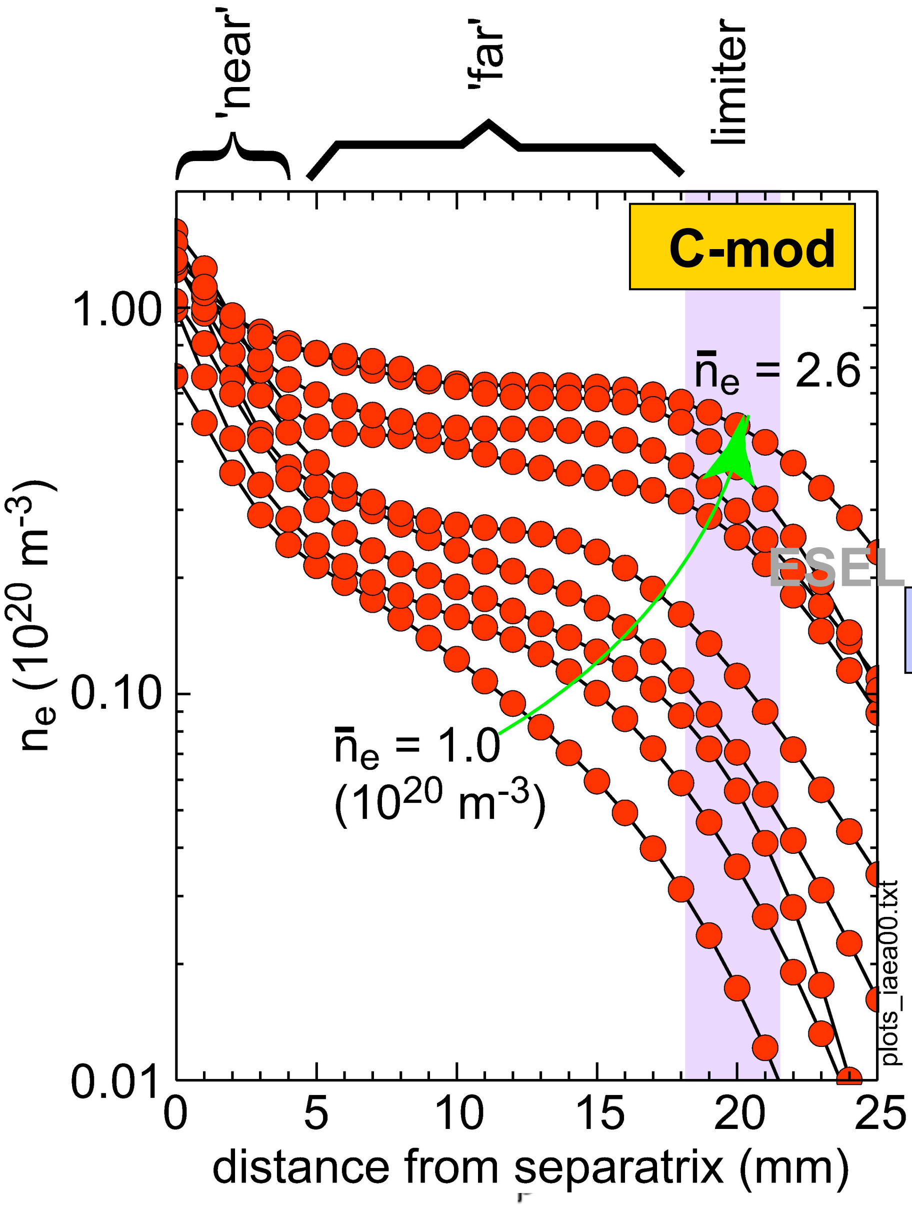

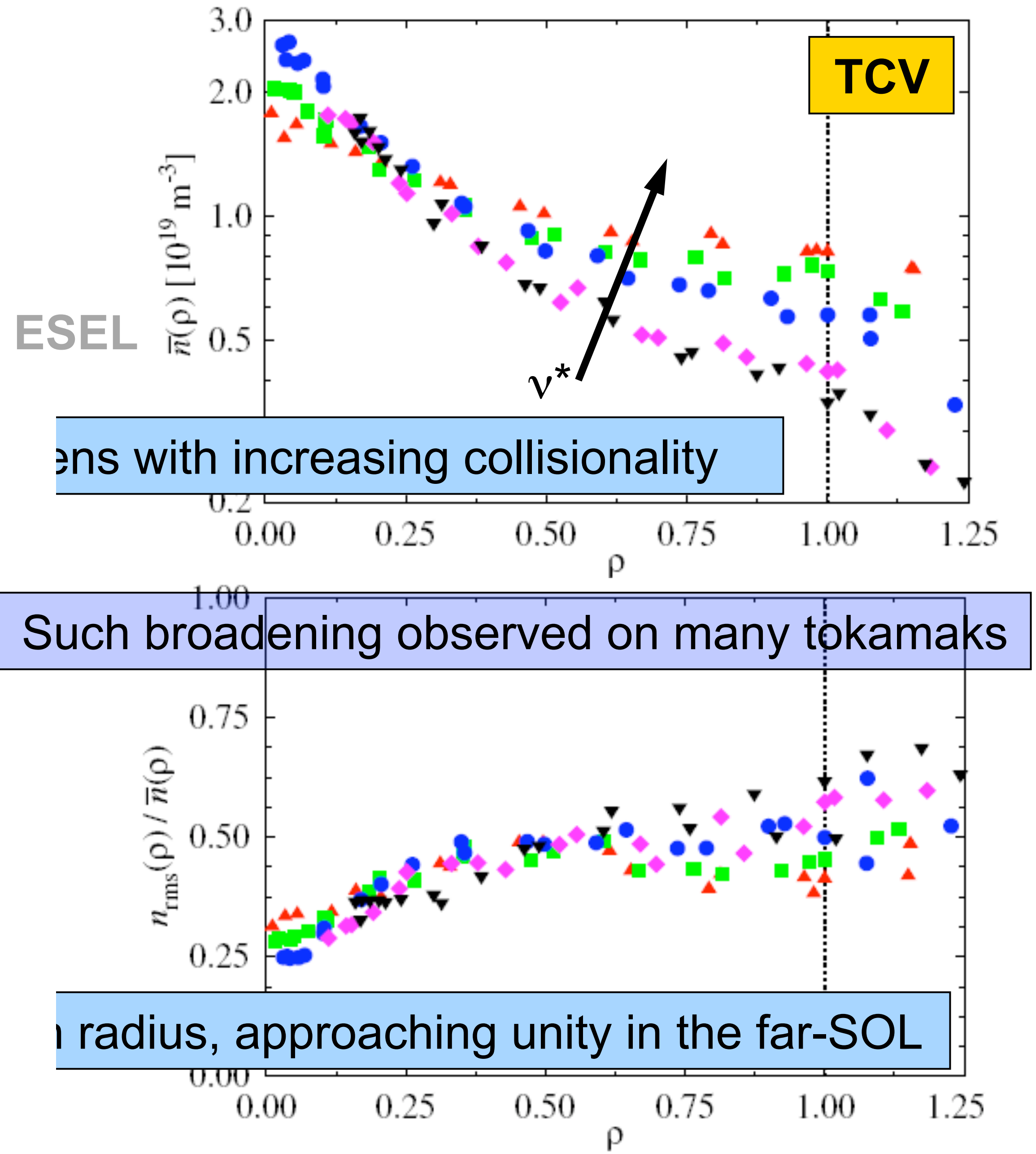

ens with increasing collisionality

Such broadening observed on many tokamaks

radius, approaching unity in the far-SOL

Radial flow profiles in the Edge-SOL

Radial plasma flux increases with collisionality

Such increase with radius observed on many tokamaks

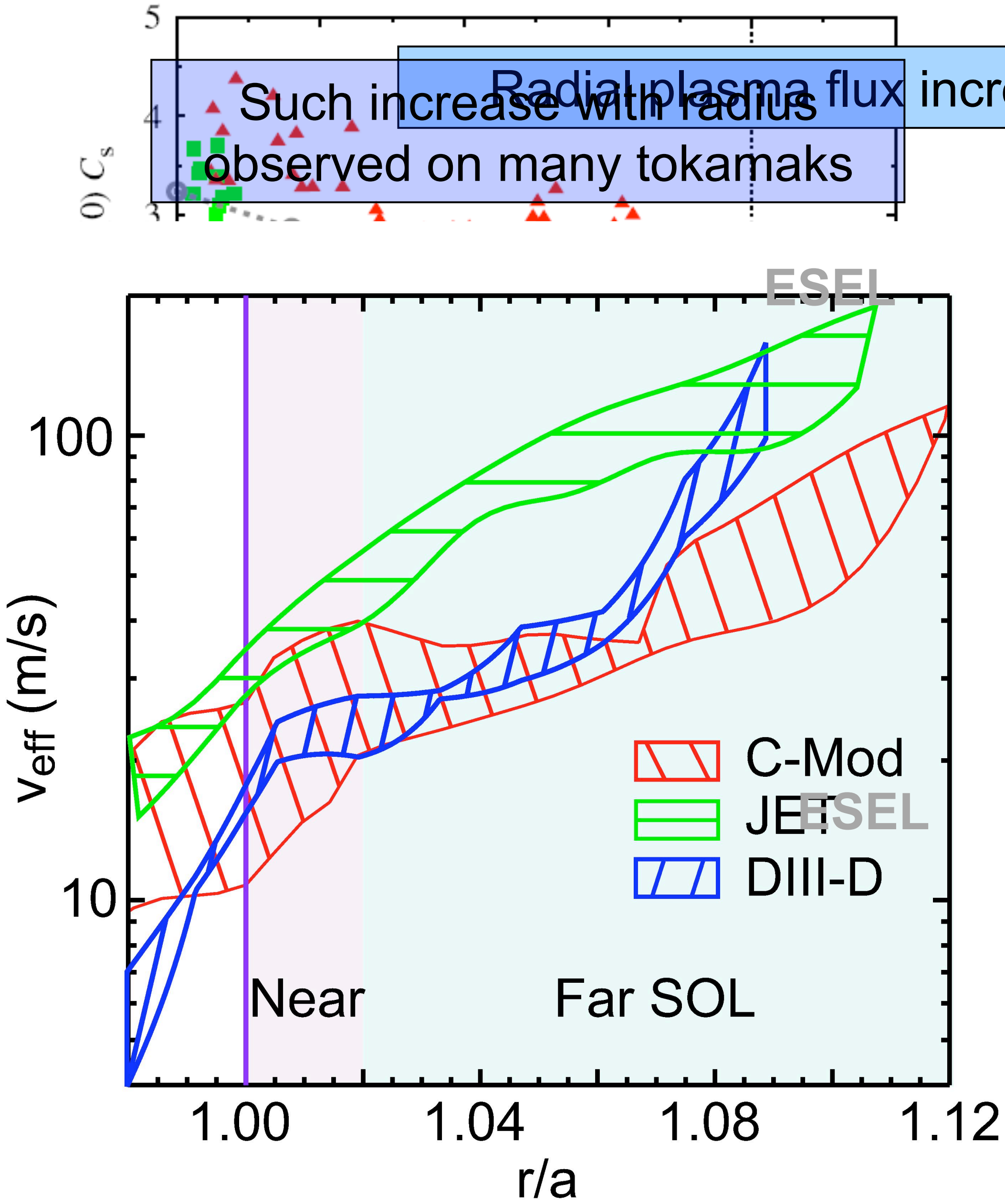

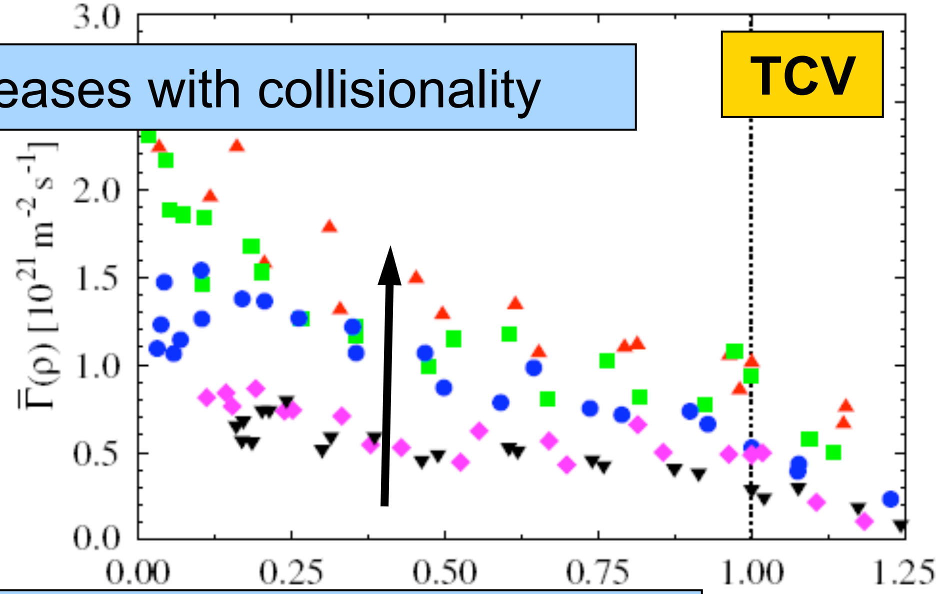

oughly constant with radius
sionality in the near-SOL

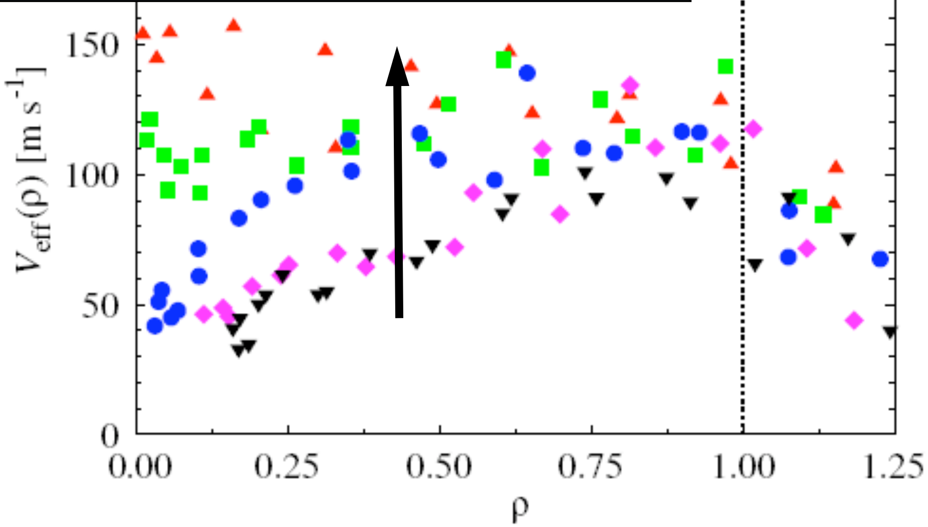

PDFs of fluctuations in the far-SOL

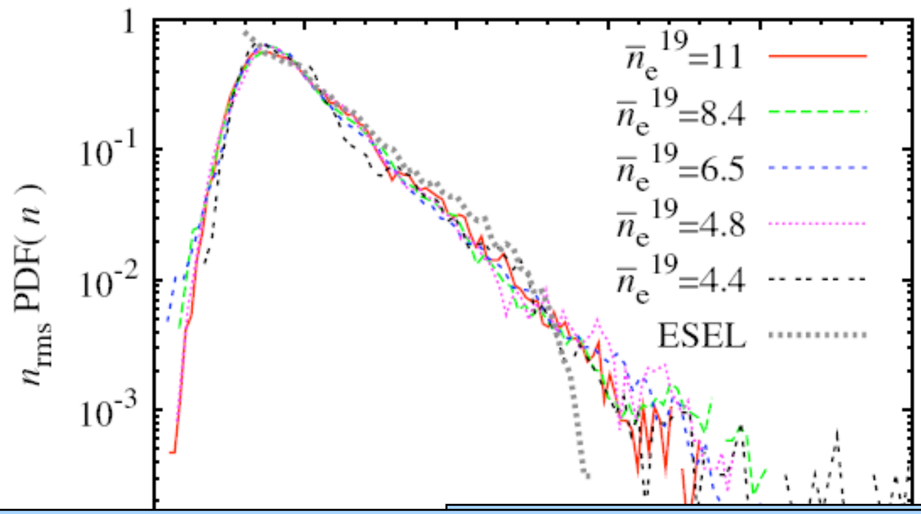

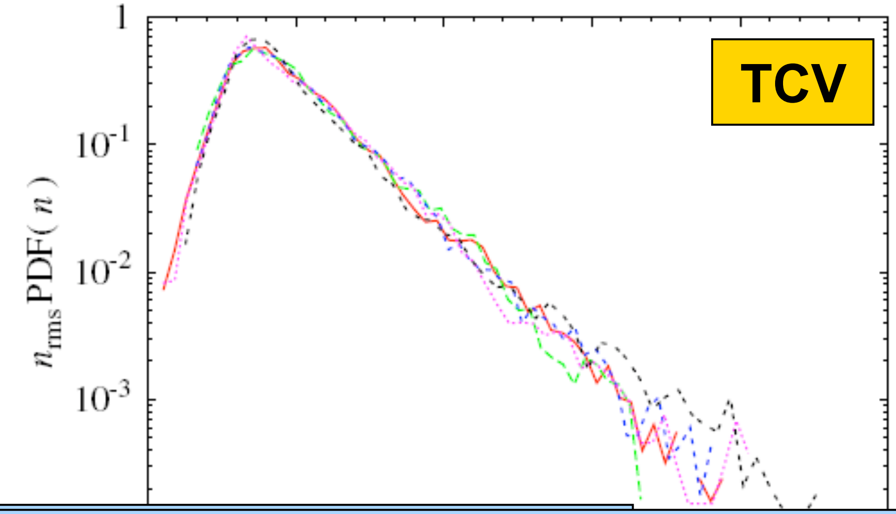

Temporal pulse shape of density ‘blobs’ reveals leading front & trailing wake

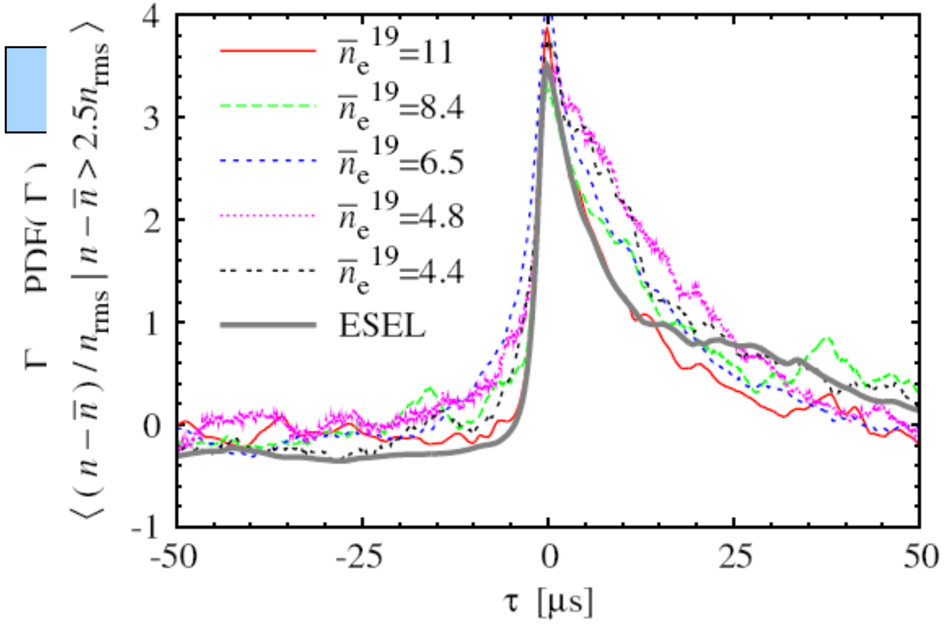

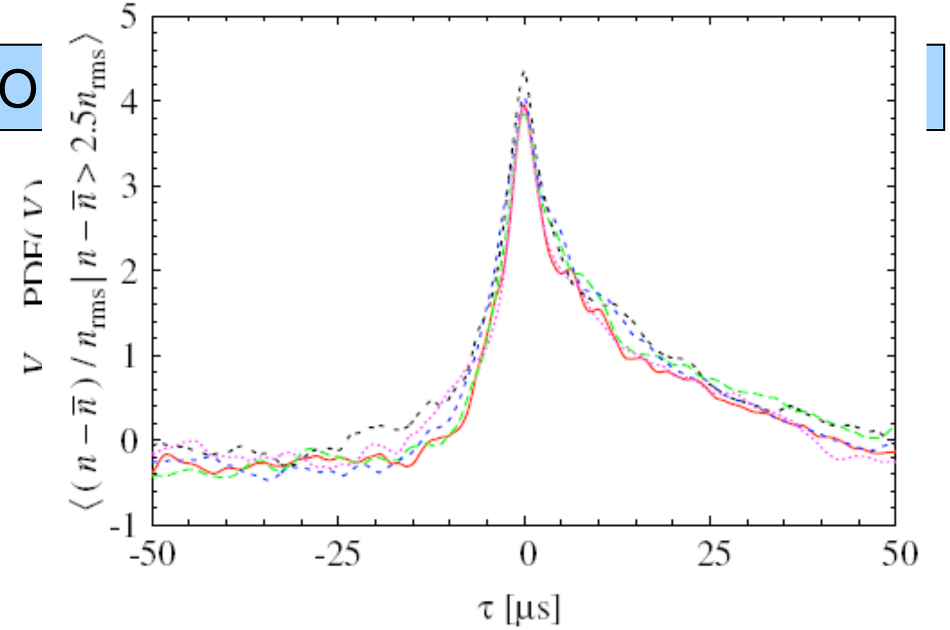

Interchange motion of plasma 'blobs'

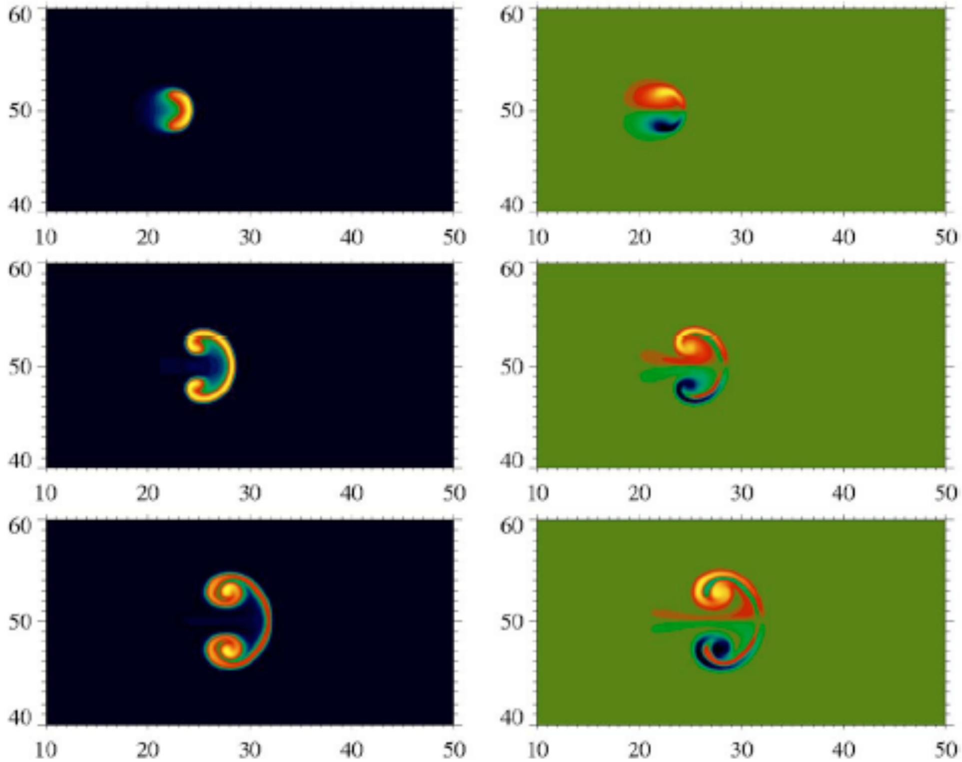

O.E.Garcia et al, PoP (2006)

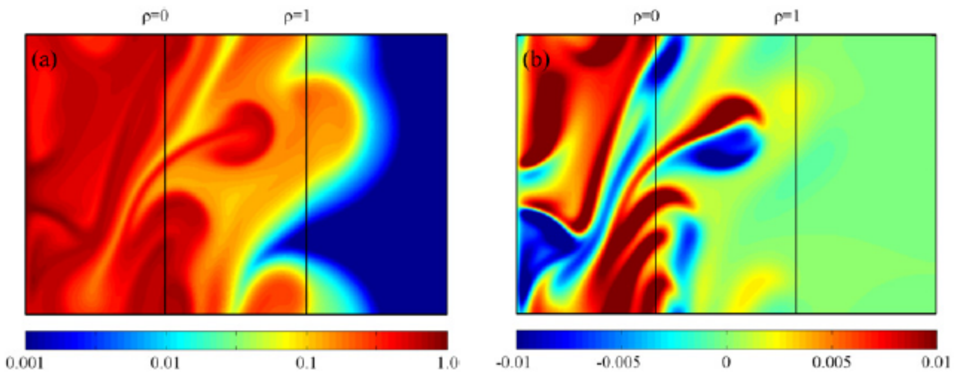

*O.E.Garcia et al, PPCF **48** (2006) L1*

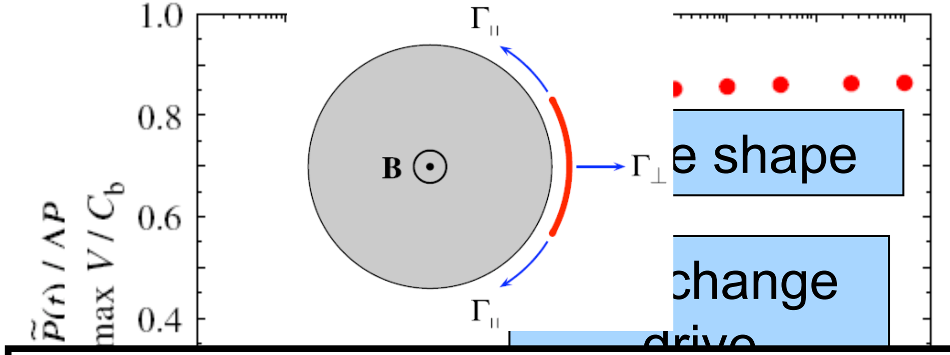

$$\nabla \cdot \mathbf{J} = \nabla \cdot (\mathbf{J}_p + \mathbf{J}_* + \mathbf{J}_{\|}) = 0$$

Dynamics of plasma filaments, or blobs, is determined by charge conservation = balance of divergences of polarization, diamagnetic and parallel currents

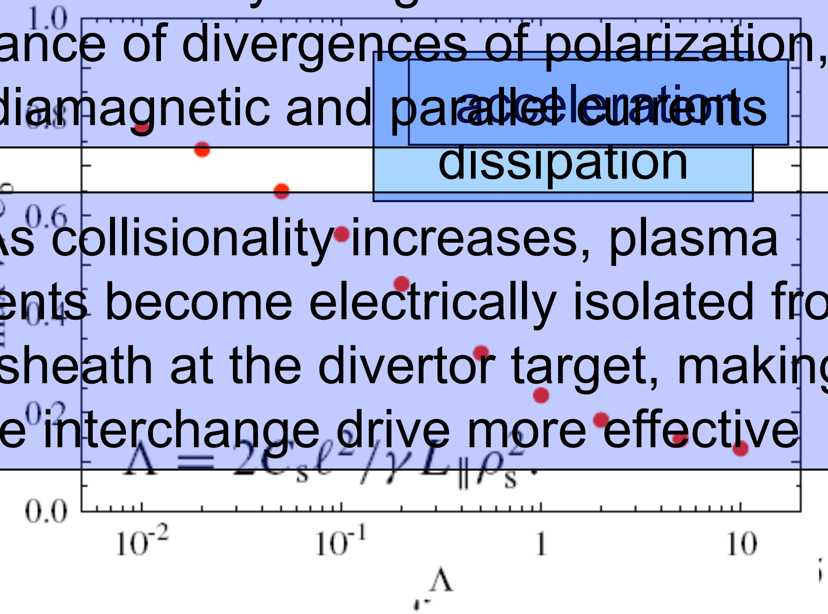

As collisionality increases, plasma filaments become electrically isolated from the sheath at the divertor target, making the interchange drive more effective

Plasma turbulence in the Edge-SOL

Intermittent transport implies strong fluctuations in far-SOL quantities

Local flux not related to local gradient!

Mean field approximation, used in most edge transport codes, is not accurate

<nT> ≠ <n><T>, etc.

Hence, need global edge turbulence codes

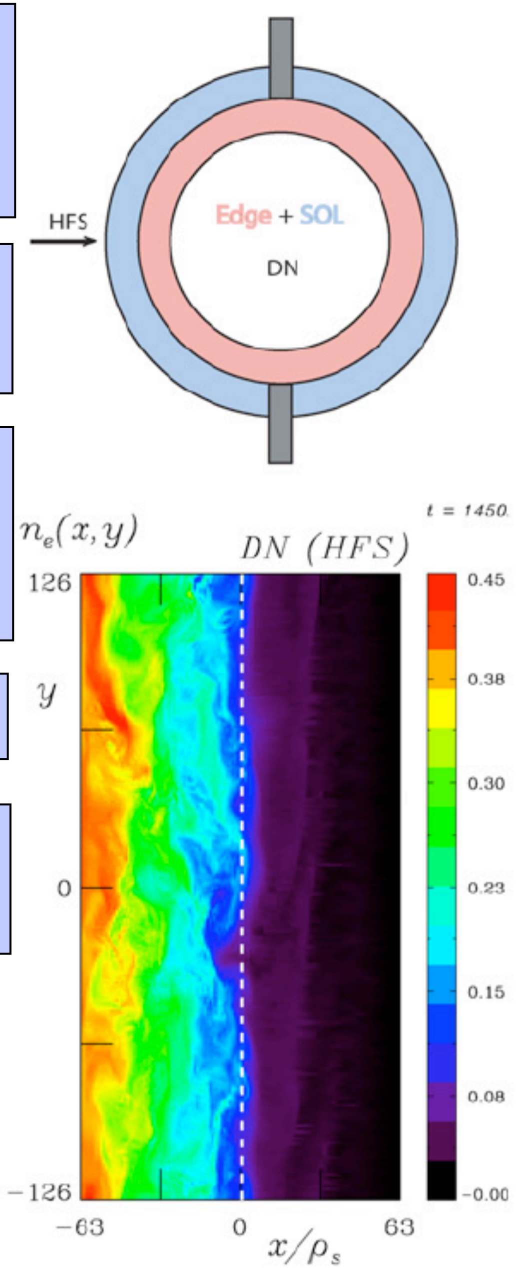

Mostly drift-Alfven dynamics in the edge region

Mostly interchange dynamics in the SOL region

Turbulence driven by edge pressure gradients, which build up together with poloidal flow shear,

damped by parallel losses and sheath dissipation

Quiescent periods interrupted by intermittent ejection of plasma filaments

These advect mass and energy into the far-SOL, while draining to the divertor

Edge-SOL turbulence not anomalous

Edge/SOL turbulence is no longer anomalous. Predictive capability in sight.

Recall that **anomalous** = abnormal, irregular, not understood

Ironically, it is the absence, rather then presence of turbulence which now appears anomalous.

We know who did it. We still don't know how.

There's just one more thing that bothers me…
How do I get this H-mode ??!

$$\nabla \cdot \mathbf{J} = \nabla \cdot (\mathbf{J}_p + \mathbf{J}_* + \mathbf{J}_{||}) = 0$$

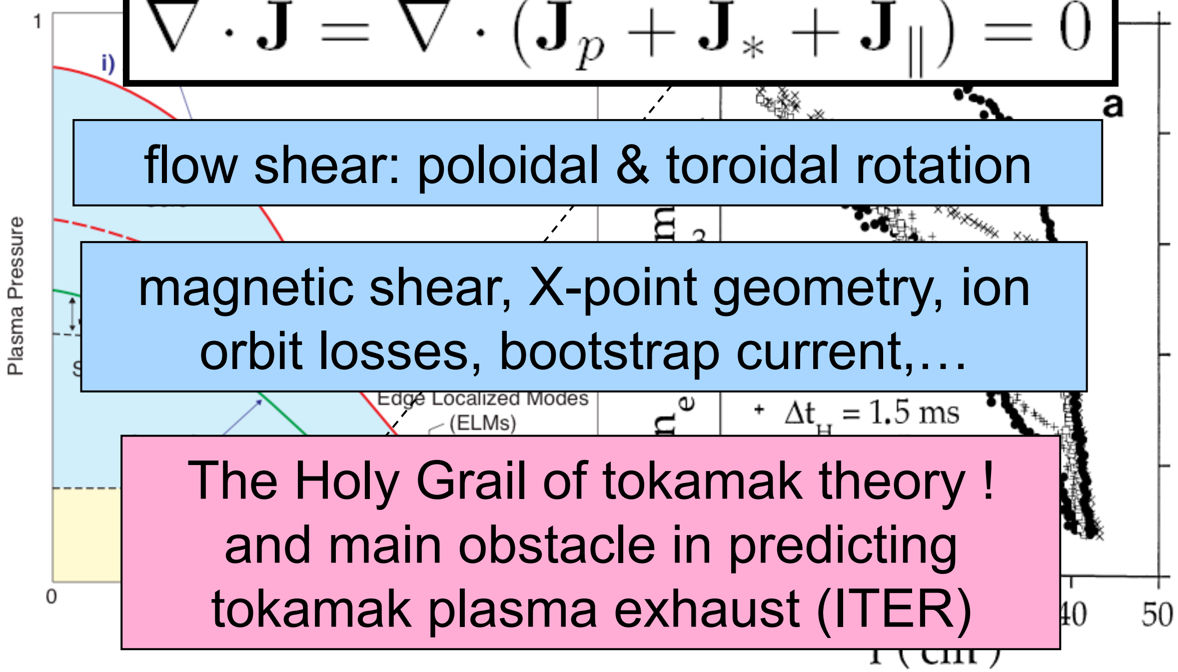

flow shear: poloidal & toroidal rotation

magnetic shear, X-point geometry, ion orbit losses, bootstrap current,…

The Holy Grail of tokamak theory ! and main obstacle in predicting tokamak plasma exhaust (ITER)

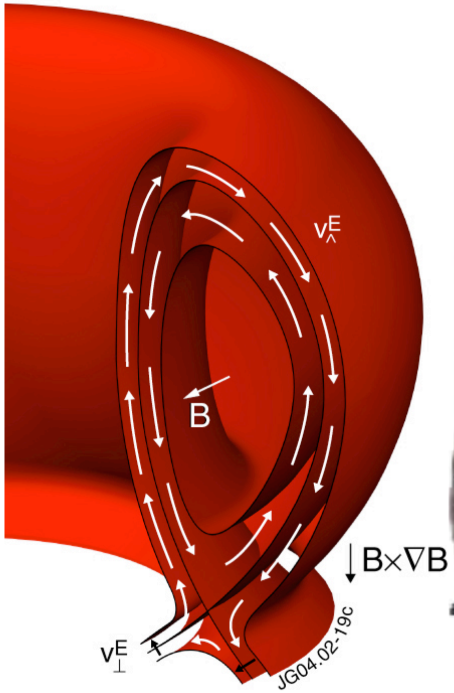

Tokamak plasma scenarios

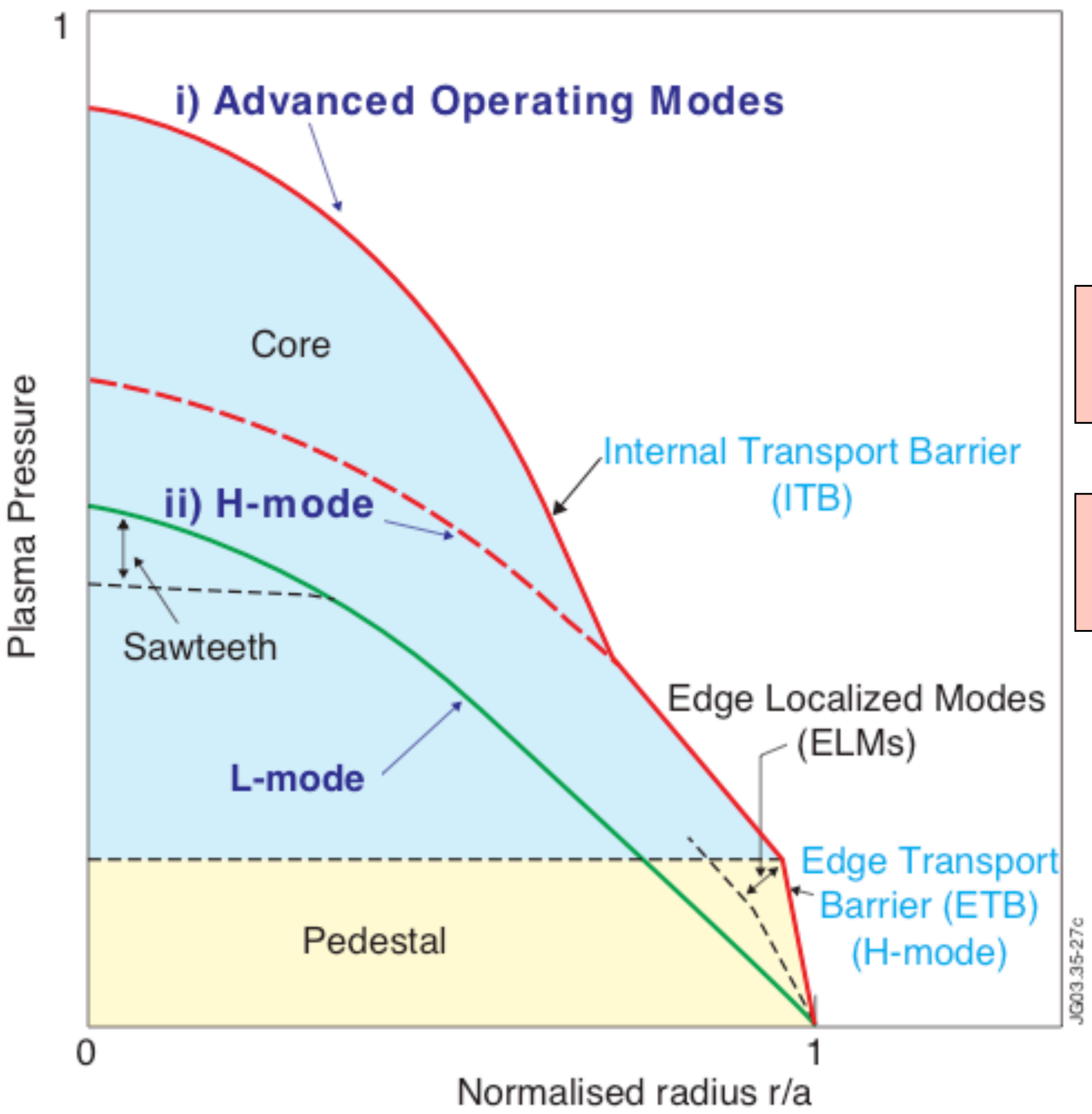

	Baseline	Advanced
current drive	inductive (pulsed)	auxiliary + bootstrap
transport barriers	edge (ETB)	edge (ETB) core (ITB)
Safety factor, q	dq/dr > 0 $q_0 \sim 1$ $q_{95} \sim 3$	dq/dr >< 0 $q_0 > 1$ $q_{95} \sim 4 - 5$

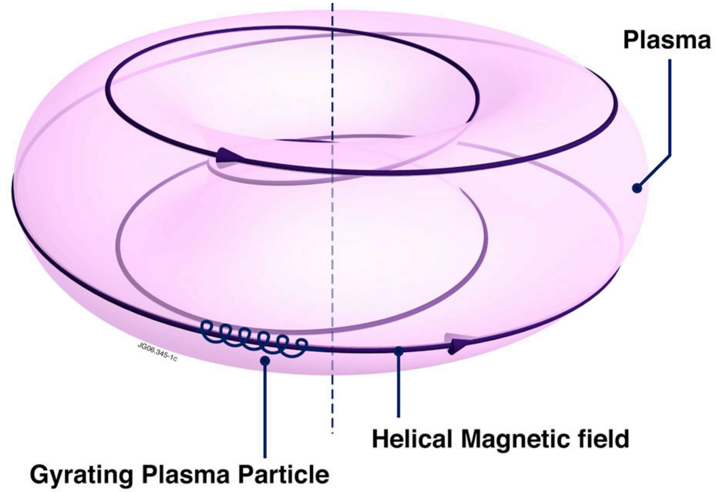

Divertor heat loads in ELMy H-mode

$$\lambda_q^{\mathrm{all}} \propto A^{\alpha} Z^{\beta} B_{\phi}^{-1.03} q_{95}^{0.6} P_{\mathrm{t}}^{-0.41} n_{\mathrm{e,u}}^{0.25}, \alpha + \beta = 1.04$$

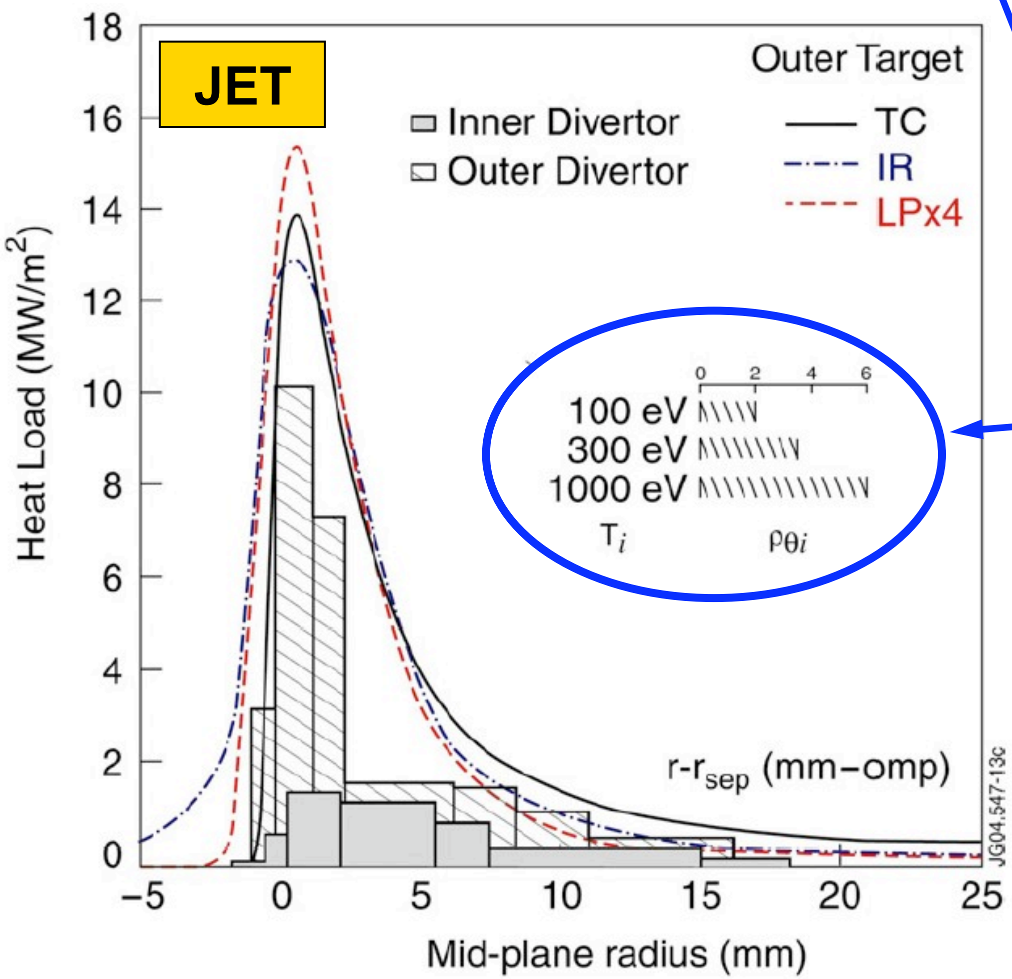

Averaged heat load profiles in natural density, ELMy H-mode

Integral power width decreases with field, current and power

Narrowest profile ~ ion poloidal gyro-radius at pedestal temperature

Narrow inter-ELM profile confirmed by high resolution IR system on JET

Most of the energy arrives at the outer target; $P_{outer} : P_{inner} = 2.5 : 1$

W.Fundamenski et al, NF ***45*** *(2005) 950*

Turbulence reduction in the near-SOL

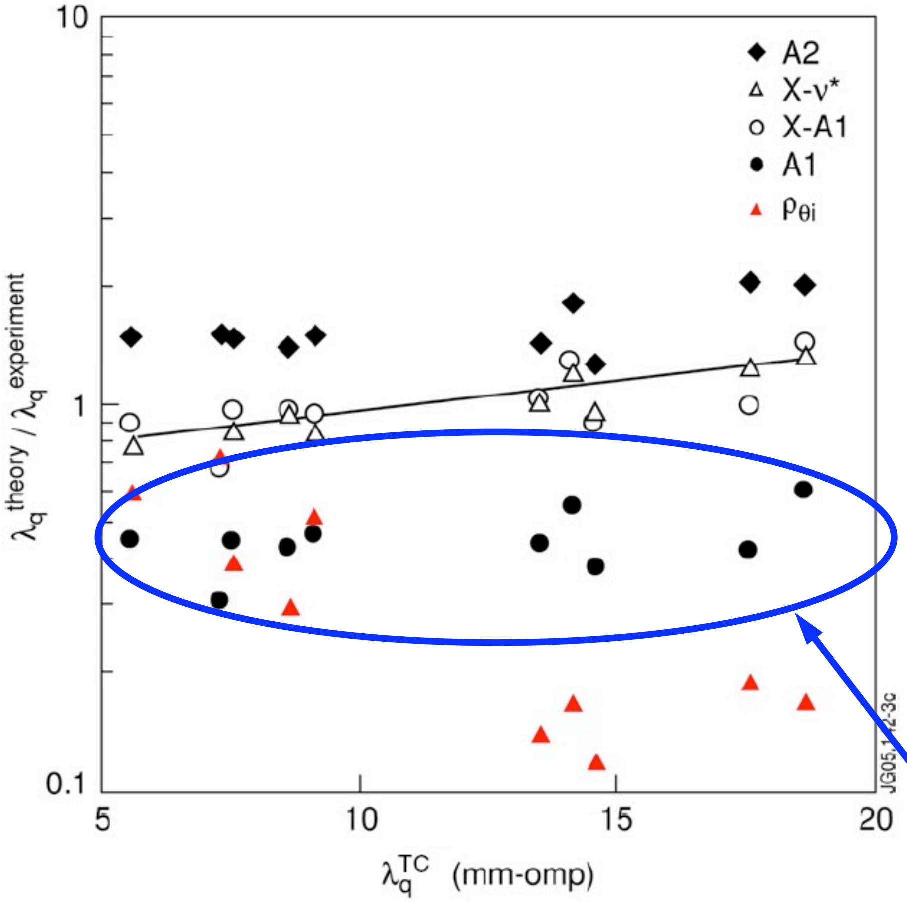

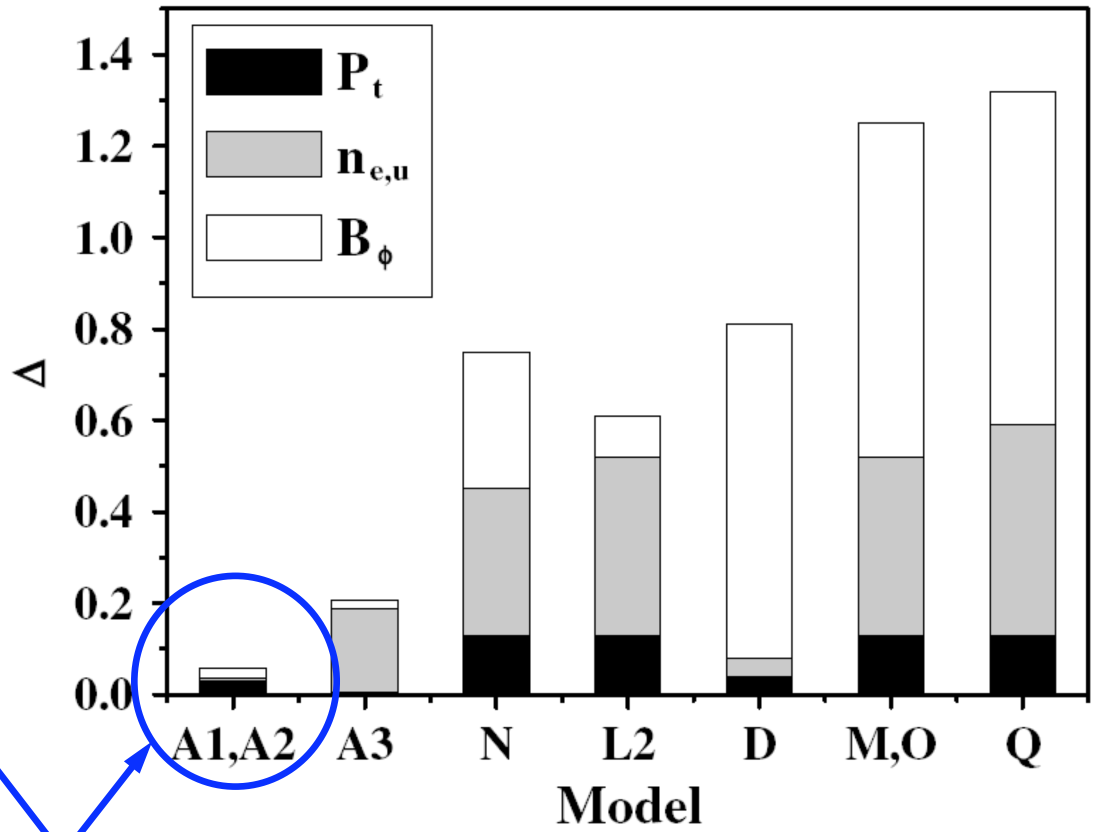

Obtained scaling is best explained by neo-classical ion conduction

$$\lambda_q^{cond} \propto B_\phi^{-1}(P_{SOL}/R^2)^{-0.5}(Rq_{95})n_{e,u}^{0.25} \propto B_\phi^{-1}P_{SOL}^{-0.5}n_{e,u}^{0.25}q_{95}R^2,$$

Consistent with partial extension of the ETB into the near-SOL

ITER prediction: ~4 mm

Recall? in wetted area

$$\lambda_q^{conv} \propto B_\phi^{-1}(P_{SOL}/R^2)^{-0.5}(Rq_{95})^{0.5}n_{e,u}^{0.25} \propto B_\phi^{-1}P_{SOL}^{-0.5}n_{e,u}^{0.25}q_{95}^{0.5}R^{1.5}.$$

Earlier analysis confirmed with multi-fluid (EDGE2D) simulations

Divertor operating regimes

Low recycling (sheath limited): $n_t \sim n_u$, $T_t \sim T_u$, $p_t \sim p_u$

Can this narrow heat load profile be broadened by a divertor 'buffering'?

high recycling (conduction limited): $n_t \sim n_u^{3}$, $T_t \sim n_u^{-2}$, $p_t \sim p_u$

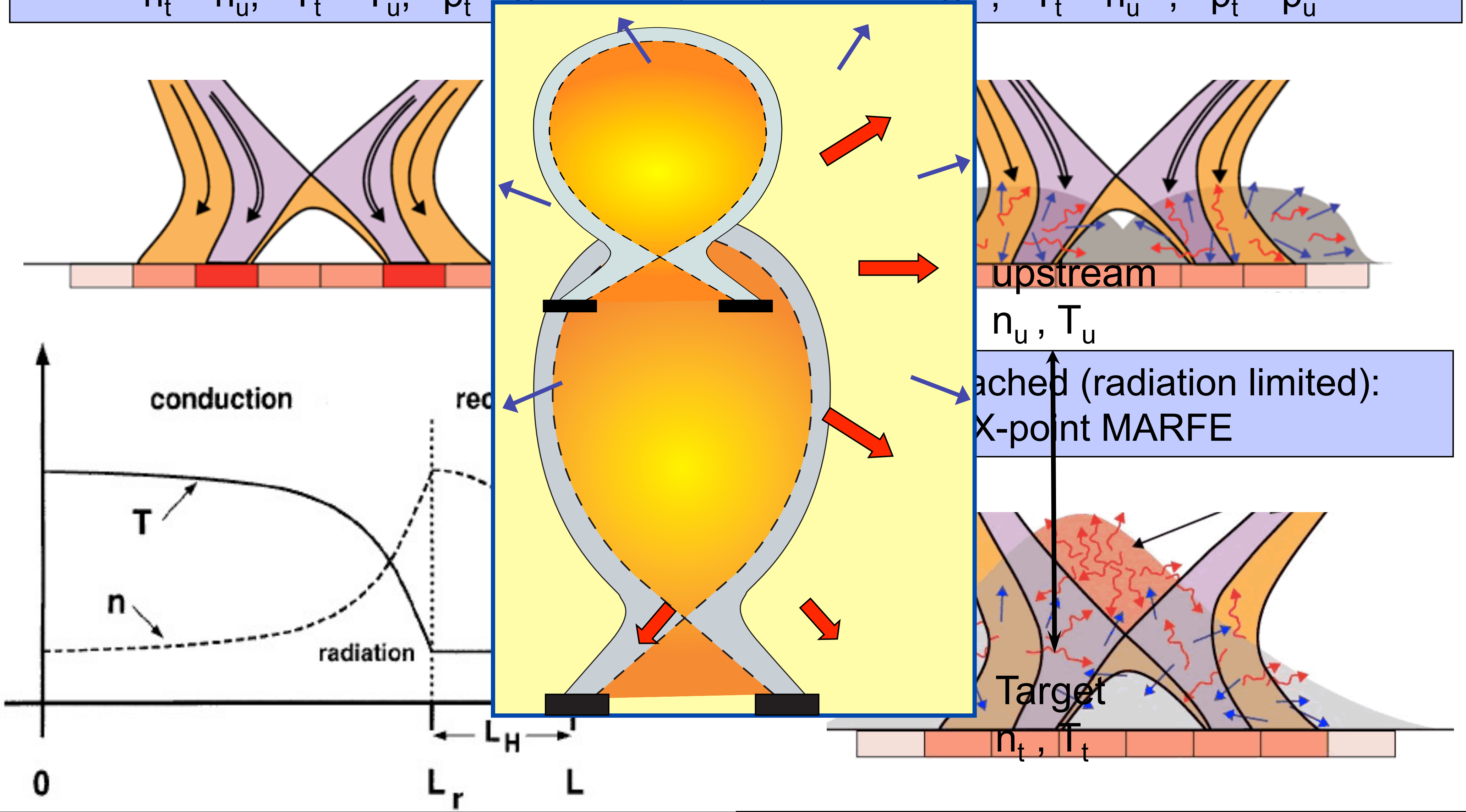

Divertor plasma detachment

A.Loarte et al, PPCF (2001)

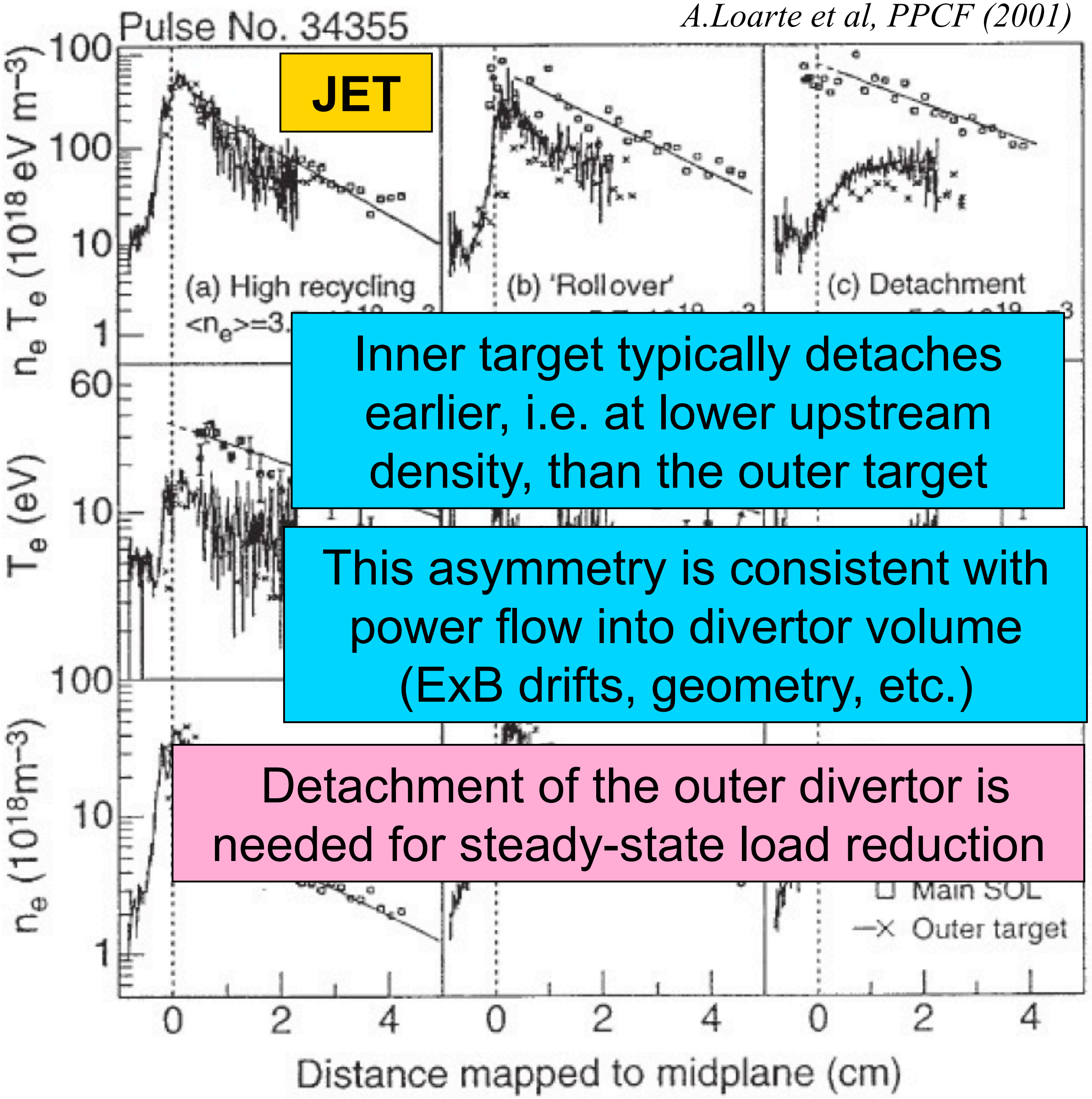

Inner target typically detaches earlier, i.e. at lower upstream density, than the outer target

This asymmetry is consistent with power flow into divertor volume (ExB drifts, geometry, etc.)

Detachment of the outer divertor is needed for steady-state load reduction

Loss of plasma pressure and energy by CX/ES & line radiation

Reduction of target plasma flux

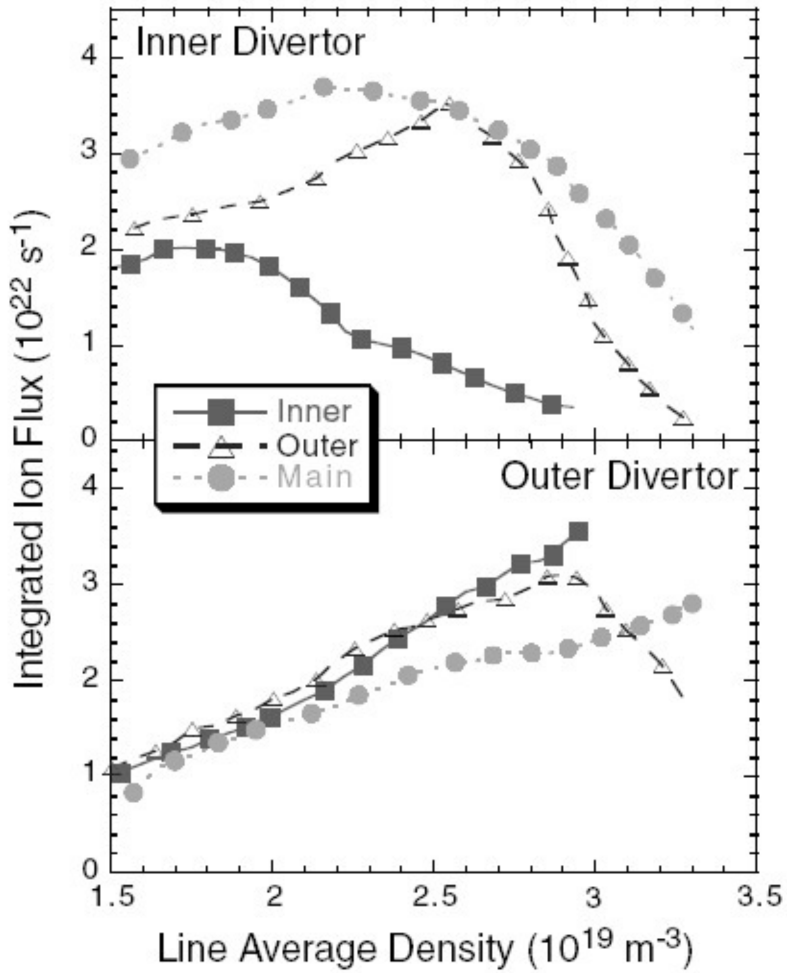

Thermal instability: X-point MARFE

Outer target detachment typically accompanied by an X-point MARFE

Results in substantial cooling of the edge plasma, reduction of pedestal stored energy and degradation of energy confinement

At higher densities transforms into an inner wall MARFE: density limit ~ n_{GW} ~ I_p/a^2

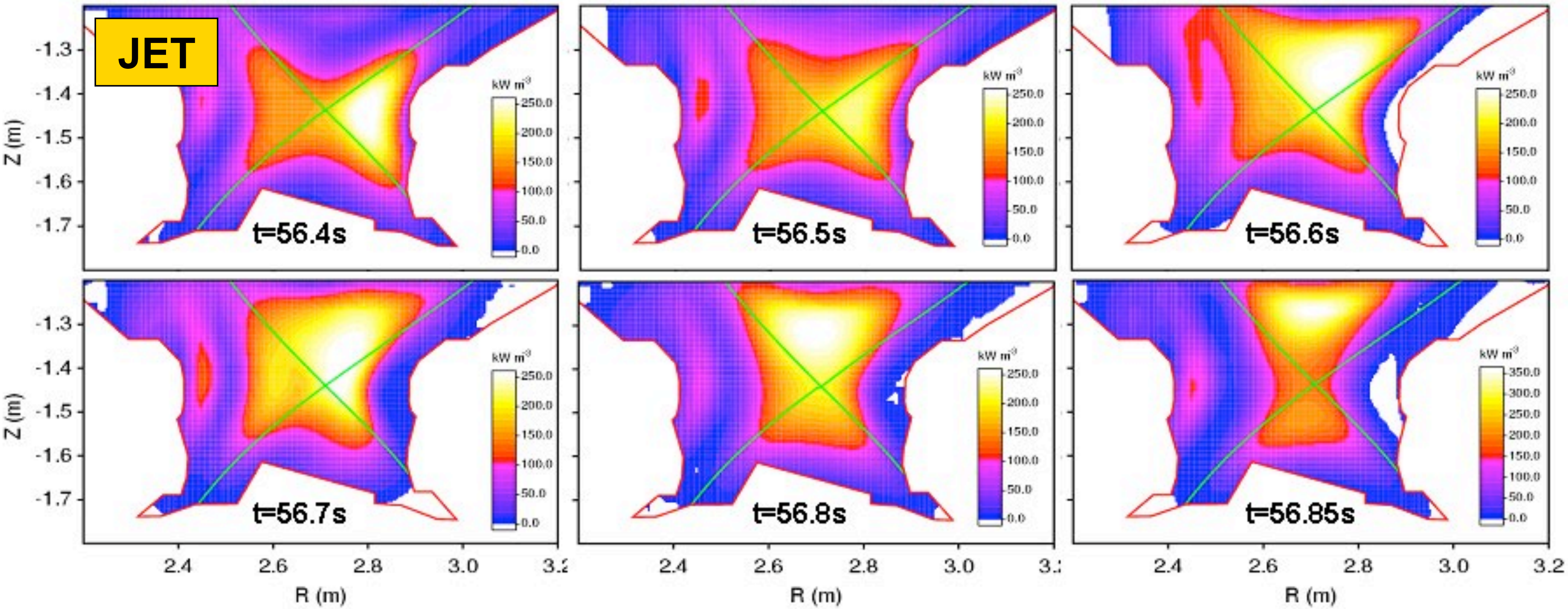

A. Huber et al, NF (2007)

Impurity seeding: confinement

Energy confinement (H98) decreases with density (f_{GW}) and radiation (f_{rad})

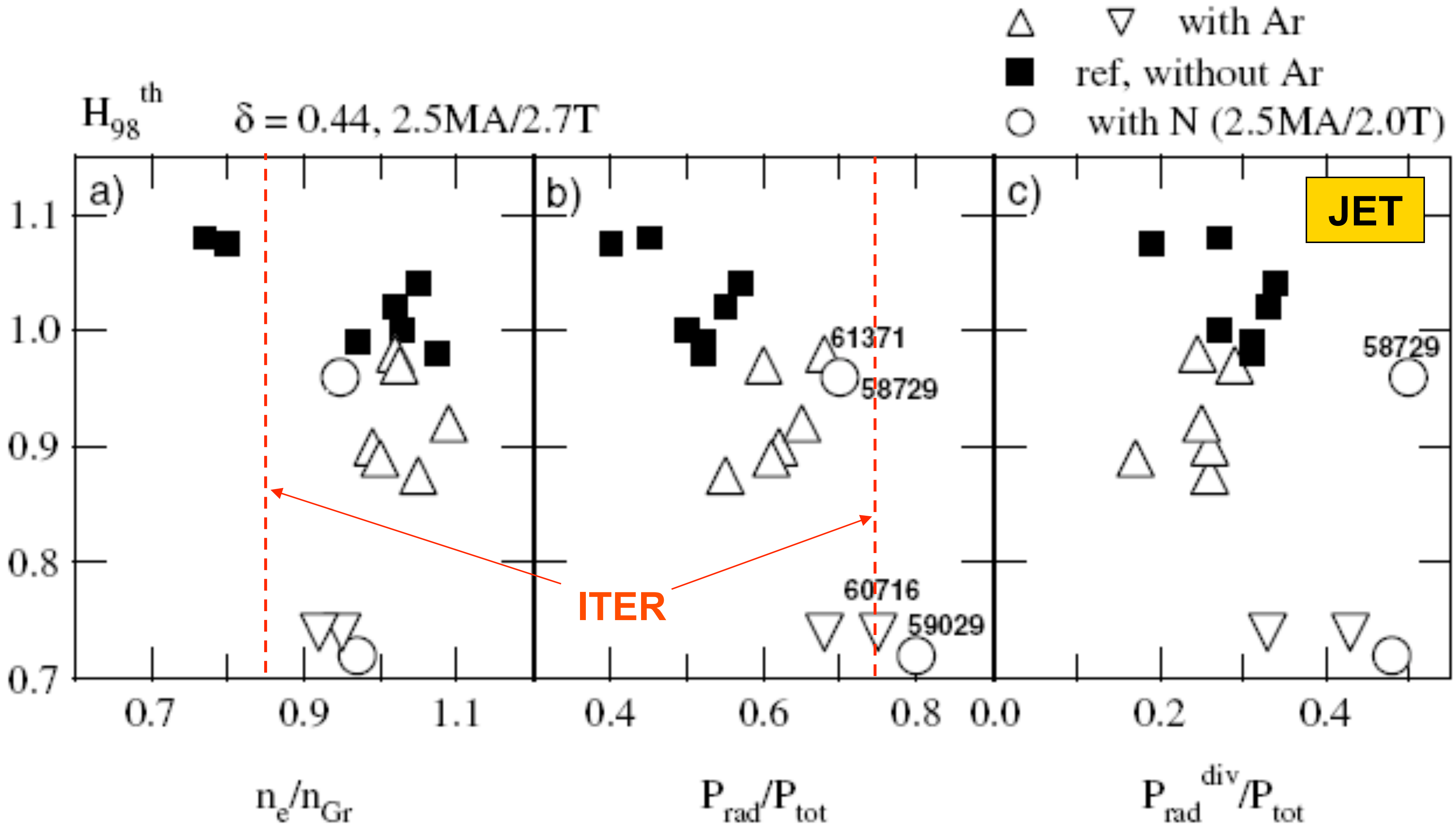

Energy confinement degradation

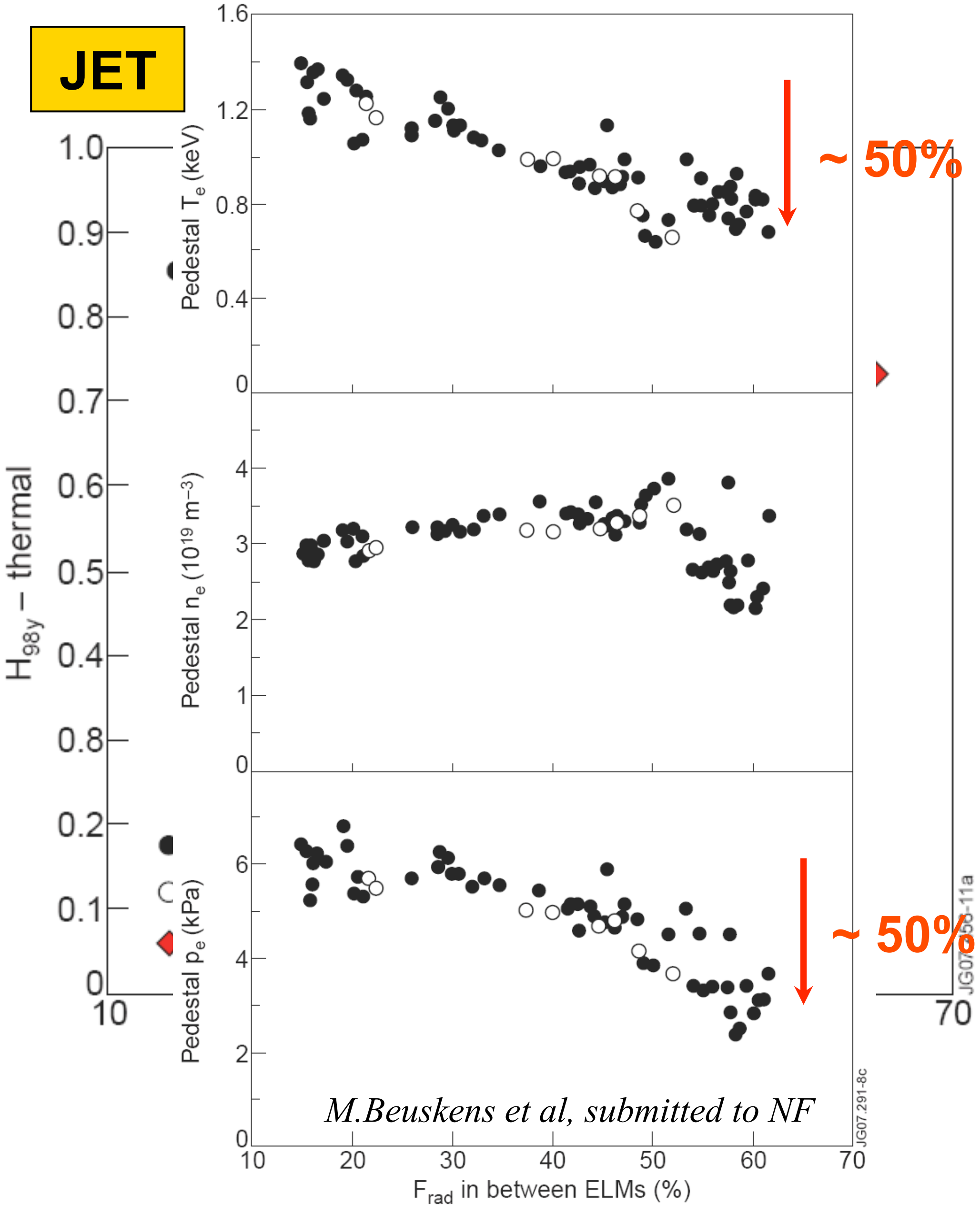

Density (fuelling) scan:

Normalised energy confinement (H98) reduced with line average density as it approaches the density limit (n_{GW})

H98 also reduced by ~15% after a Type-I to Type-III ELM transition

Radiation (impurity seeding) scan:

H98 reduced with radiative fraction

Caused by reduction of pedestal temperature and pressure

Since W_{ped} ~ 1/3 W, hence a 50% drop in W_{ped} means a ~15-20% drop in H98

Impurity accumulation in the core

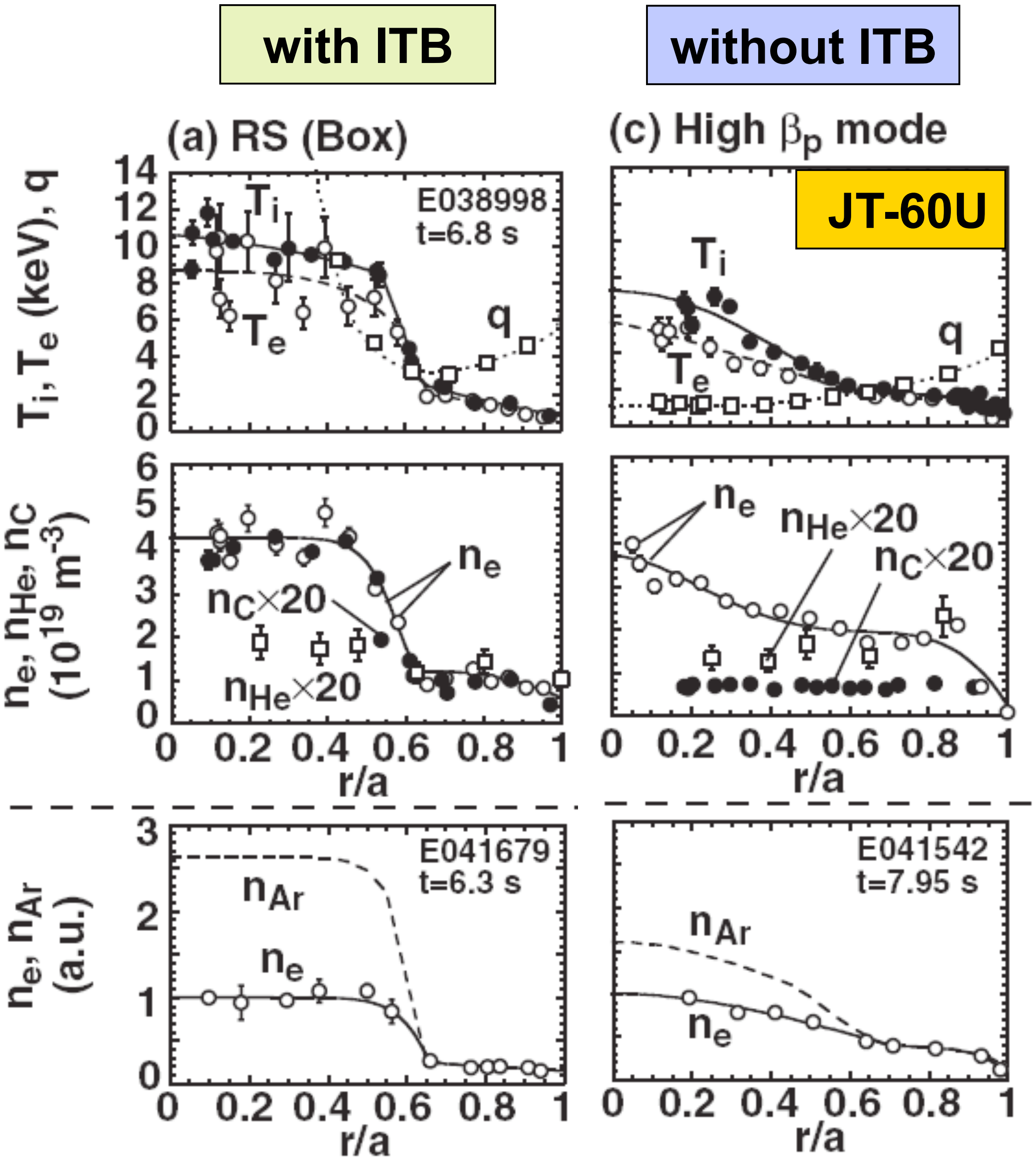

$Z_{eff} - 1 \sim P_{rad} / n_e^2$

Impurity density roughly uniform in the absence of an ITB

ITB acts as a barrier for impurity transport as well as for transport of fuel ions and energy

Inward velocity of impurities (neoclassical and turbulent pinch) overcomes outward diffusion

Impurity accumulation increases with ion charge

Cause for concern for both medium and high-Z impurities

*H.Takenaga et al, NF **43** (2003) 1235*

Transient exhaust

- **Compatibility between the plasma scenarios and PFCs**
  - Ignition vs. exhaust criteria
  - Impact of PFCs on fusion gain
  - Power balance on ITER
- **Steady-state particle and power exhaust**
  - Limiter vs Divertor exhaust
  - Steady plasma loads
    - on main chamber PFCs
    - on divertor PFCs
  - Divertor plasma detachment
- **Transient particle and power exhaust**
  - Edge localised modes (ELMs)
  - Plasma loads associated with ELMs
    - on divertor PFCs
    - on main chamber PFCs
  - ELM mitigations techniques
    - Magnetic perturbations
    - Pellet pacing
    - Impurity injection
- **Conclusions**

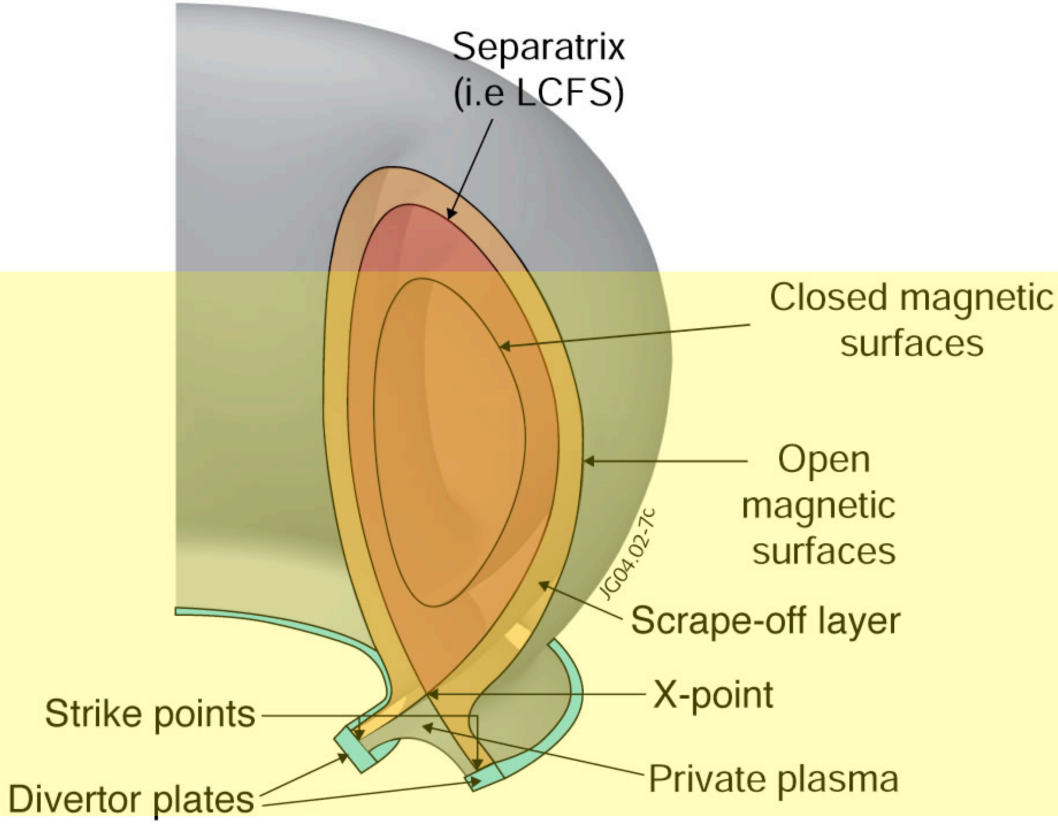

Edge localized modes (ELMs)

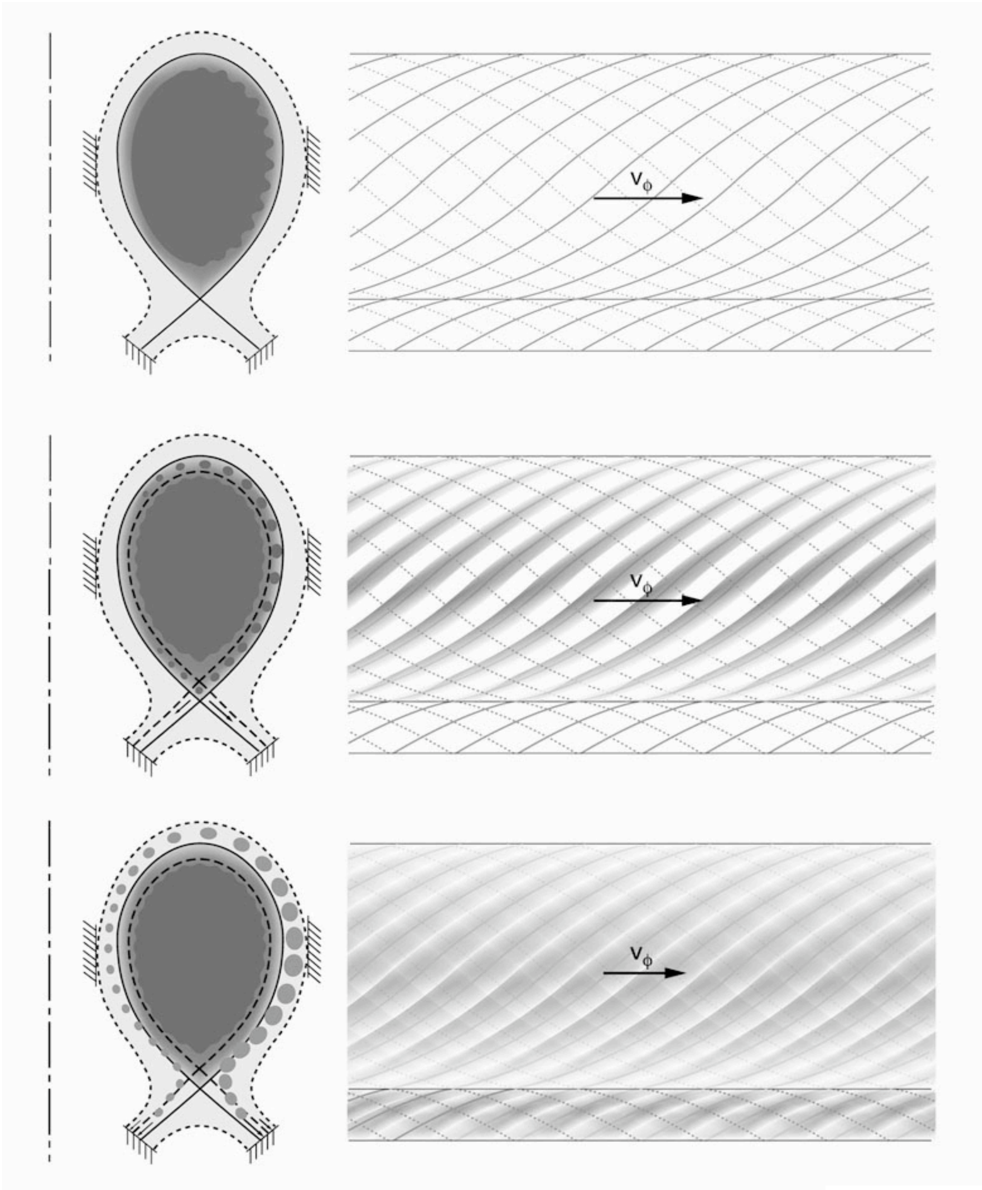

Growth stage:

• Linear instability (e.g. ideal/resistive MHD mode) forms n flute-like ripples in pedestal quantities

Saturation stage:

• These develop into n filaments during the non-linear phase of the instability; beginning of transport, parallel losses, magnetic reconnection, ergdodization?

Exhaust stage:

• Filaments move outward, driven by interchange (curvature + pressure), while draining to the divertor targets

Fundamenski W *et al* 2006 *Plasma Phys. Control. Fusion* **48** 109

Free streaming approach

Ions released during an ELM from an initially Maxwellian distribution stream freely along field lines to the (inner/outer) divertor targets *(W.Fundamenski et al., PPCF48 (2006))*

$$P_{div}(t) = E_{ELM}^{div} \Big/ \sqrt{\pi}\tau_{FS} \times \exp\left(-\left(\frac{\tau_{FS}}{t} - M_{ELM}\right)^2\right) \times \frac{\tau_{FS}^2}{t^2} \times \left(1 + \frac{\tau_{FS}^2}{t^2}\right)$$

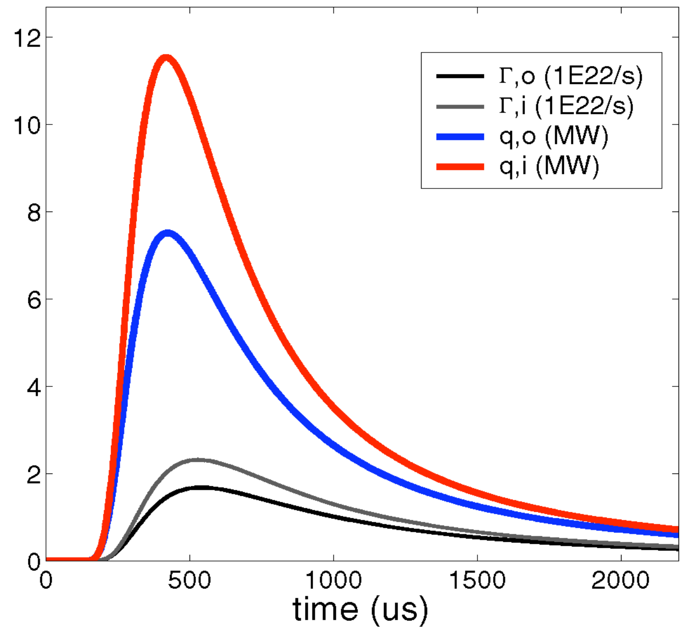

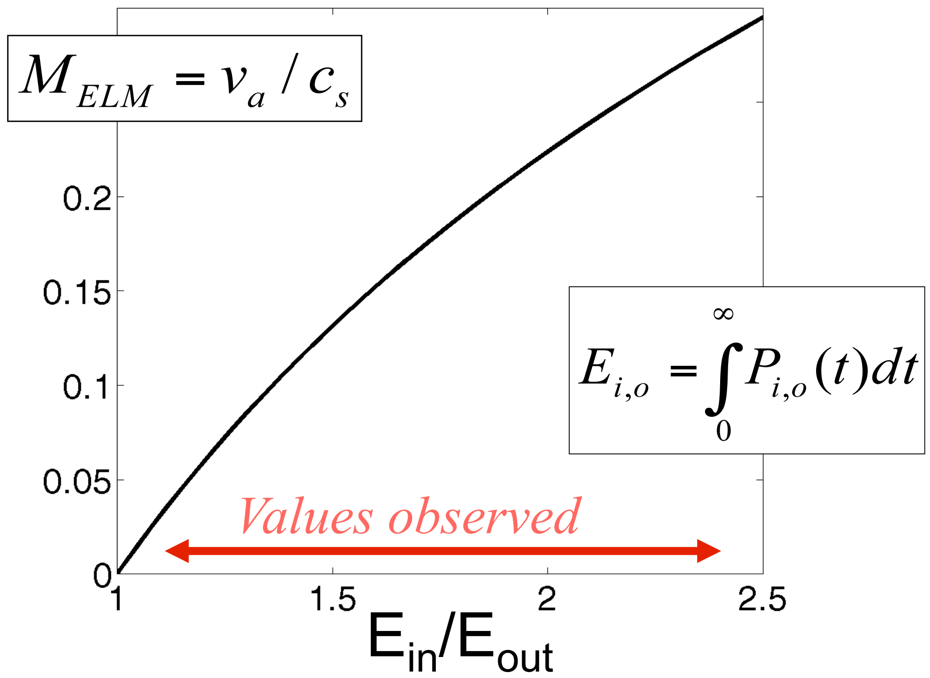

Power load can be fitted by 4 parameters $E_{in}+E_{out}$, τ_{in} , τ_{out} and M_{ELM}

Comparison with IR data: AUG

ASDEX Upgrade

+0.8MA/-2.0T, E_i/E_o = 0.6 Upper Single Null	+0.8MA/+2.0T: E_i/E_o = 1.4 Upper Single Null

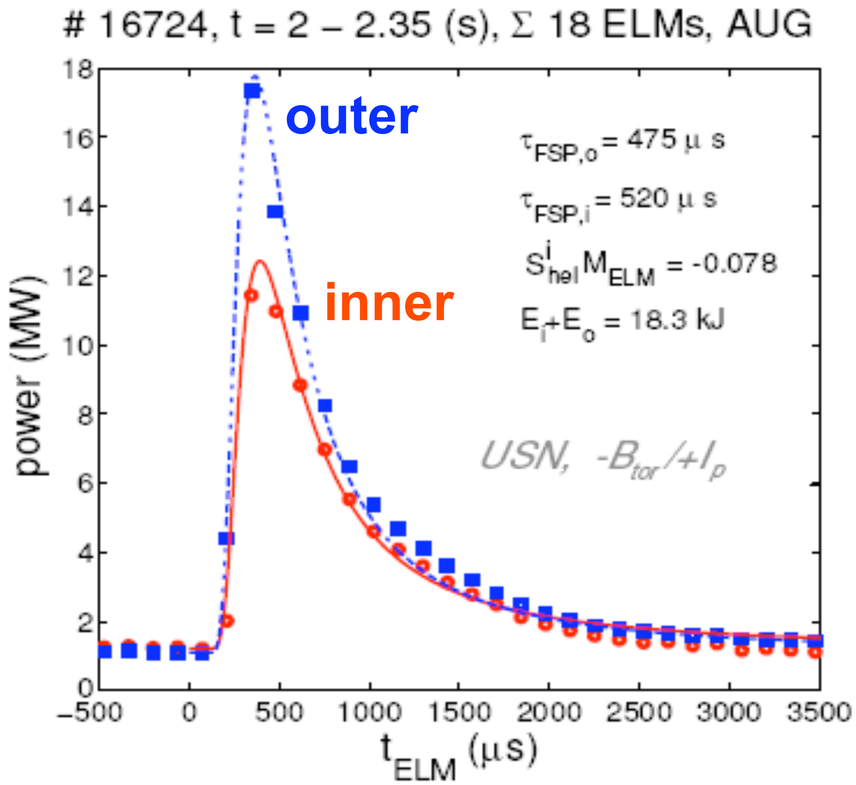

$\nu^*_{ped,top} \sim 0.6$

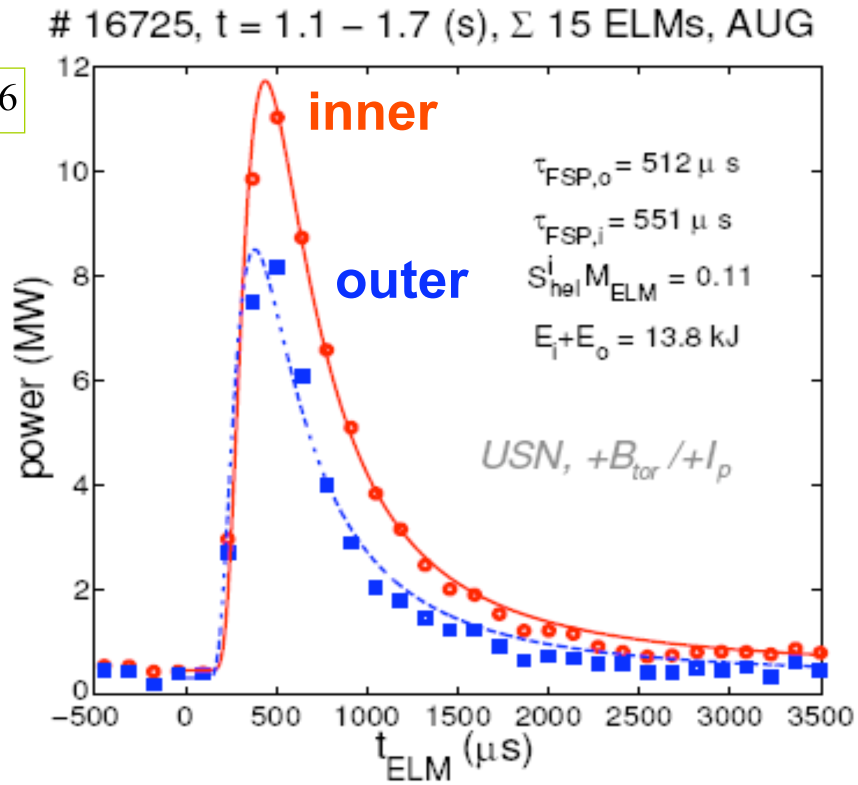

- In/out ELM energy asymmetry changes with field direction
- Inferred Mach number consistent with magnitude/direction of toroidal rotation
- Comparable FS times to both targets ($\tau_{in} \sim 1.1 \times \tau_{out}$); not affected by helicity

Type-I ELM structure at AUG

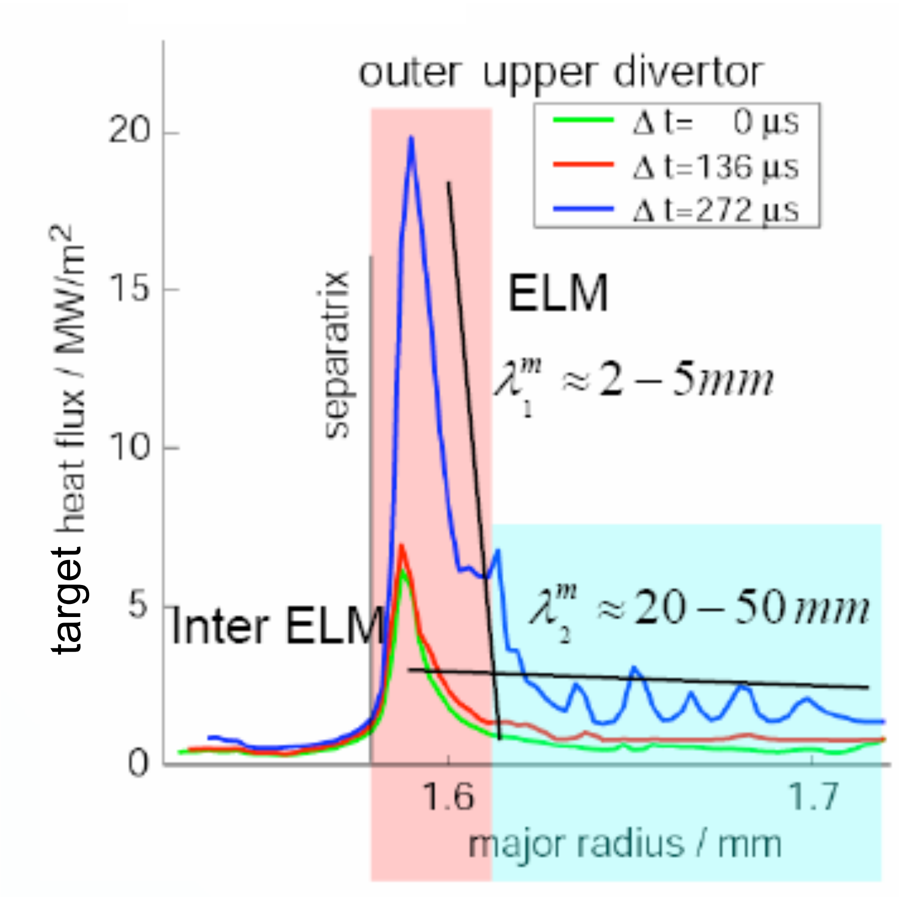

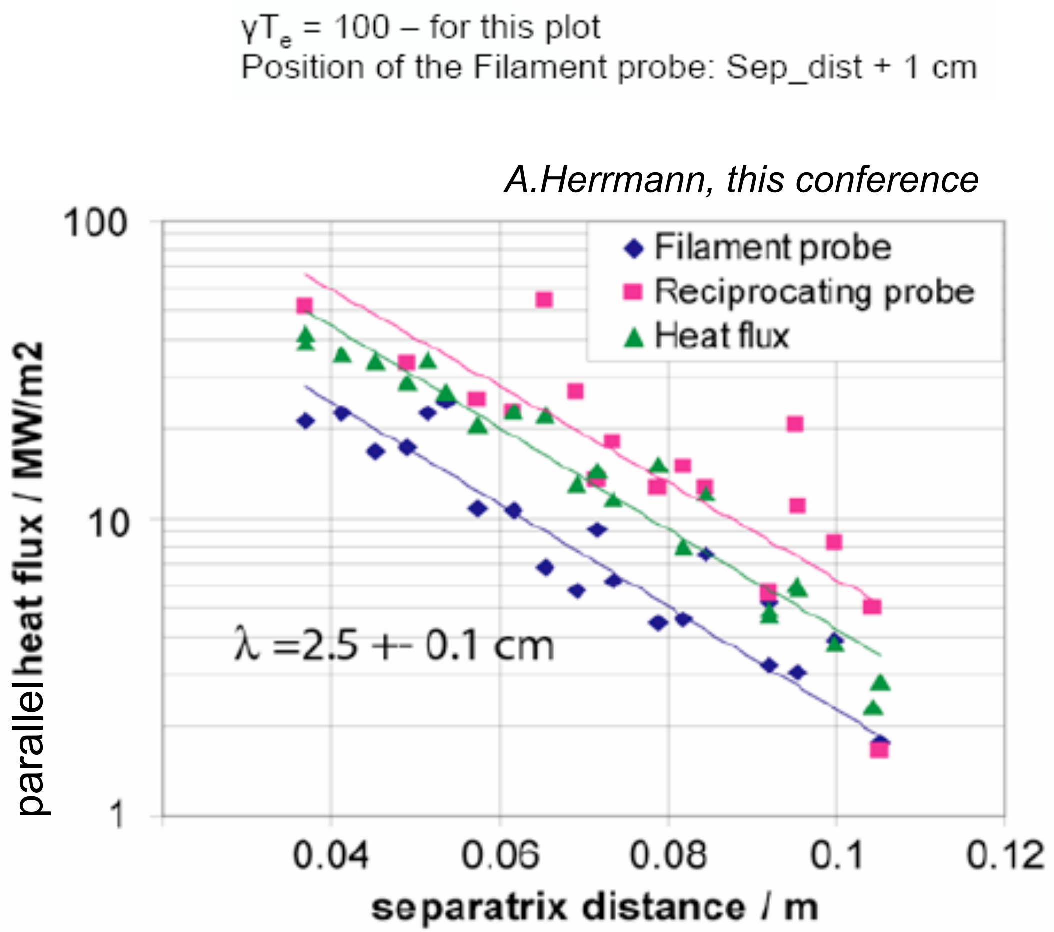

- Near separatrix profile shape roughly similar between and during ELMs
- Imprints of single filaments resolved in the far scrape-off layer
- Comparable radial power decay lengths observed at target and outer mid-plane

Type-I ELM structure on JET divertor

Pre-ELM magnetic equilibriu

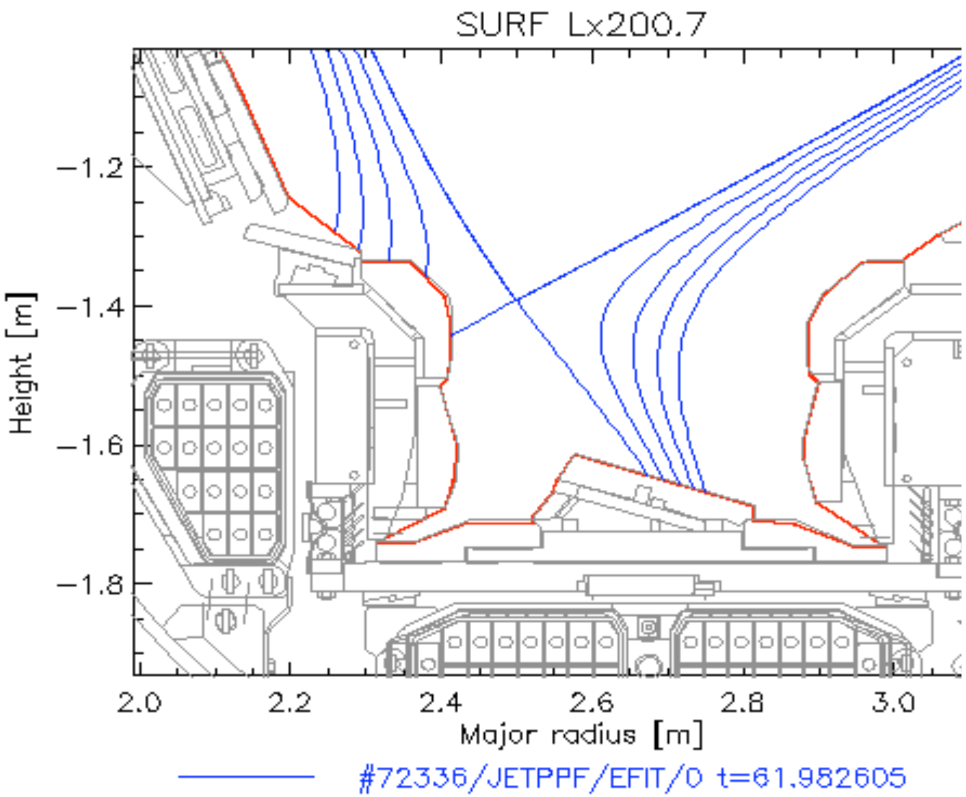

Heat load imprints of individual ELM filaments

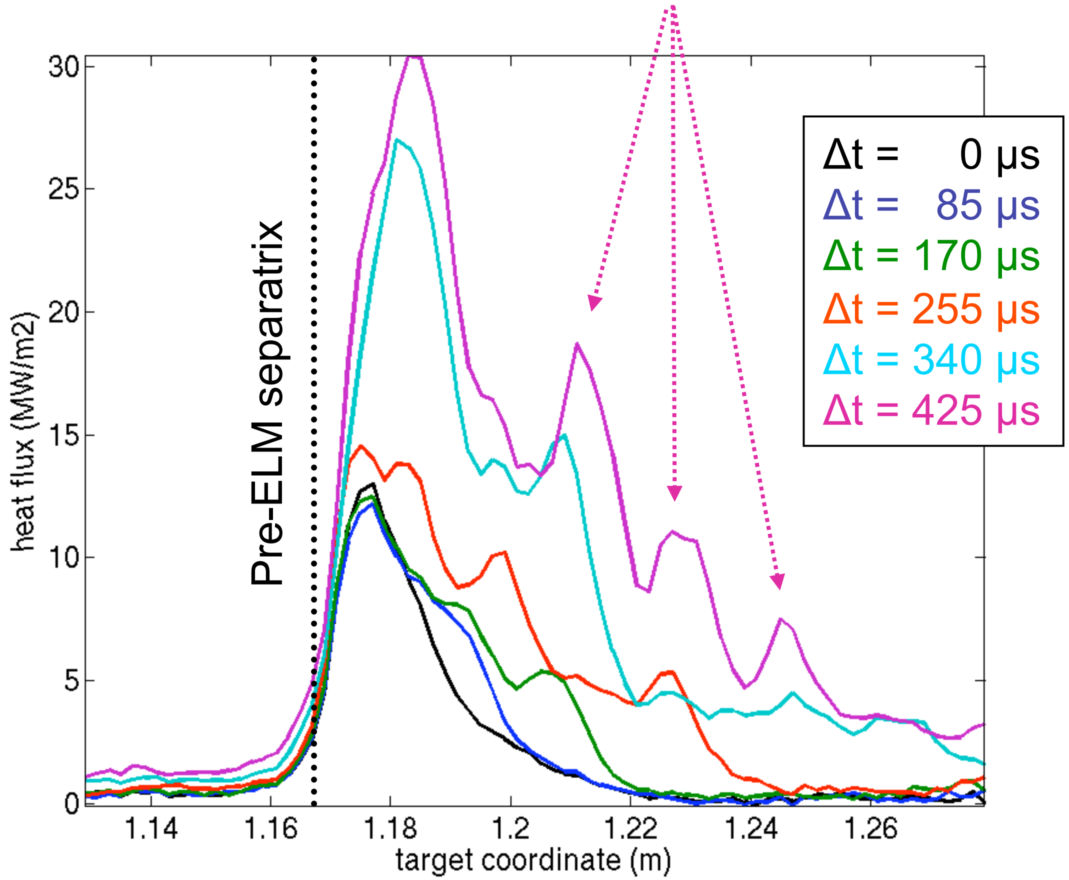

Snapshot of IR camera displaying the divertor target plates during ELM power load

- Near separatrix heat load profile roughly similar between and during ELMs
- Heat load imprints of single filaments resolved in the far scrape-off layer
- Using pre-ELM SOL magnetic field, the quasi-toroidal mode number can be found

Spatial resolution is 1.7mm, picture integration time 20

Quasi-toroidal mode number

JET (#74380), 160 ELMs

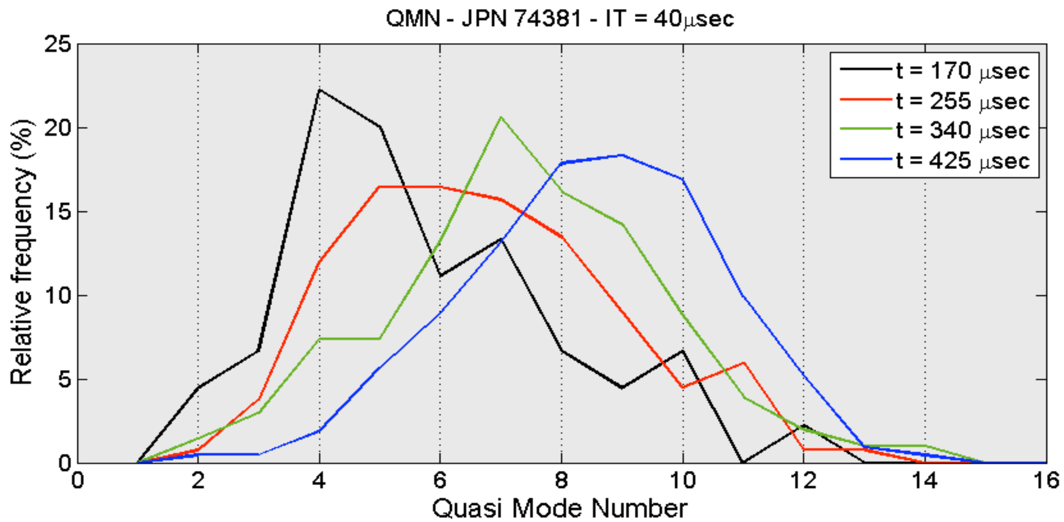

- ELM mode structure derived from striations in divertor heat fluxes
- Similar quasi-toroidal mode number, n~4-12, as observed previously on AUG
- Mode number increases with time, by a factor of ~ 2-3, during the ELM (exhaust)
- Suggests break-up into smaller structures

ASDEX Upgrade, 243 ELMs

ELM structure seen in heat fluxes

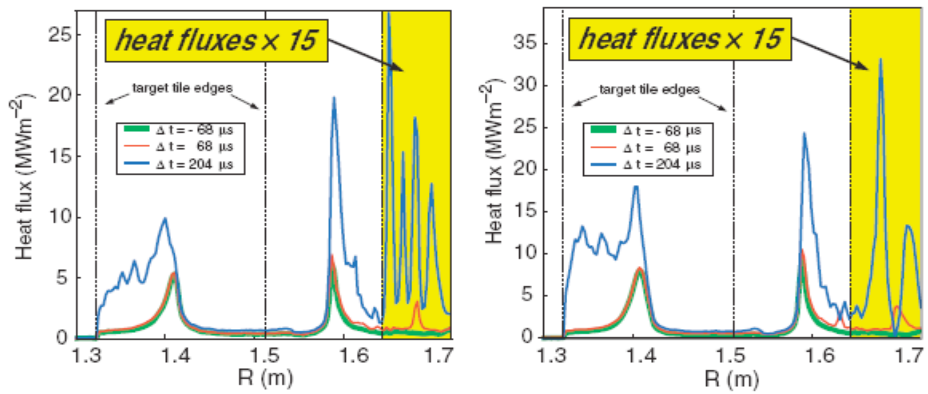

Derived (quasi) mode numbers

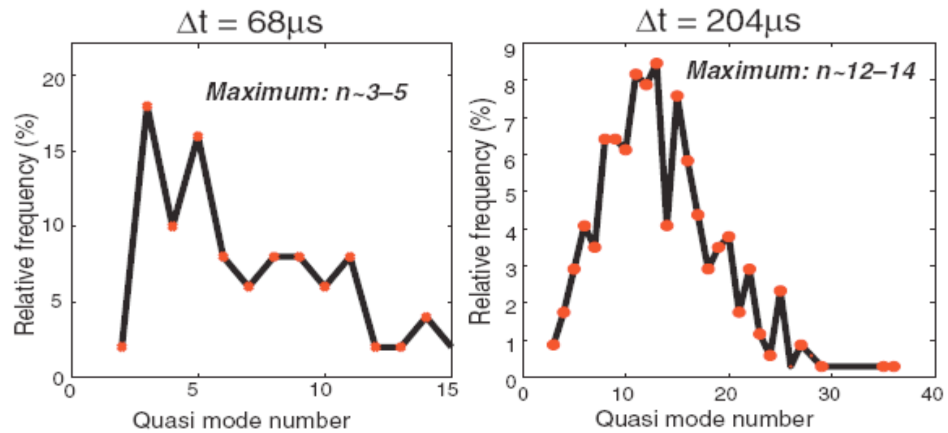

T.Eich et al., PPCF 47, p.841 (2005)

IR imprint on outer limiters

ELM heat load superimposed on ambient background

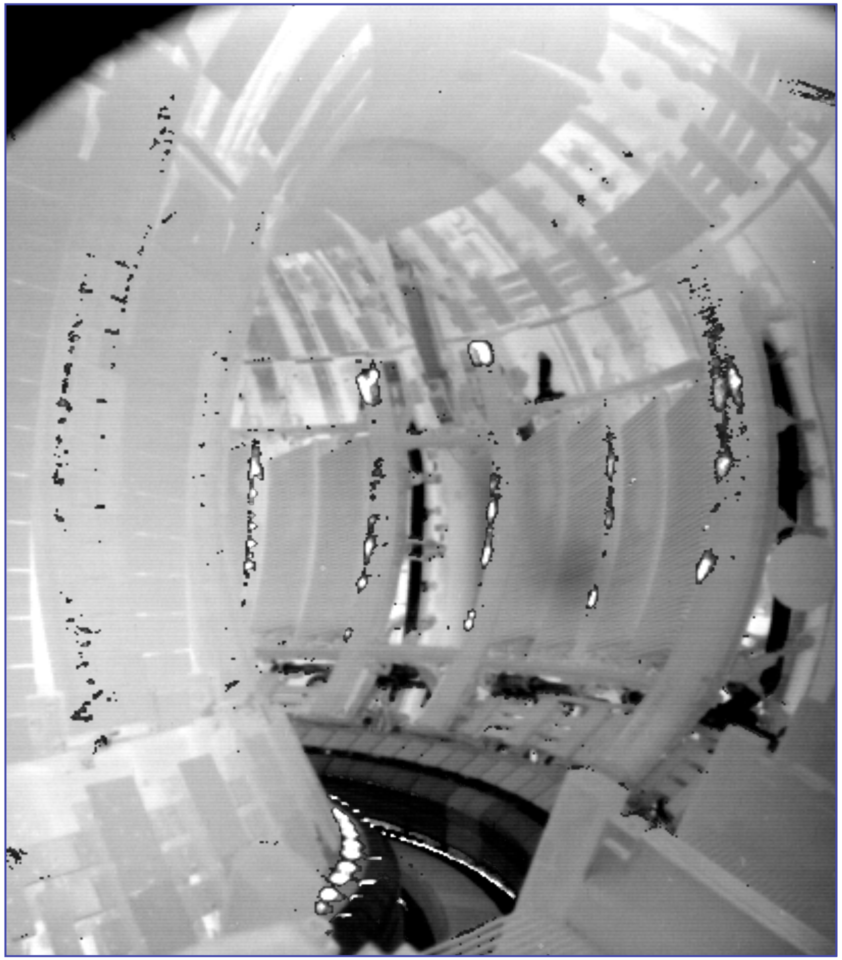

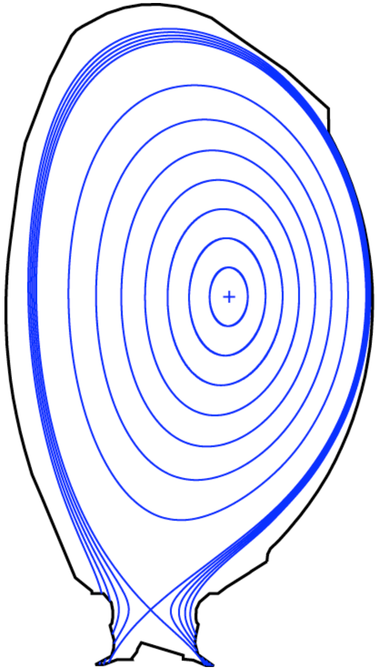

ΔW_{ELM} ~ 200 kJ
t = 7.6 s
Exp. time 300 µs
Frame time 7.8 ms

Difference between ELM and pre-ELM frames

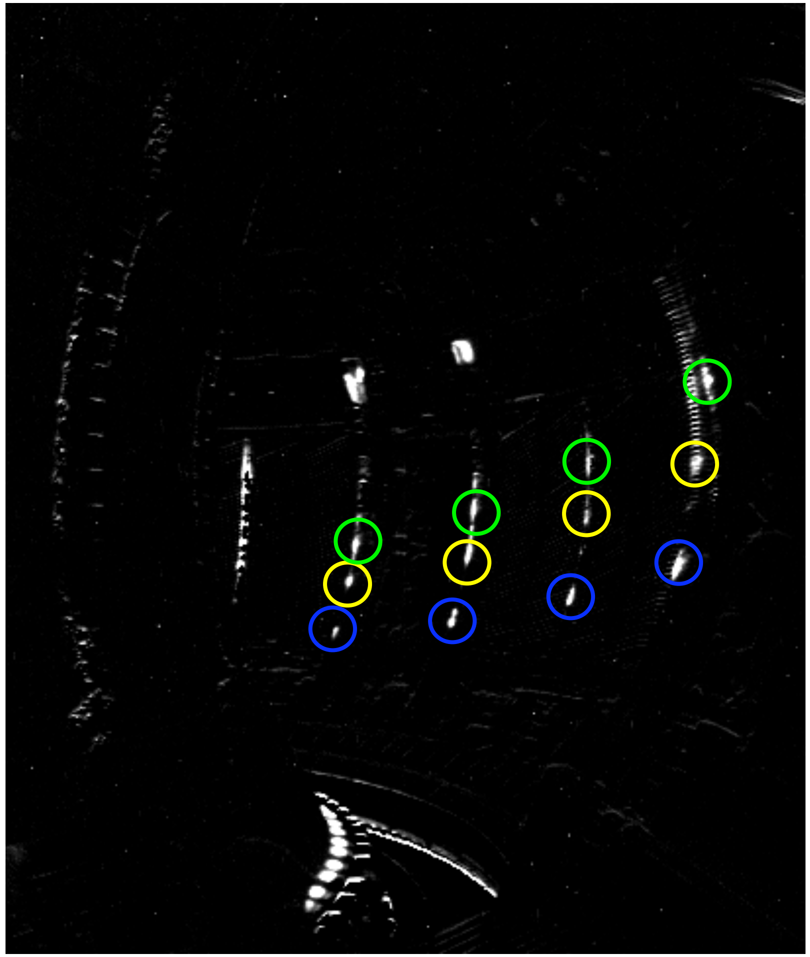

- New wide angle IR camera diagnostic using ITER-like front mirrors.
- 640x512 pixel FPA, max. full frame rate 100 Hz (E. Gauthier et al., CEA)

W. Fundamenski, M. Jakubowski, ITPA Garching May 2007, P. Andrew et al., EPS 2007

IR imprint field aligned

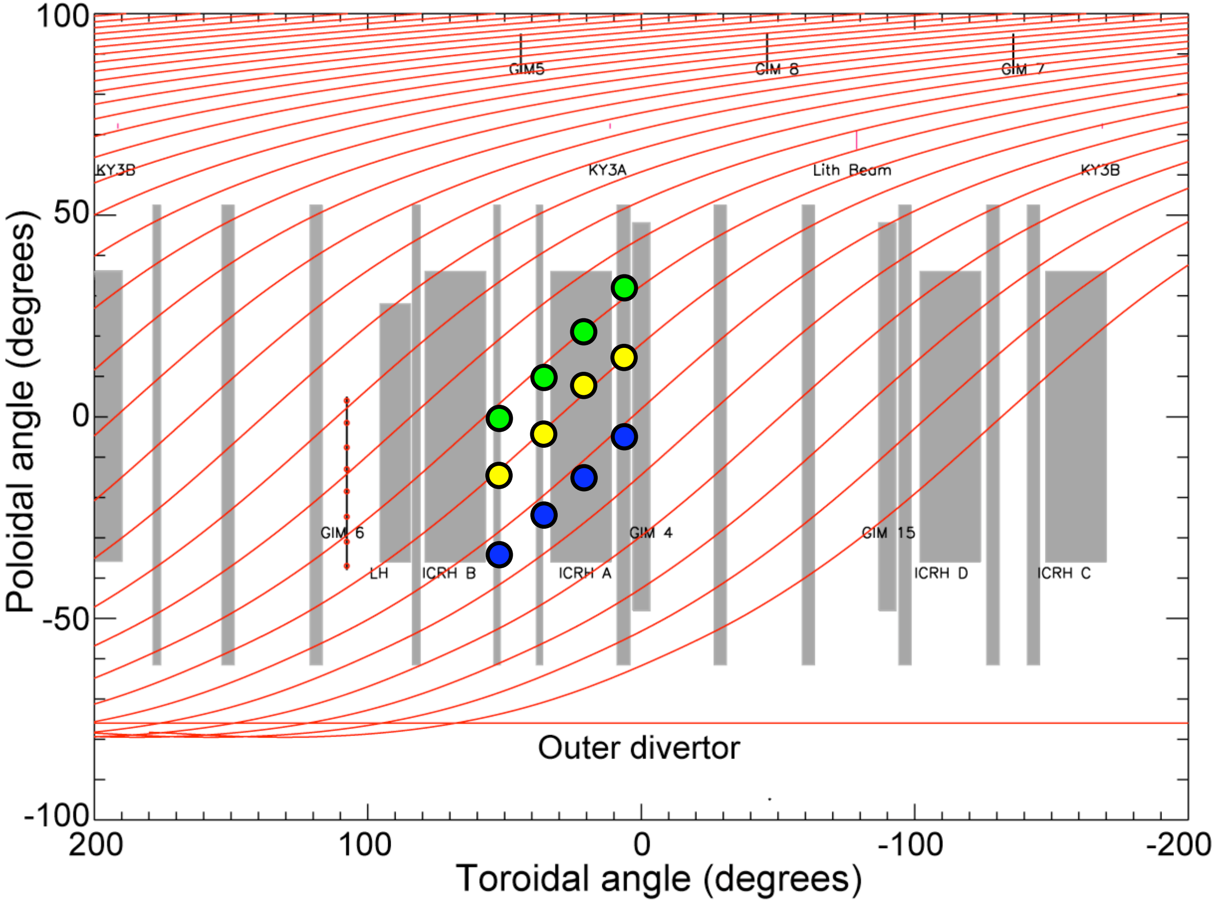

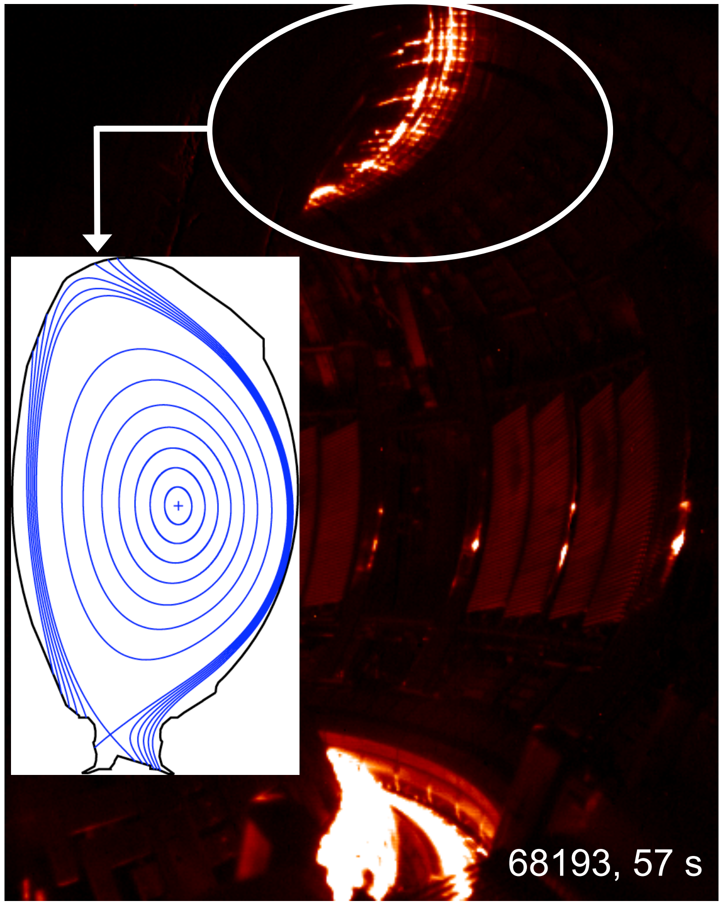

ELM filaments follow pre-ELM magnetic field lines in the poloidal-toroidal plane

Also observed on the upper dump plates

Fast-visible images of filaments

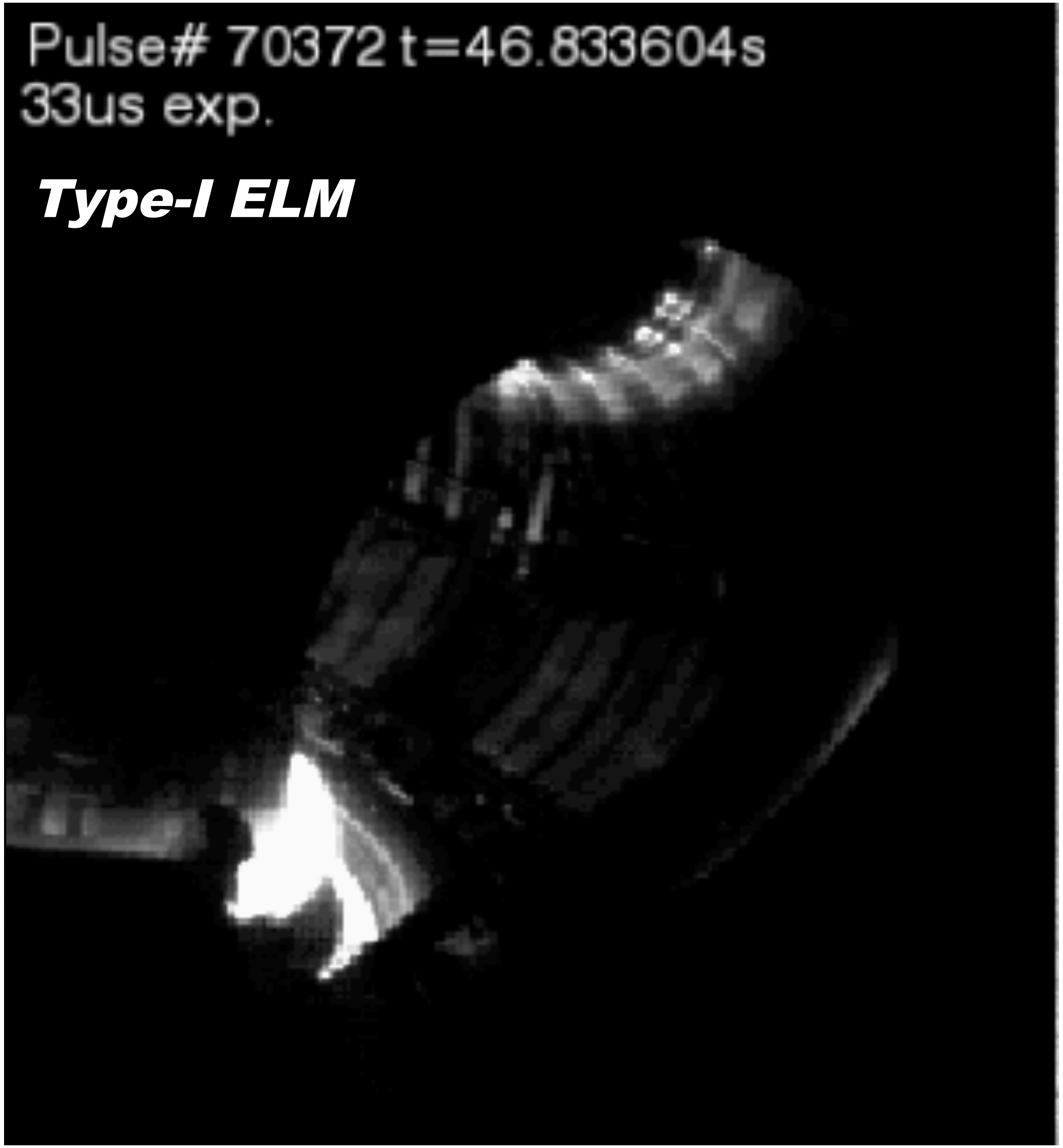

- Exposure time 33 μs
- Ten successive frames showing ELM-filaments striking the upper dump plate
- Less contact at outer limiter

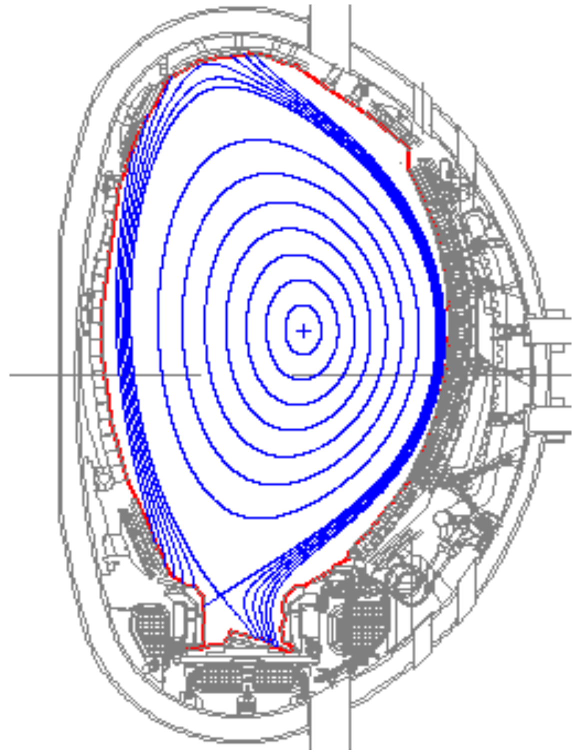

IR imprint on upper dump plate

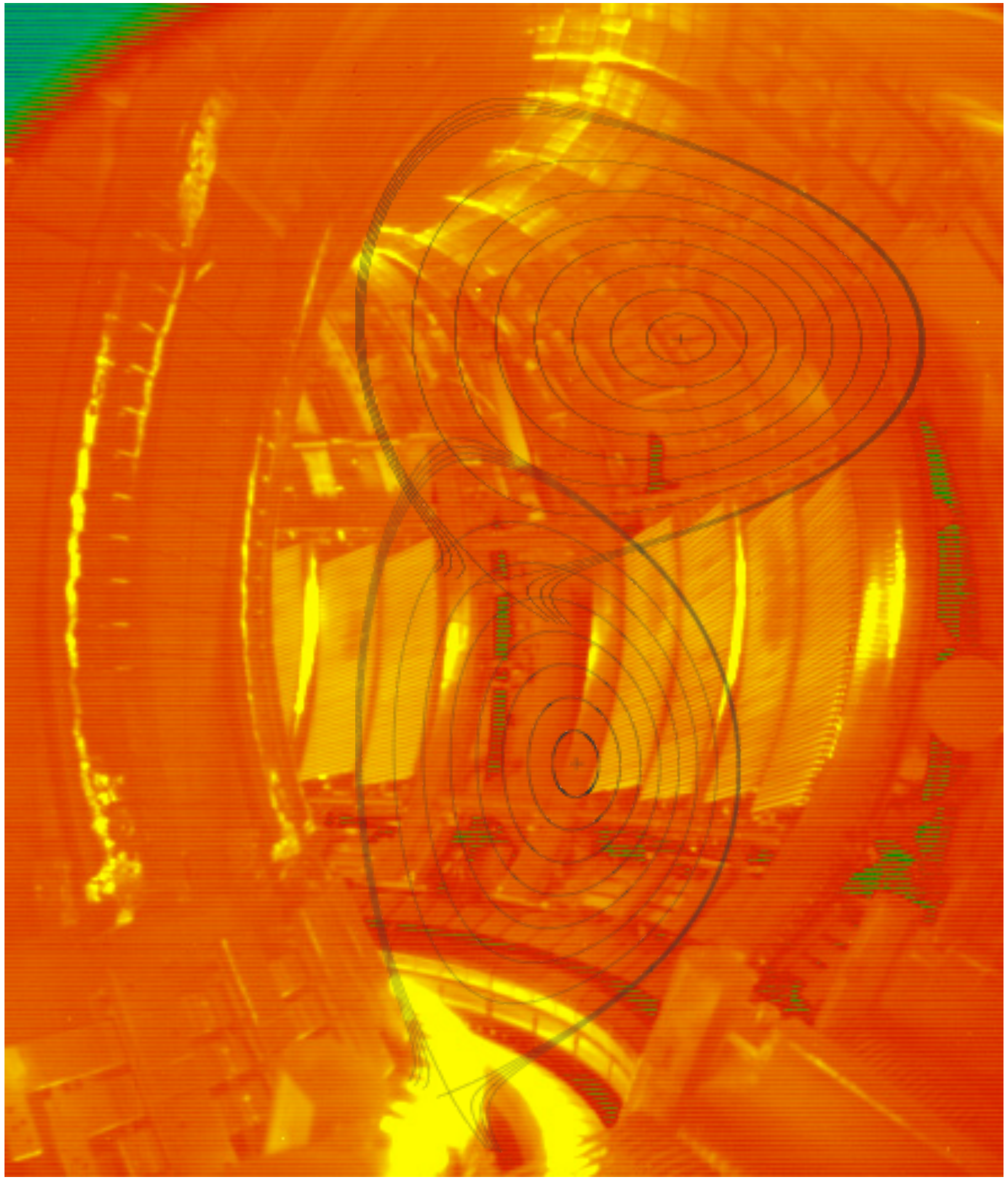

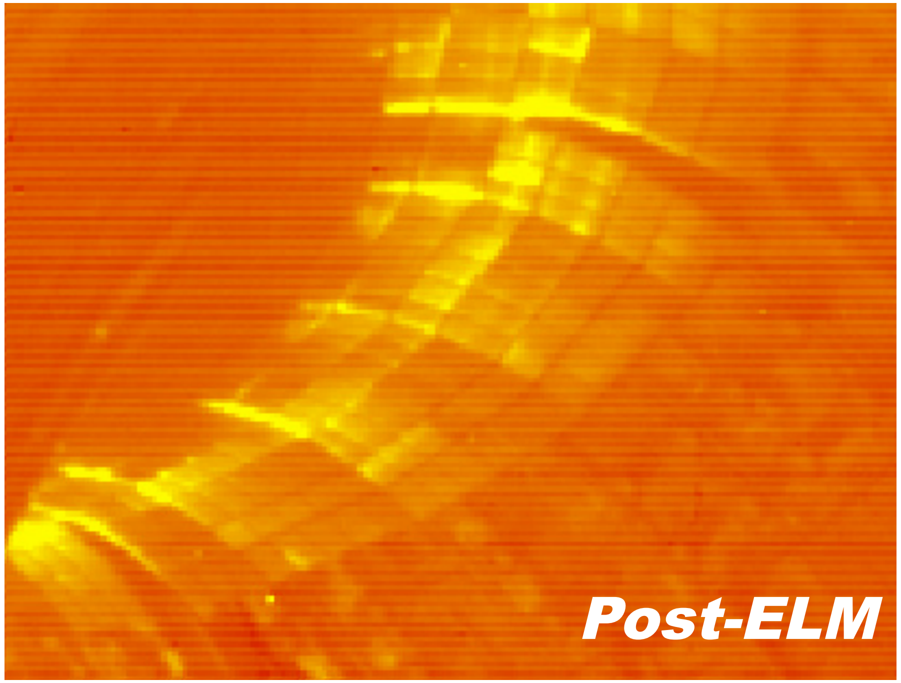

Courtesy of G. Arnoux

- Wide angle IR image during an ELM
- Combined with EFIT reconstruction
- Helical stripes on upper dump plate
- Closely aligned with local magnetic field – smaller pitch angle than at omp

IR imprint on upper dump plate

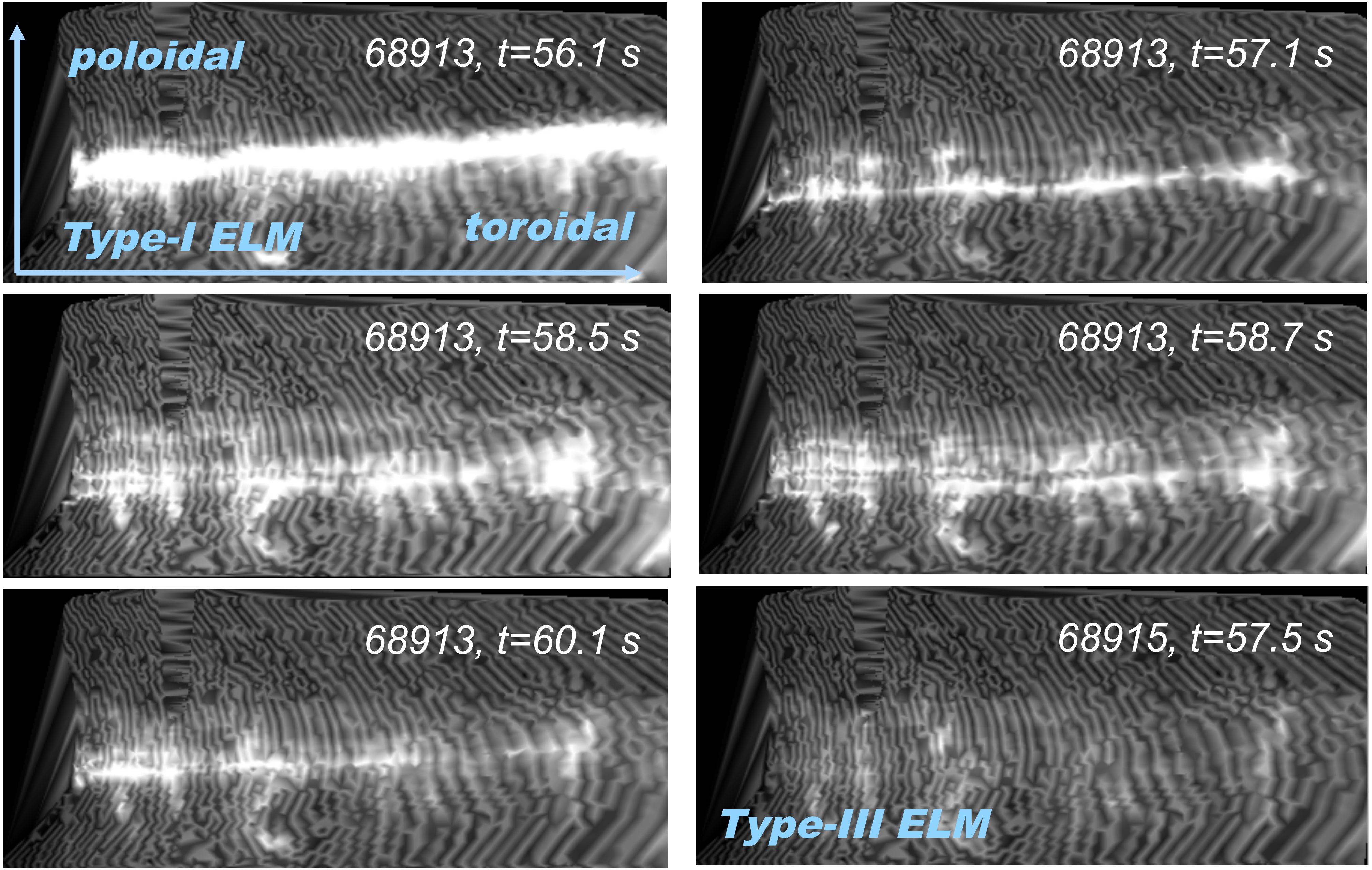

Results of IR imprint analysis

- Quasi-toroidal mode number, $n_w \sim 2\pi/\Delta\phi$, inferred as:
  - $n_w \sim 30 - 40$ at the outer limiter ($\Delta r = r - r_{sep} \sim 5$ cm), with little dependence on ELM size, $\Delta W_{ELM}/W_{ped}$
  - $n_w \sim 20 - 60$ at the upped dump plate ($\Delta r \sim 2$ cm), with a roughly inverse linear dependence on ELM size, $n_w \sim 6/(\Delta W_{ELM}/W_{ped})$.
- The relative width, $\delta\theta/\Delta\theta$, is roughly independent of ELM size
  - Mean $\delta\theta/\Delta\theta \sim 0.6 \pm 0.2$ at the upper dump plates
  - Mean $\delta\theta/\Delta\theta \sim 0.8 \pm 0.2$ at the outboard limiters
- The observed range of quasi-toroidal mode numbers is somewhat higher than predicted by the Peeling-Ballooning model of the ELM instability:
  - in which $n_0 \sim 10$ at low density to $n_0 \sim 30$ at high density
- This suggests a break-up of initial ELM filaments into roughly ~ 2 - 3 smaller fragments in the SOL before hitting the wall
  - Consistent with IR observation at the divertor tiles
  - Consistent with break-up of filaments under interchange drive

ELM energy to outer limiters

- main chamber IR camera too slow to follow single ELMs and filaments
- hence, use energy balance for a single outboard poloidal limiter during H-mode phase

Assumptions:

- only ELMs can deposit energy on limiters
- no energy to upper dump plates
- no energy deposited in compound phases
- same energy on 16 limiters

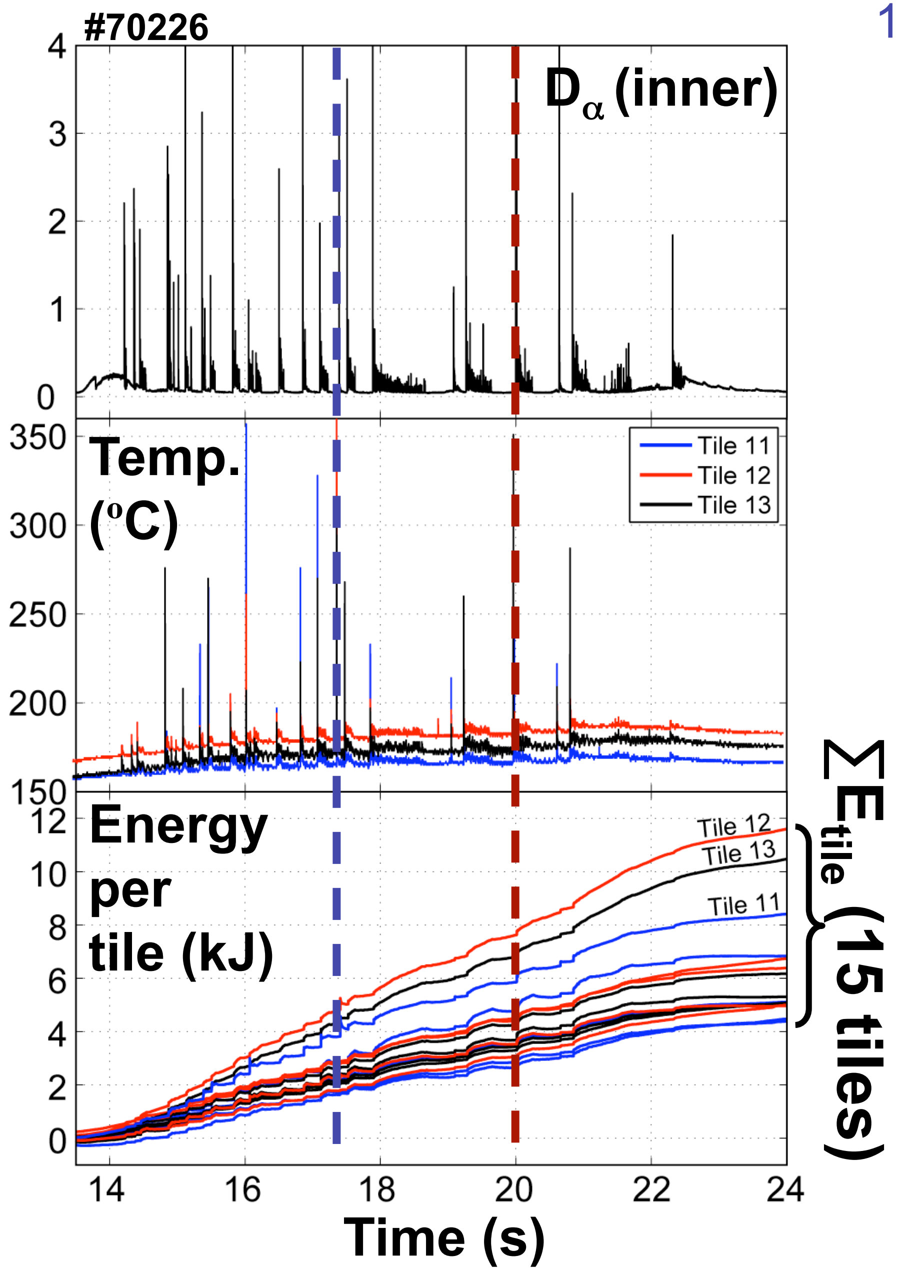

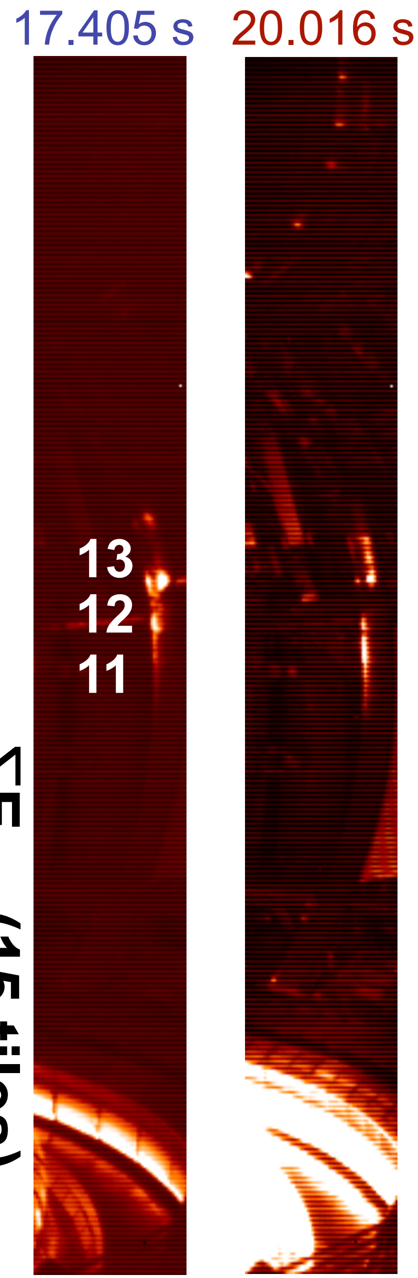

R.A.Pitts el al, PSI-2008; submitted to JNM

Fraction of energy to limiters

I_p = 3.0 MA, B_φ = 3.0 T, gas scan. Separatrix-midplane outer wall gap fixed at ~5.0 cm.
ΔW_{ELM} estimated for first ELM peak only

Pulse No.	Γ_{gas} (10^{22}e⁻/s)	No. ELMs	$\sum \Delta W_{ELM}$ (MJ)	$\sum E_{LIM}$ (MJ)	$\langle \Delta W_{ELM} \rangle$ (kJ)	$\frac{\sum E_{LIM}}{\sum \Delta W_{ELM}}$ (%)
70221	1.47	133	29.7	1.49	**224**	**5.3**
70222	1.24	87	23.9	1.02	**275**	**4.3**
70223	0.89	50	18.0	0.85	**360**	**4.7**
70224	0.38	16	8.34	0.71	**521**	**8.8**
70225	0	30	14.9	1.37	**497**	**9.2**
70226	0	24	12.7	1.49	**528**	**11.8**

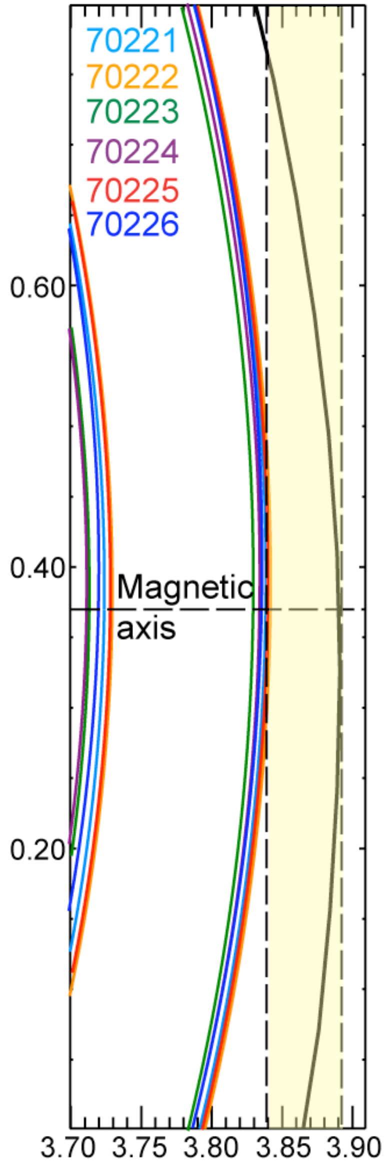

- For fixed wall gap, larger ELMs deposit (on average) more energy on to the outer limiters
- How does wall energy fraction compare with theory?

R.A.Pitts el al, PSI-2008; submitted to JNM

Simulations of filament motion

density, pressure   vorticity

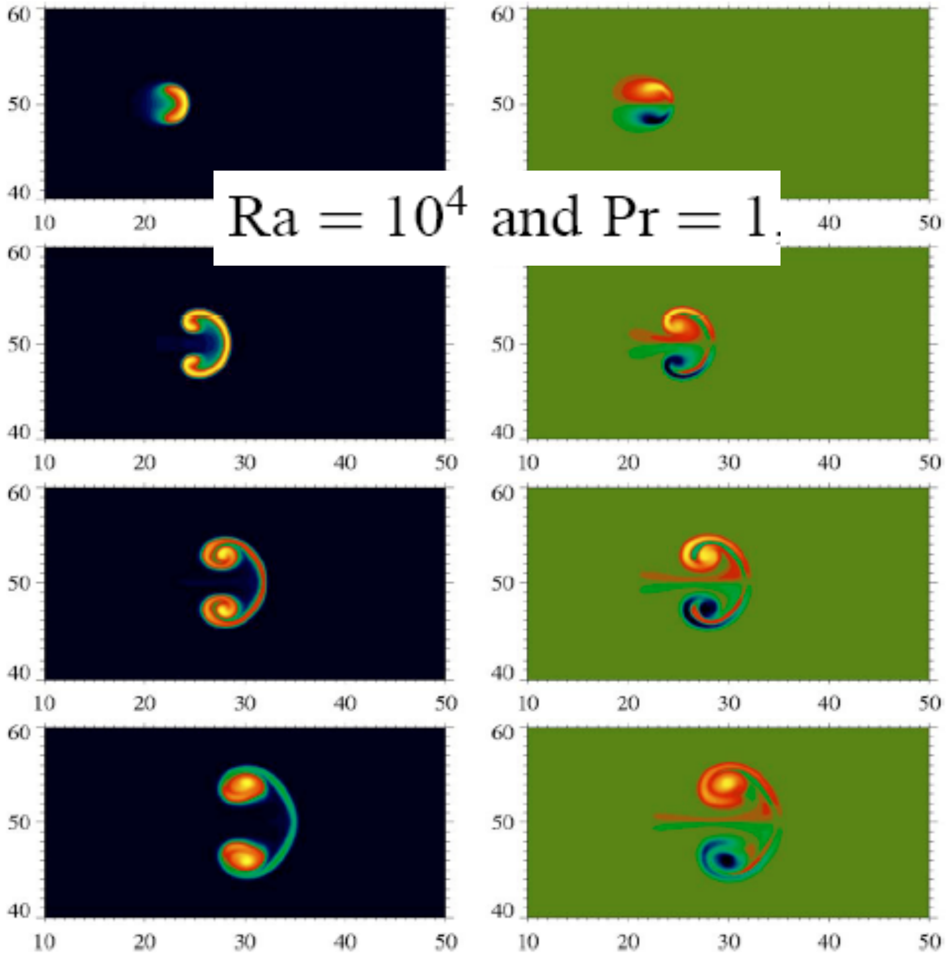

Ra $= 10^4$ and Pr $= 1$.

Radial distance

$$M_{\perp}^{\text{int}} = \frac{V_{\perp}^{\text{int}}}{c_S} = \left(\frac{2l}{R} \frac{\Delta p}{p_0} \right)^{1/2}$$

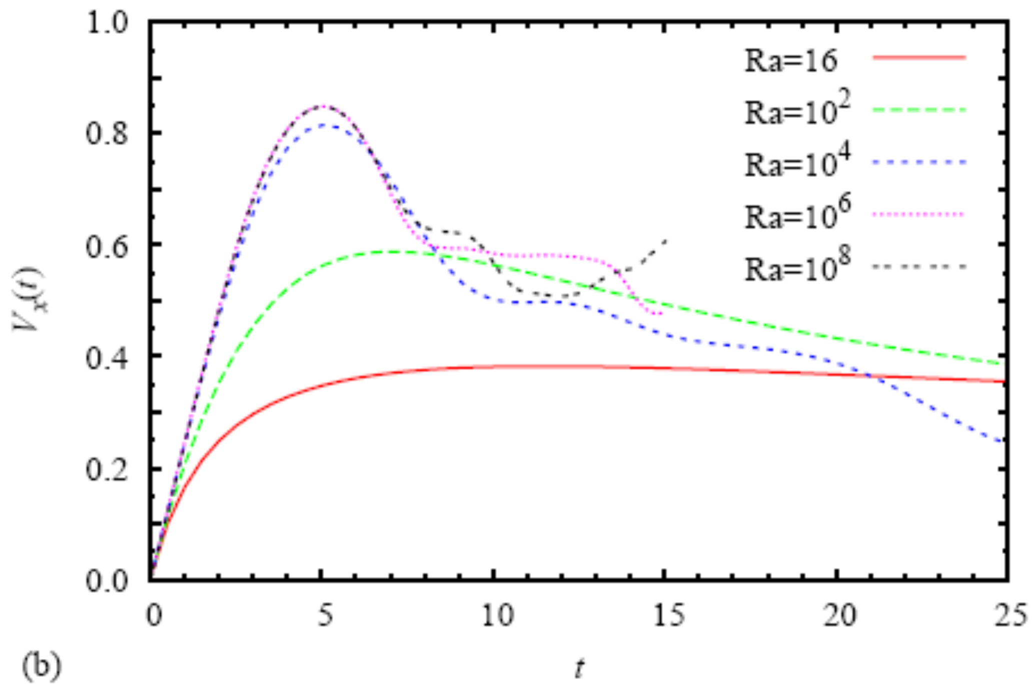

O.E.Garcia, N.H. Bian and W.Fundamenski., Phys. Plasmas (2006)

Expression for ELM energy to wall on JET

Interchange driven amplitude scaling with convective ion losses

$$\lambda_W \approx V_\perp \tau_\| \approx \frac{V_\perp L_\|}{C_s} \qquad \Rightarrow \qquad \frac{\lambda_W^{ELM}}{L_\|} \approx \frac{V_\perp^{ELM}}{C_s} \propto \left(\frac{W_{ELM}}{W_{ped}}\right)^{1/2}$$

combined with moderate-ELM ($\Delta W/W = 5\%$, $\Delta W/W_{ped}=12\%$) e-folding length, yields

$$\lambda_W^{ELM,JET}[\mathrm{mm}] \approx 35\left(\frac{W_{ELM}/W}{0.05}\right)^{1/2} \approx 35\left(\frac{W_{ELM}/W_{ped}}{0.12}\right)^{1/2}$$

so that **fraction of ELM energy to wall** can be approximated as

$$\frac{W_{wall}^{ELM}}{W_0^{ELM}} \approx \exp\left(-\frac{\frac{1}{2}\Delta_{ped}+\Delta_{SOL}}{\lambda_W^{ELM}}\right) \approx \exp\left(-\frac{const}{\sqrt{W_{ELM}/W}}\right)$$

where Δ_{ped} is the **pedestal width** and Δ_{SOL} is the **separatrix-wall gap**.

eg. when $\Delta W/W$ reduced by a third, then (W_{wall}/W_0) = 10 % for 3 cm gap, see below.

W.Fundamenski et al, PSI 2006; subm. to J.Nucl.Mater

Small ELMs = less energy to the wall

$$\frac{\lambda_W^{ELM}}{L_{\parallel}} \approx \frac{V_{\perp}^{ELM}}{C_s} \propto \left(\frac{W_{ELM}}{W_{ped}}\right)^{1/2}$$

$$\lambda_W^{ELM,ITER}[\mathrm{mm}] \approx 30\left(\frac{W_{ELM}/W}{0.05}\right)^{1/2} \approx 30\left(\frac{W_{ELM}/W_{ped}}{0.12}\right)^{1/2}$$

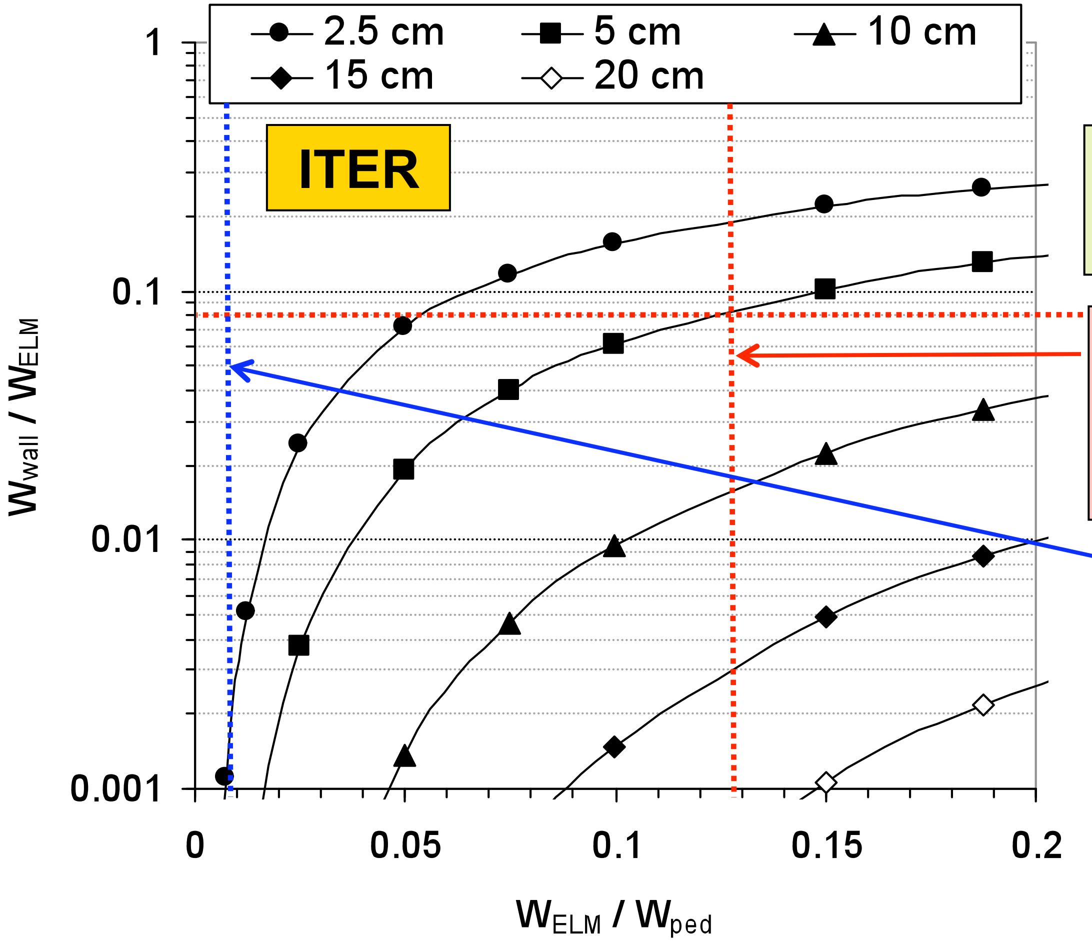

Smaller ELM filaments travel slower, consistent with interchange dynamics

Predicted power width scaling on ELM filament energy in the far-SOL

For a natural (unmitigated) ELM on ITER, expect ~ 10 % of its energy to main wall PFCs

For a small (mitigated) ELM expect only a tiny fraction (<<1%) of ELM energy to main wall PFCs

Maximum ELM size on ITER determined by divertor PFCs !!!

Pedestal n_e & T_e profiles

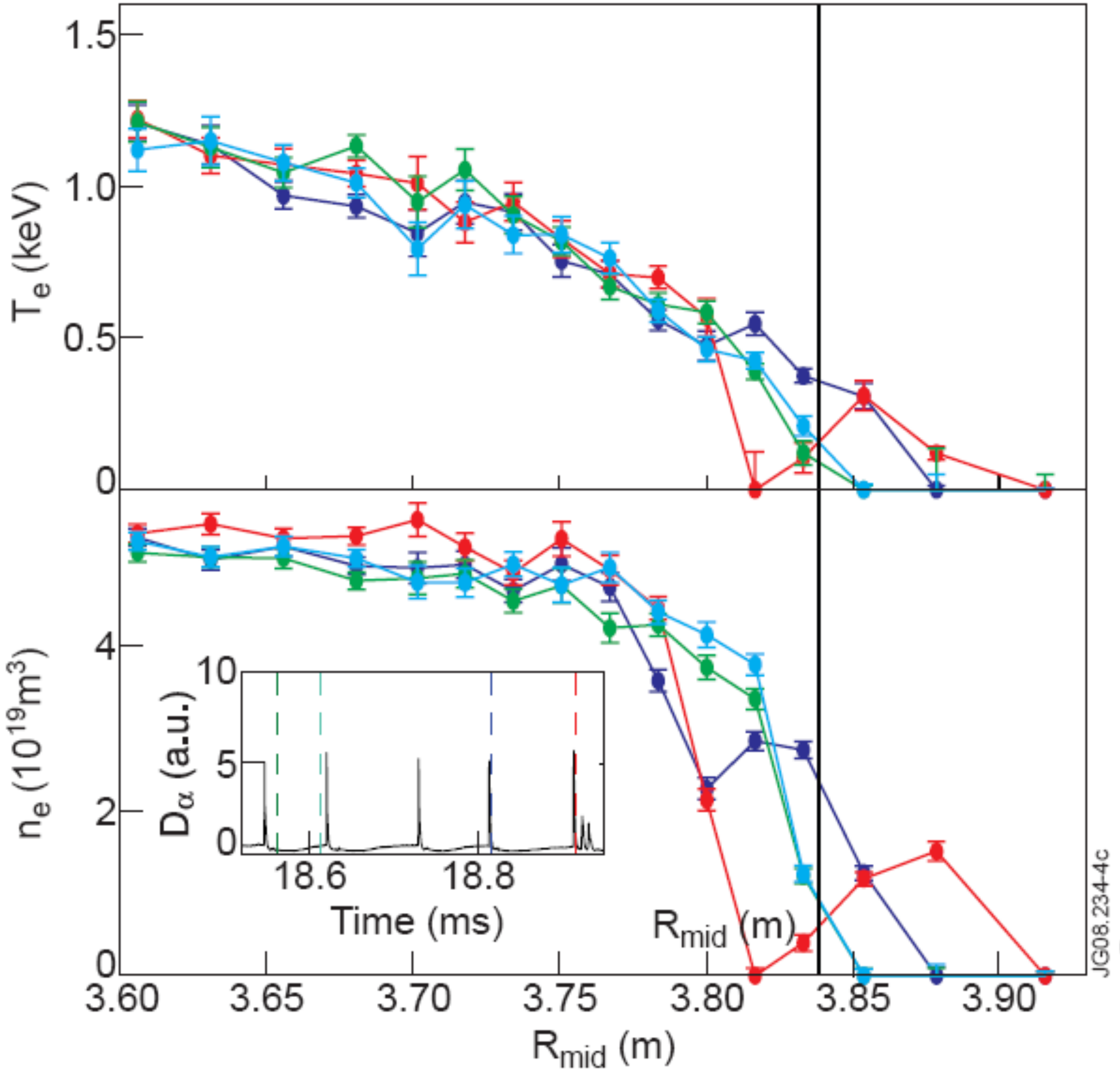

- Assume ELM filament begins to experience parallel losses from the mid-pedestal values of n_e and T_e
- Apply the parallel loss model of ELM filament evolution (W. Fundamenski, R. A. Pitts, PPCF **48** (2006) 109)
- Pre-ELM profiles and ELM filament evolution measured using Thomson scattering

M. Beurskens el al, this conference

Parallel loss model of ELM exhaust

Consider the radial motion of the pedestal plasma subject to parallel losses.

Low ν^*: plasma cools faster than it dilutes: mainly conductive losses

Describe as an 'effective' plasma filament, moving with some average radial velocity.

High ν^*: cooling and rarefaction comparable: significant convective losses

Evolve the density and temperature of the filament using a fluid model

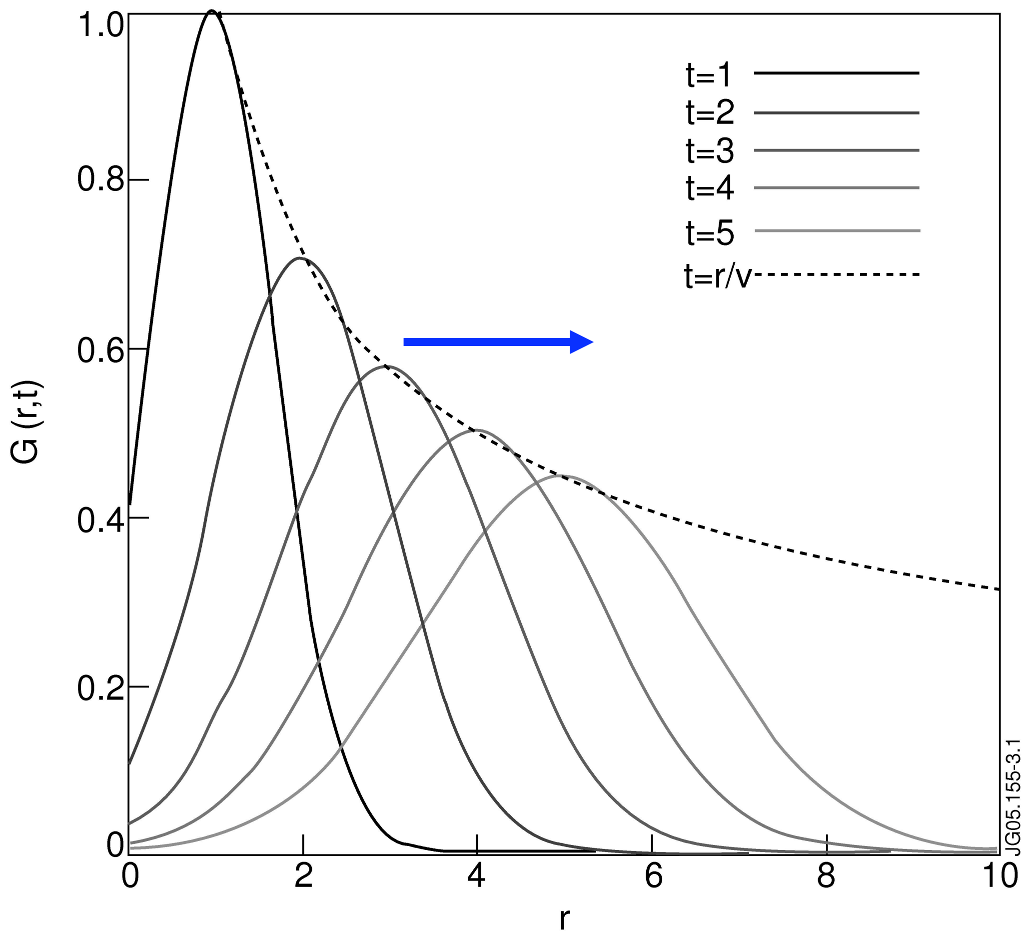

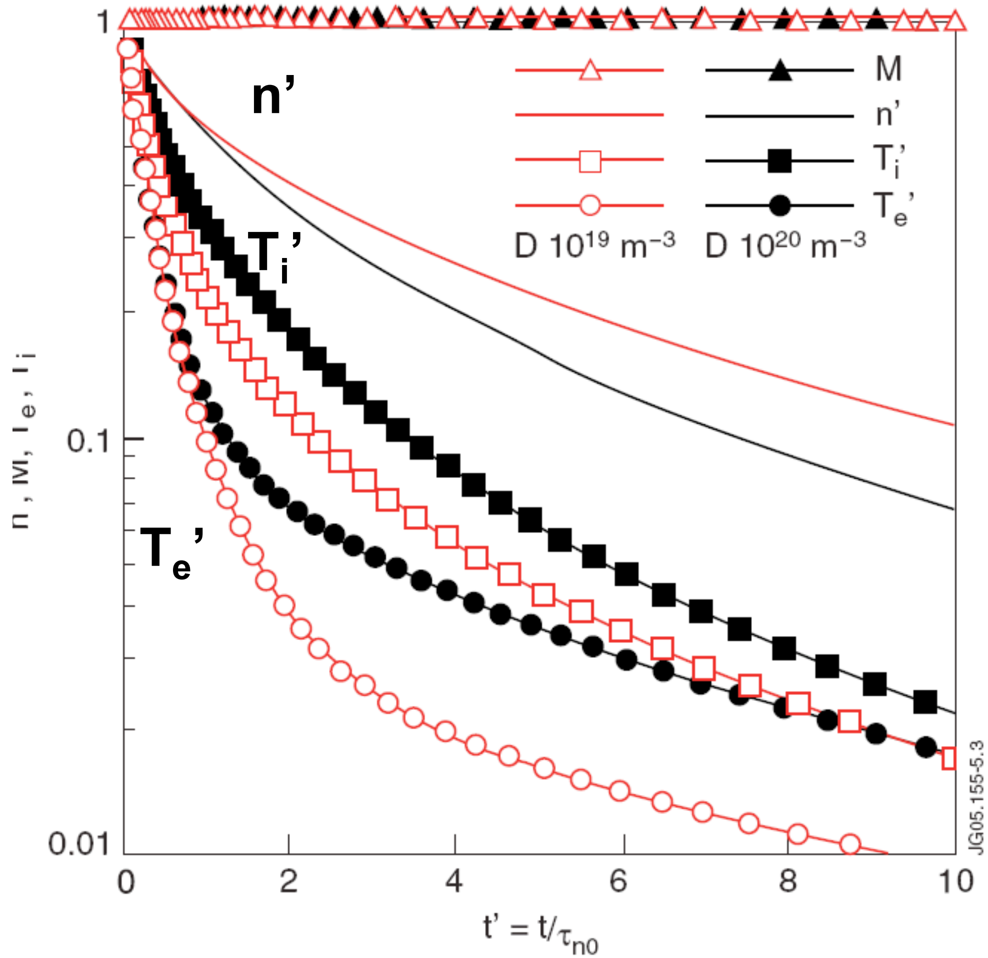

Pedestal changes during an ELM

Pedestal plasma eroded during the ELM:

Density drop = ‘convective’ losses

Temperature drop = ‘conductive’ losses

Small ELMs are mostly convective

ELM size decreases with collisionality

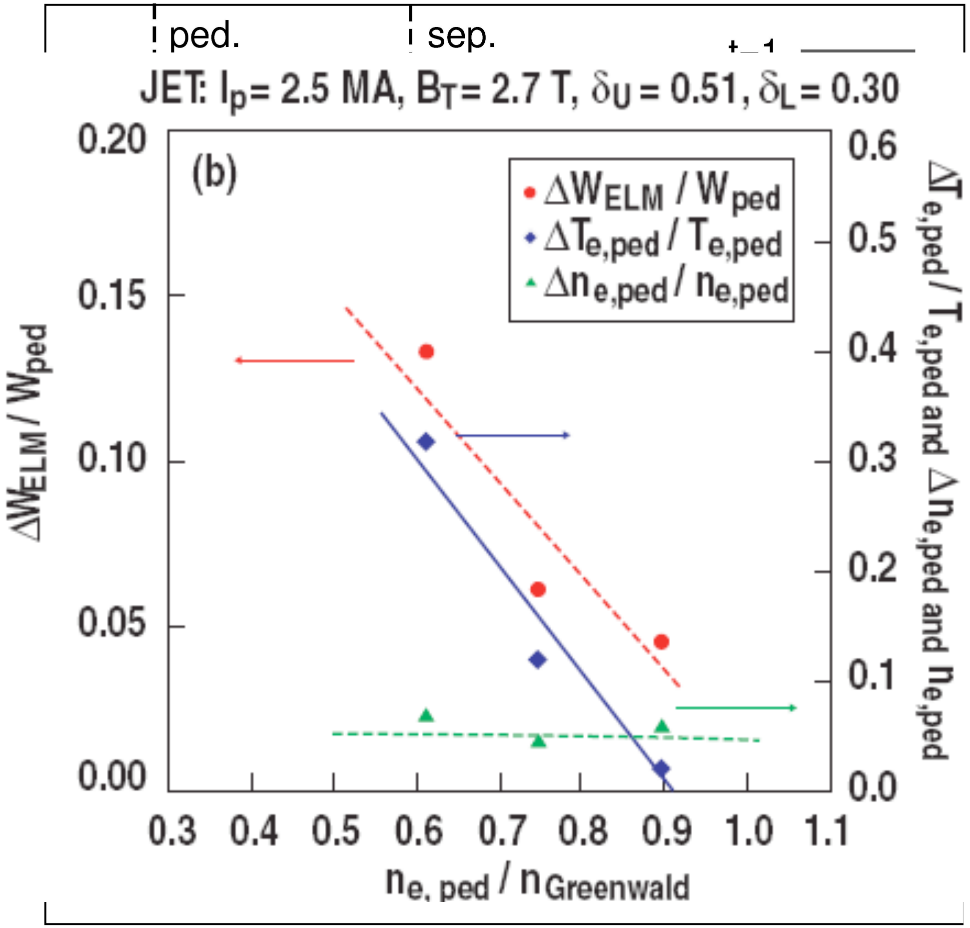

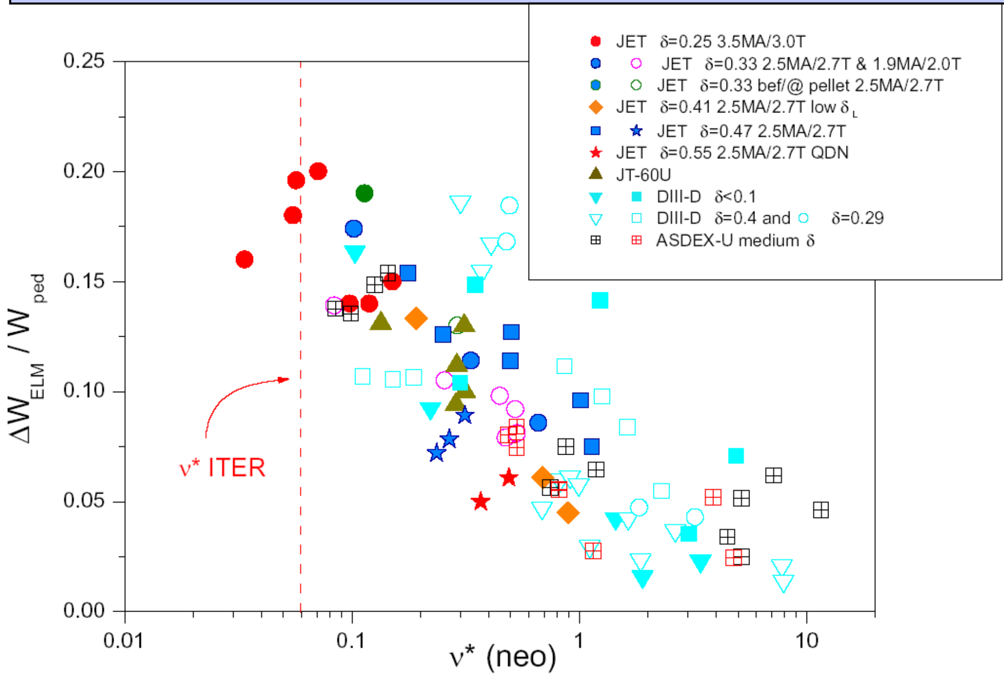

Comparison with model

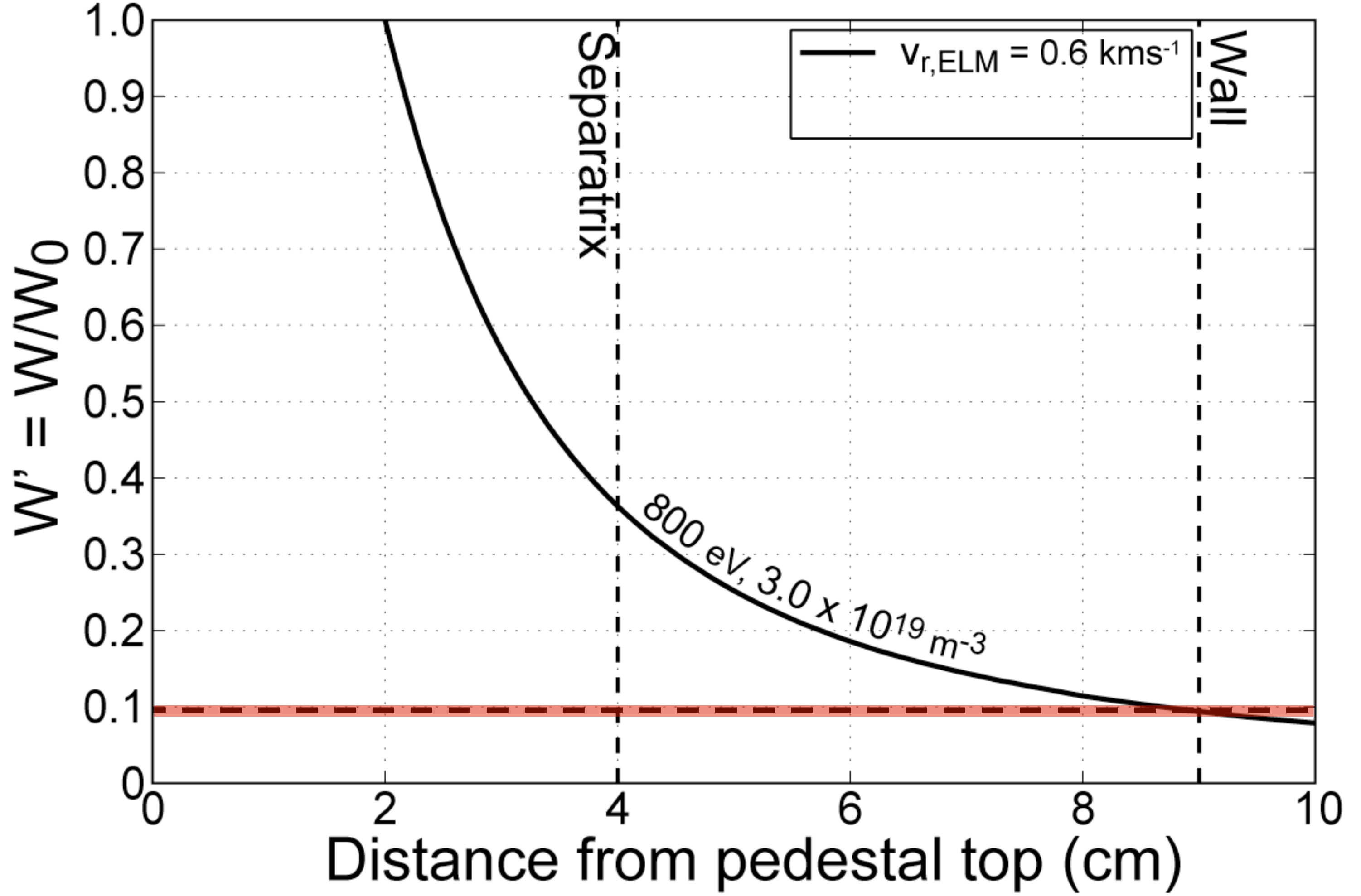

Mid-pedestal:
$T_{e,0} = T_{i,0} \sim 800$ eV
$n_{e,0} \sim 3.0 \times 10^{19}$ m^{-3}
$\Delta_{ped} \sim 4$ cm
$v_{ELM} = 600$ ms^{-1} → from previous JET studies

W' = 0.094 (model)
W' = 0.088 (experiment)

$$W_0 = \frac{3}{2} n_0 (T_{e,0} + T_{i,0})$$

Good agreement given the model approximations and measurement errors !

R.A.Pitts el al, PSI-2008; submitted to JNM

Comparison with model

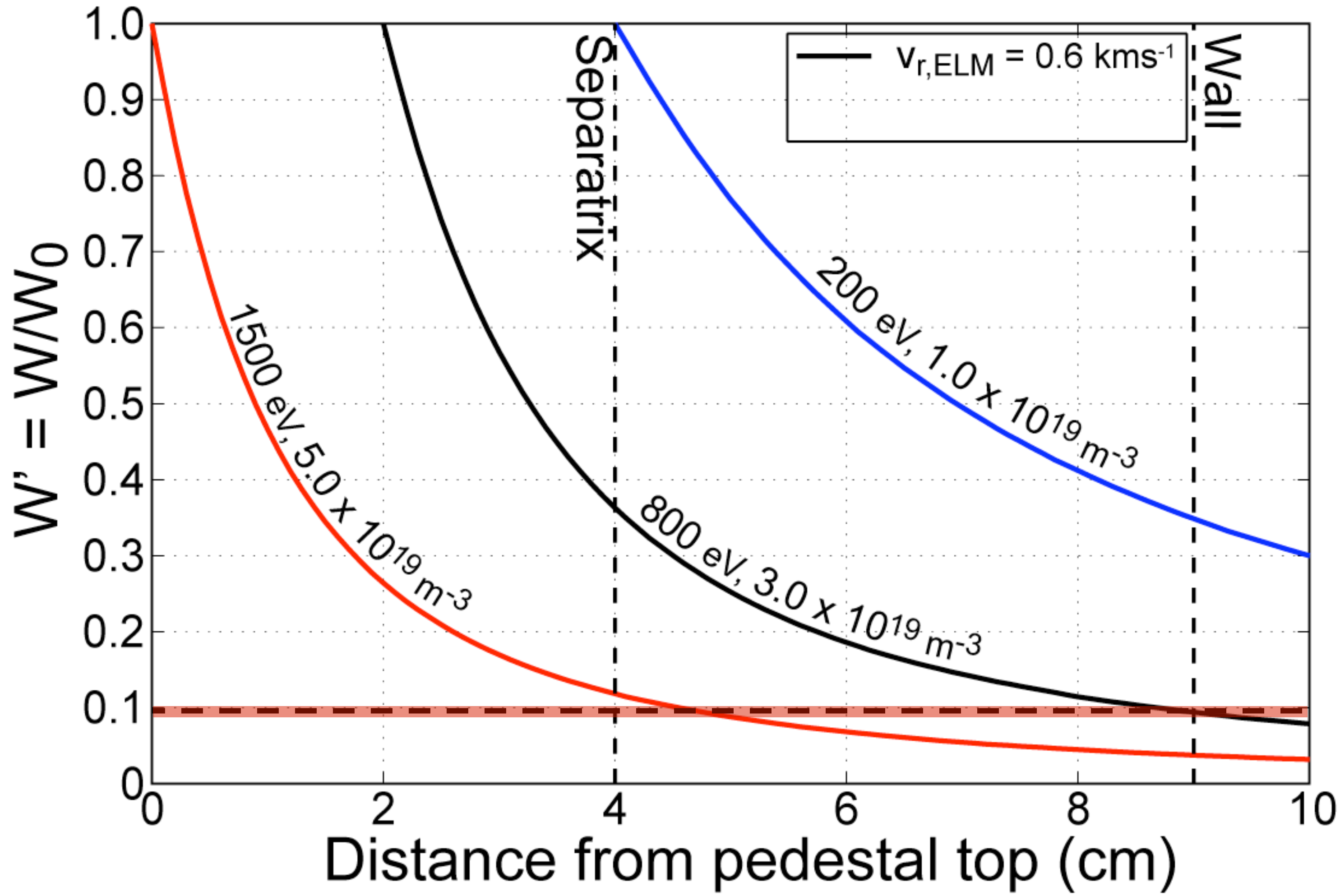

Pedestal top:
$T_{e,0} = T_{i,0} \sim 1500$ eV
$n_{e,0} \sim 5.0\times10^{19}$ m^{-3}

Separatrix:
$T_{e,0} = T_{i,0} \sim 200$ eV
$n_{e,0} \sim 1.0\times10^{19}$ m^{-3}

v_{ELM} = 600 ms^{-1}

0.394

0.094

0.037

R.A.Pitts el al, PSI-2008; submitted to JNM

Comparison with model

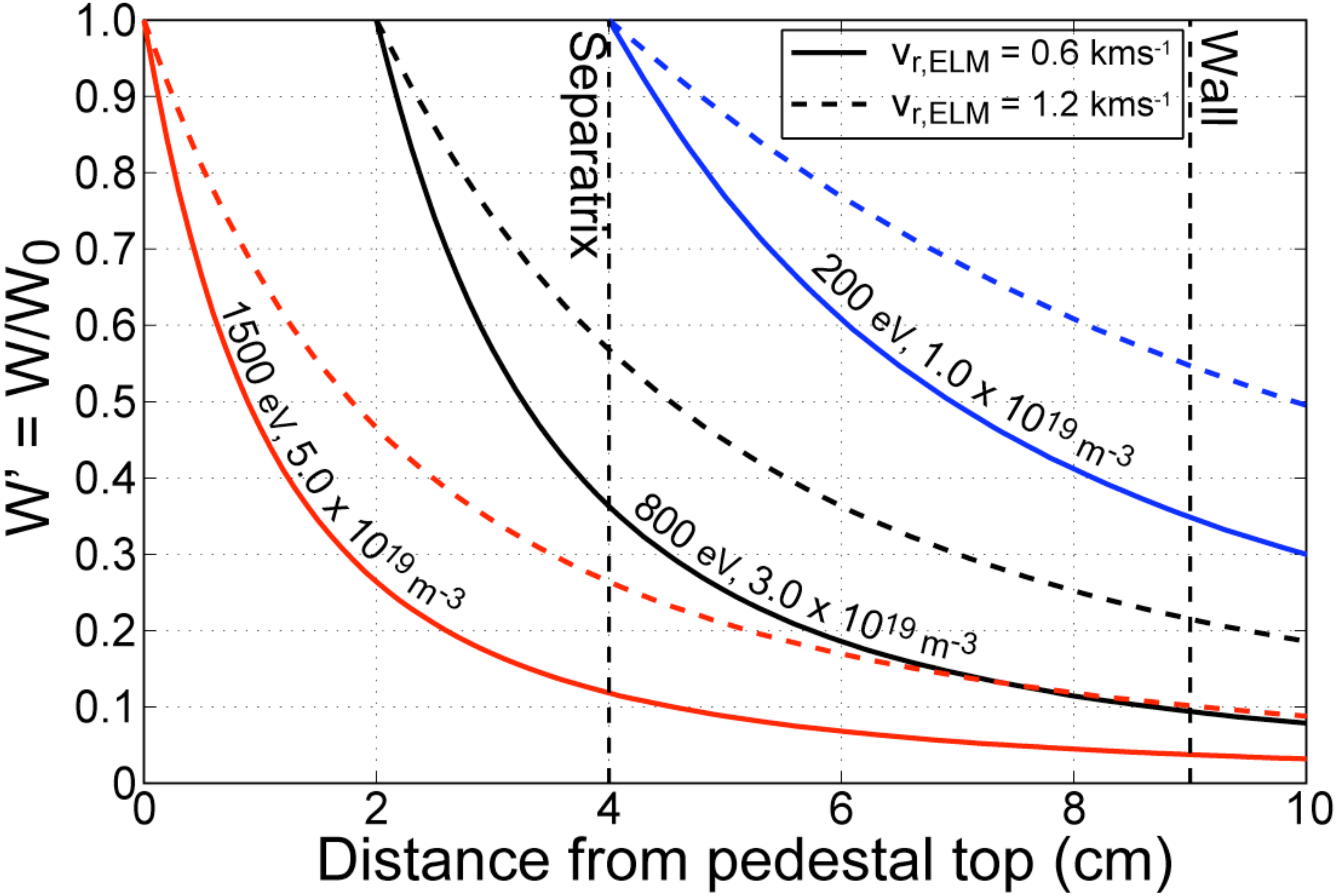

Pedestal top
Mid-pedestal
Separatrix

v_{ELM} = 600 ms^{-1}
v_{ELM} = 1200 ms^{-1}

Filaments starting at:

- the pedestal top with twice higher v_{ELM} deposit the same energy at the limiter
- the separatrix must travel much slower ~180 m/s to match the observation
- the separatrix with pedestal quantities, could explain the data

R.A.Pitts el al, PSI-2008; submitted to JNM

Extrapolation to ITER

- Results indicate that larger ELMs travel faster
- Consistent with mainly interchange driven filament motion

$$M_\perp^{int} = \frac{V_\perp^{int}}{c_S} = \left(\frac{2l}{R}\frac{\Delta p}{p_0}\right)^{1/2} \sim \left(\frac{\Delta W_{ELM}}{W_{ped}}\right)^{1/2}$$

- use the parallel loss model with earlier measurements (v_{ELM} = 600 m/s for $\Delta W_{ELM}/W_{ped}$ ~ 0.12)

$$V_{ELM}^{ITER}[m/s] \sim 600\left(\frac{T_{ped}^{ITER}}{T_{ped}^{JET}}\frac{\Delta W_{ELM}^{ITER}}{W_{ped}^{ITER}}\frac{1}{0.12}\right)^{1/2}$$

JET experiments ⇒ exponent ~ 0.4

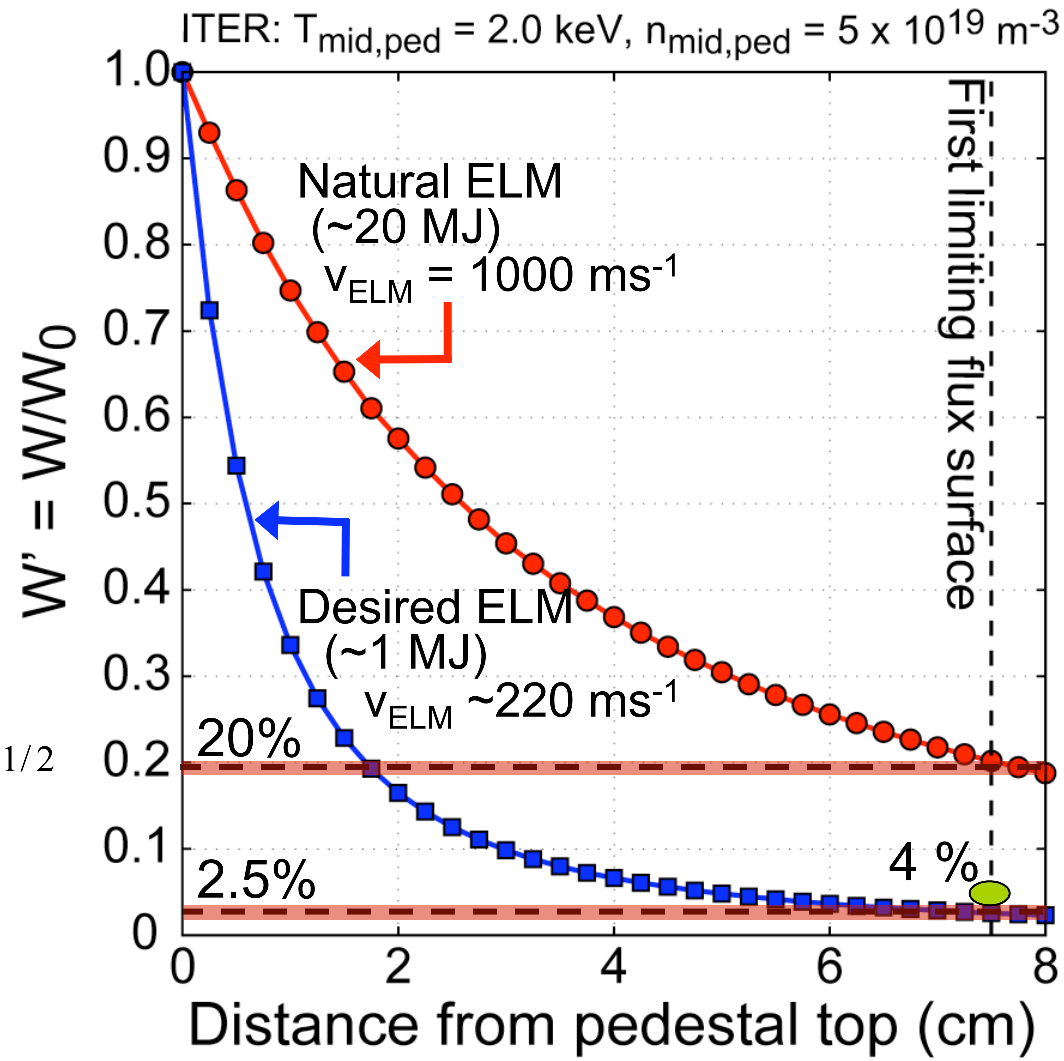

Hence, mitigated (~1 MJ) ELMs on ITER deliver a small fraction of their energy to wall

Ion impact energies on JET and ITER

Predicted peak ELM filament quantities on JET and ITER (moderate Type-I ELMs)

- JET: $T_{i,max}(r_{lim}) \sim 185$ eV (ion impact energy ~ 0.6 keV) at 4 cm
- ITER: $T_{i,max}(r_{lim}) \sim 350$ eV (ion impact energy > 1 keV) at 5 cm; ~ 100 eV at 15 cm
- Lower bound estimates for moderate ($\Delta W/W \sim 5$ %) Type-I ELMs

	JET	***ITER***
n_{max} *(m^{-3})*	*8.25×10^{18}*	*1.2×10^{19}*
$T_{i,max}$ *(eV)*	*185*	*350*
$T_{e,max}$ *(eV)*	*74*	*140*
$\lambda_{n,max}$ *(mm)*	*47*	*54.5*
$\lambda_{Ti,max}$ *(mm)*	*41*	*42.5*
$\lambda_{Te,max}$ *(mm)*	*25*	*27.5*

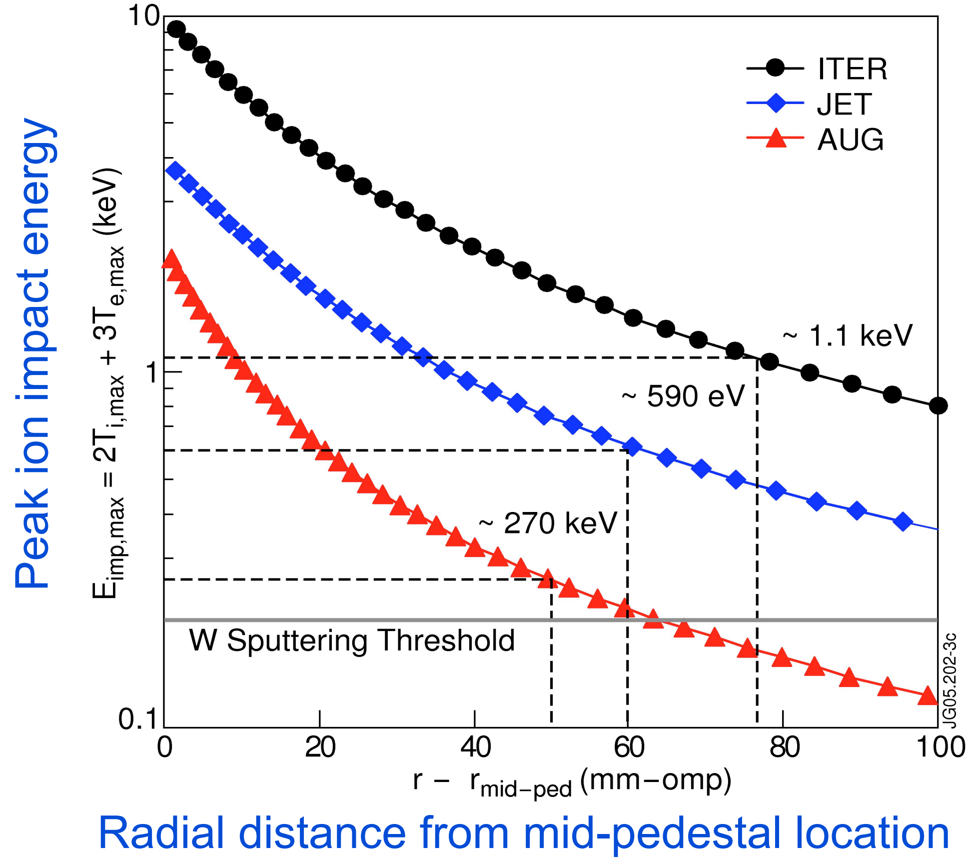

*W.Fundamenski et al., Plasma Phys. Control..Fusion, **48** (2006) 109*

In-out energy asymmetries

Steady-state power deposited mostly on the outer target (factor of ~ 2.5).

ELM energy deposited mostly on the inner target (factor of ~ 2).

What is the reason for these opposite in-out energy asymmetries?

?

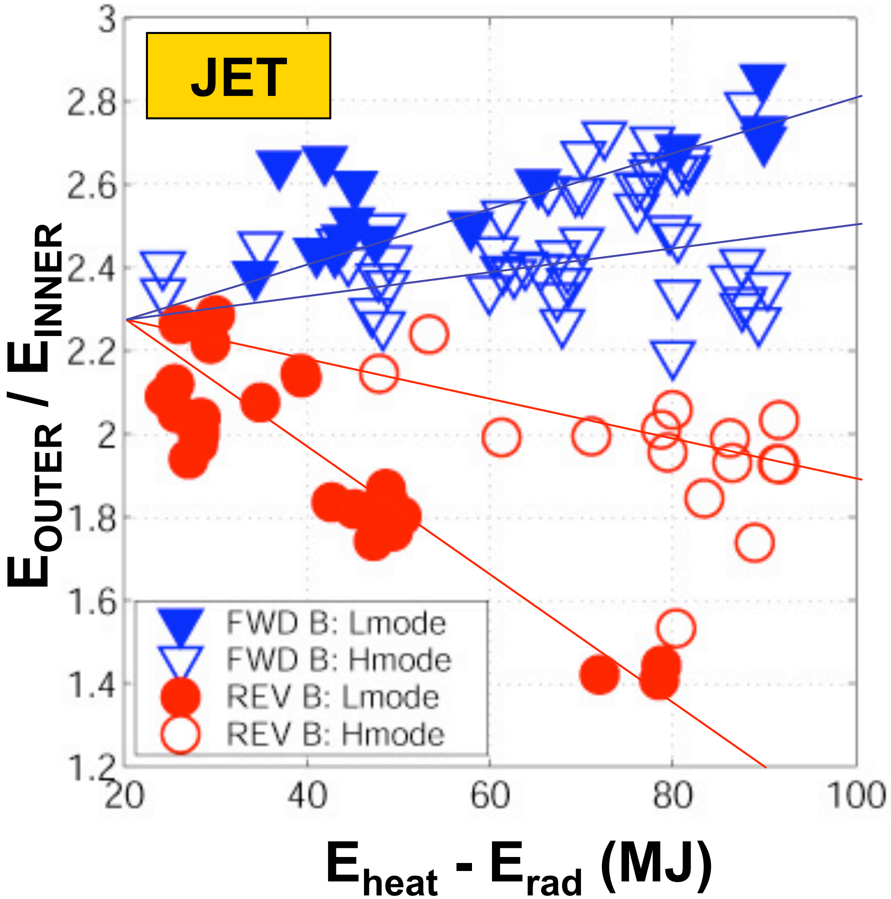

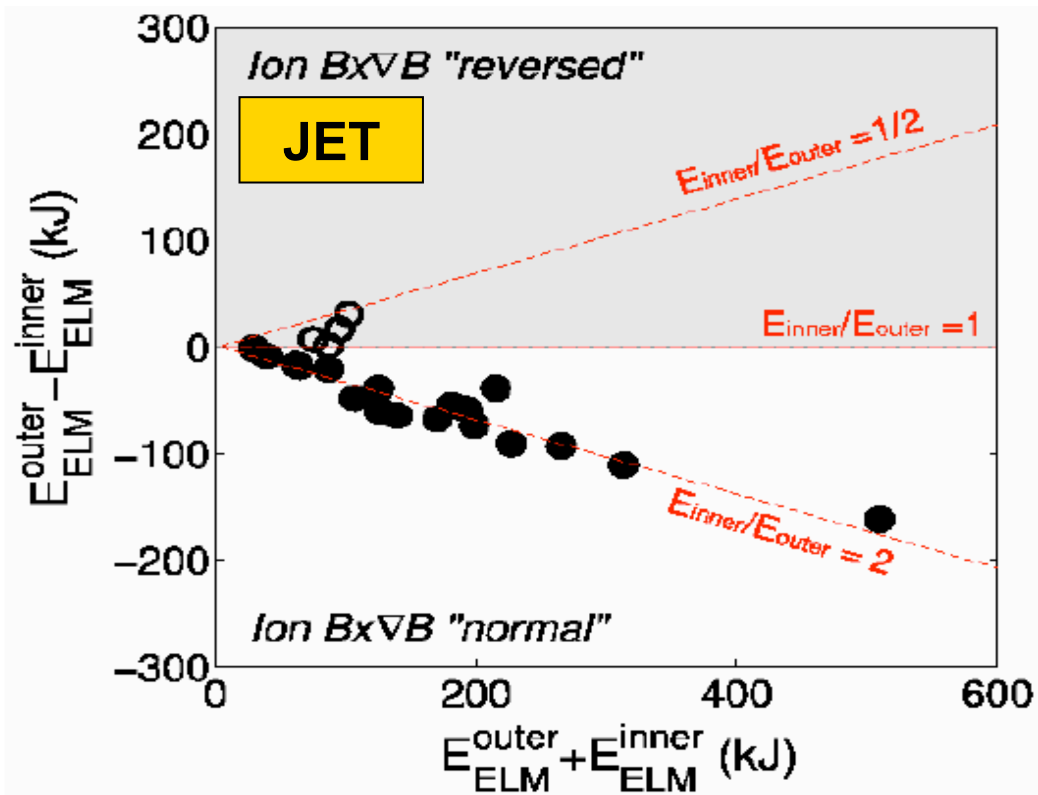

In-out energy asymmetries

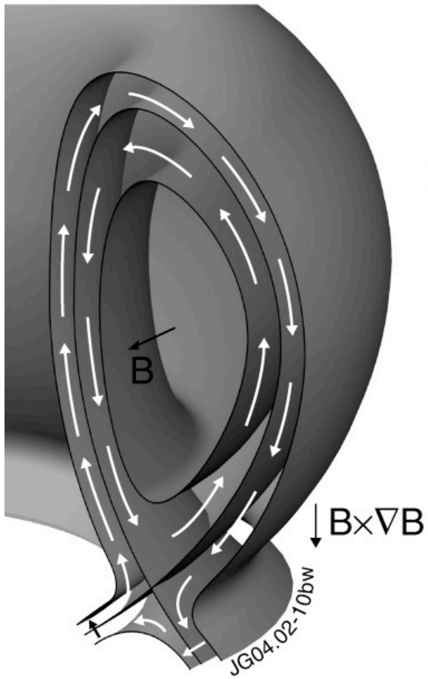

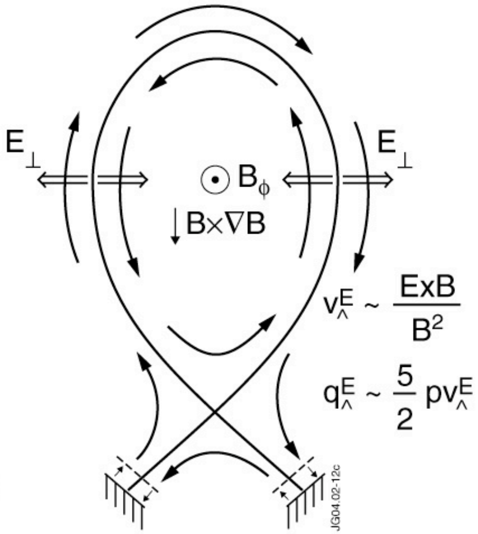

Radial electric field in the edge and SOL regions points in opposite directions !!!

For normal field direction:

Electric drifts in the SOL increase the convective power flow to the outer target

Electric drifts in the edge increase the convective energy flow to the inner target

Parallel motion of ions and electrons convects energy towards both targets

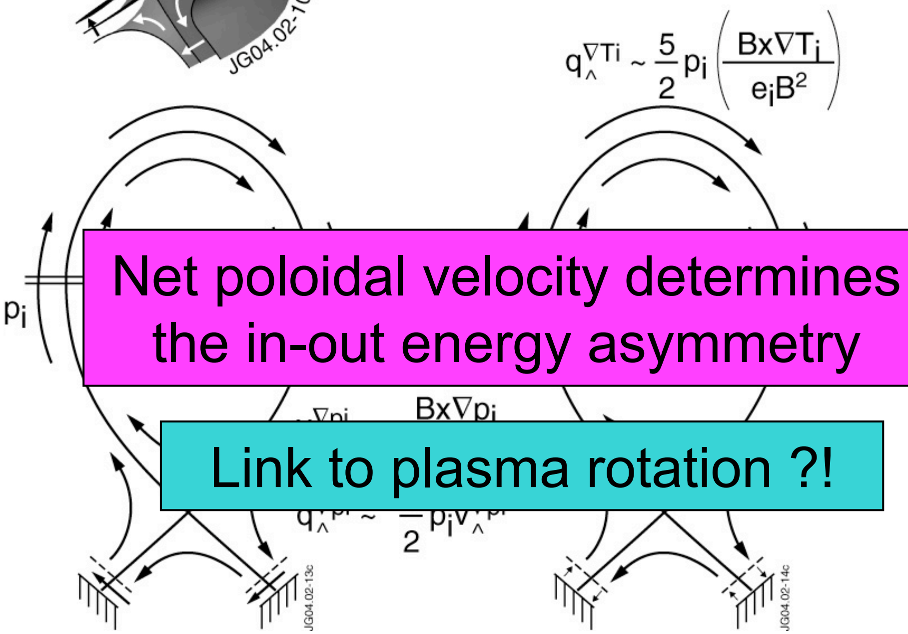

Net poloidal velocity determines the in-out energy asymmetry

Link to plasma rotation ?!

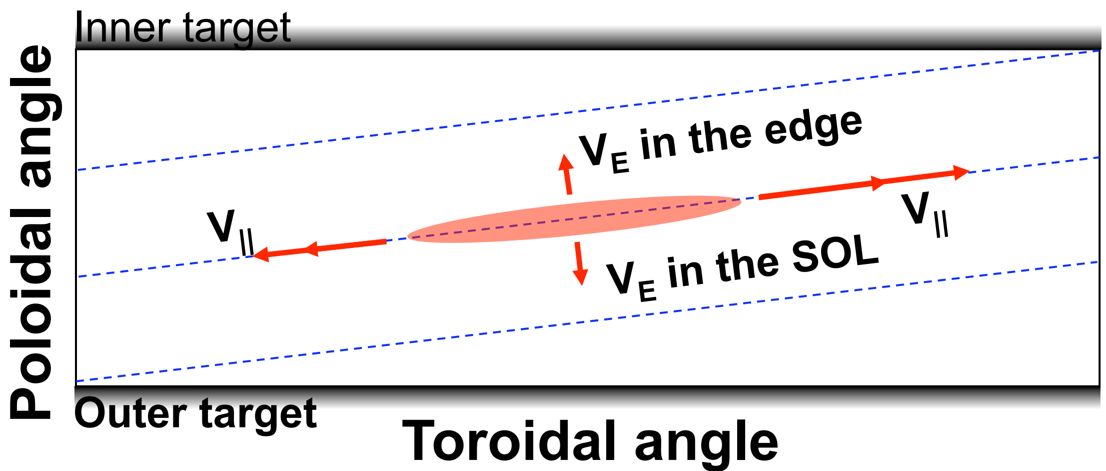

Parallel transport of ELM energy

When M=0, the energy deposition is symmetric; however, M ~ 0.2 towards the inner target can account for the observed deposited energy asymmetry

$$P_\alpha^{ELM}(t)\tau_{\|\alpha} / E_\alpha^{ELM} = \frac{2}{3\sqrt{\pi}}\left[1 + x_\alpha{}^2\right] x_\alpha{}^2 e^{-(x_\alpha - M)^2},$$

$$x_\alpha = \tau_{\|\alpha} / t \qquad \tau_{\|\alpha} = L_{\|\alpha} / v_{Ti} \qquad M = u / v_{Ti}$$

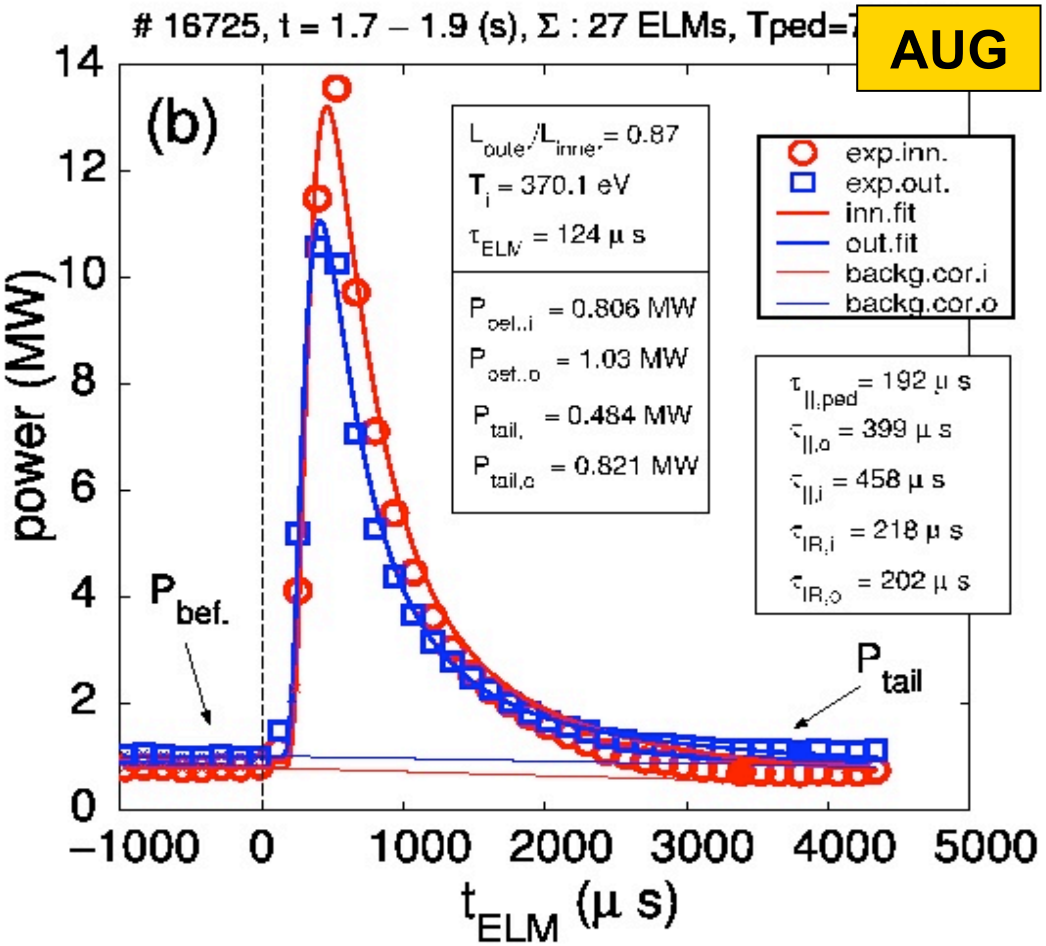

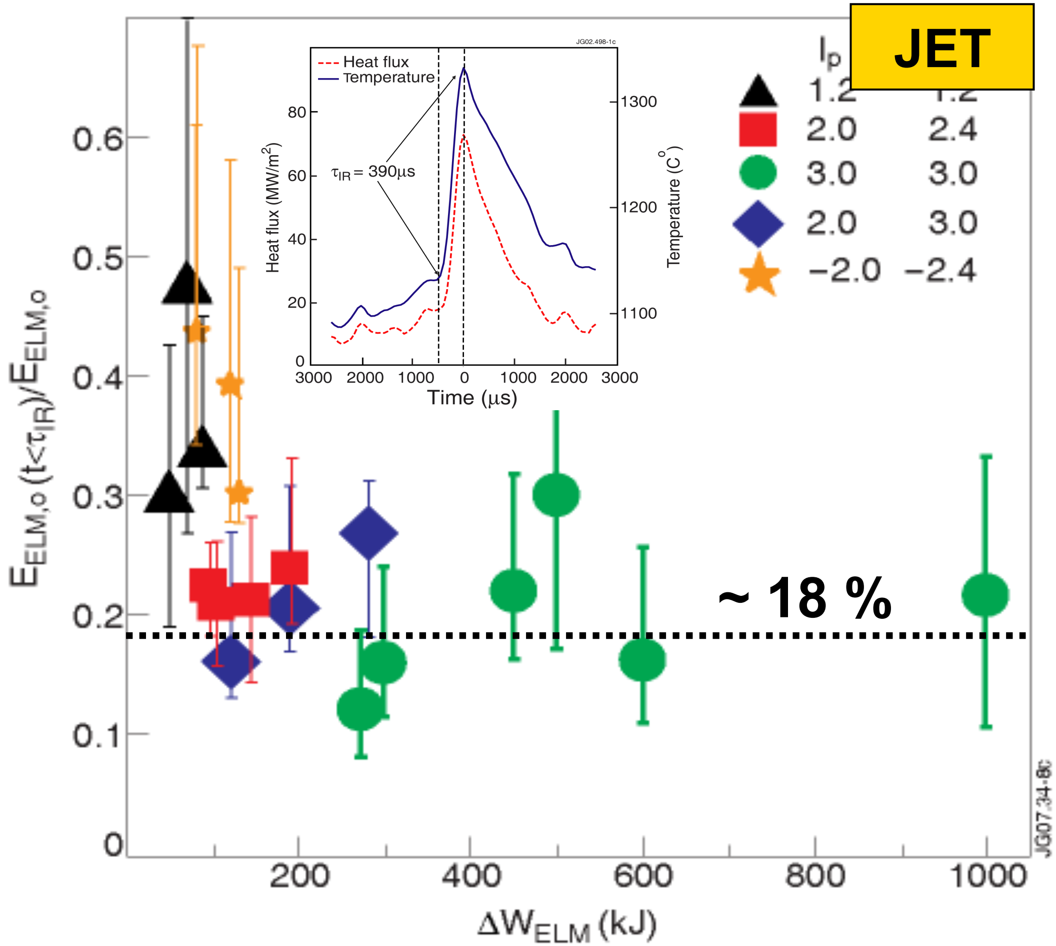

Transient heat load limits in ITER

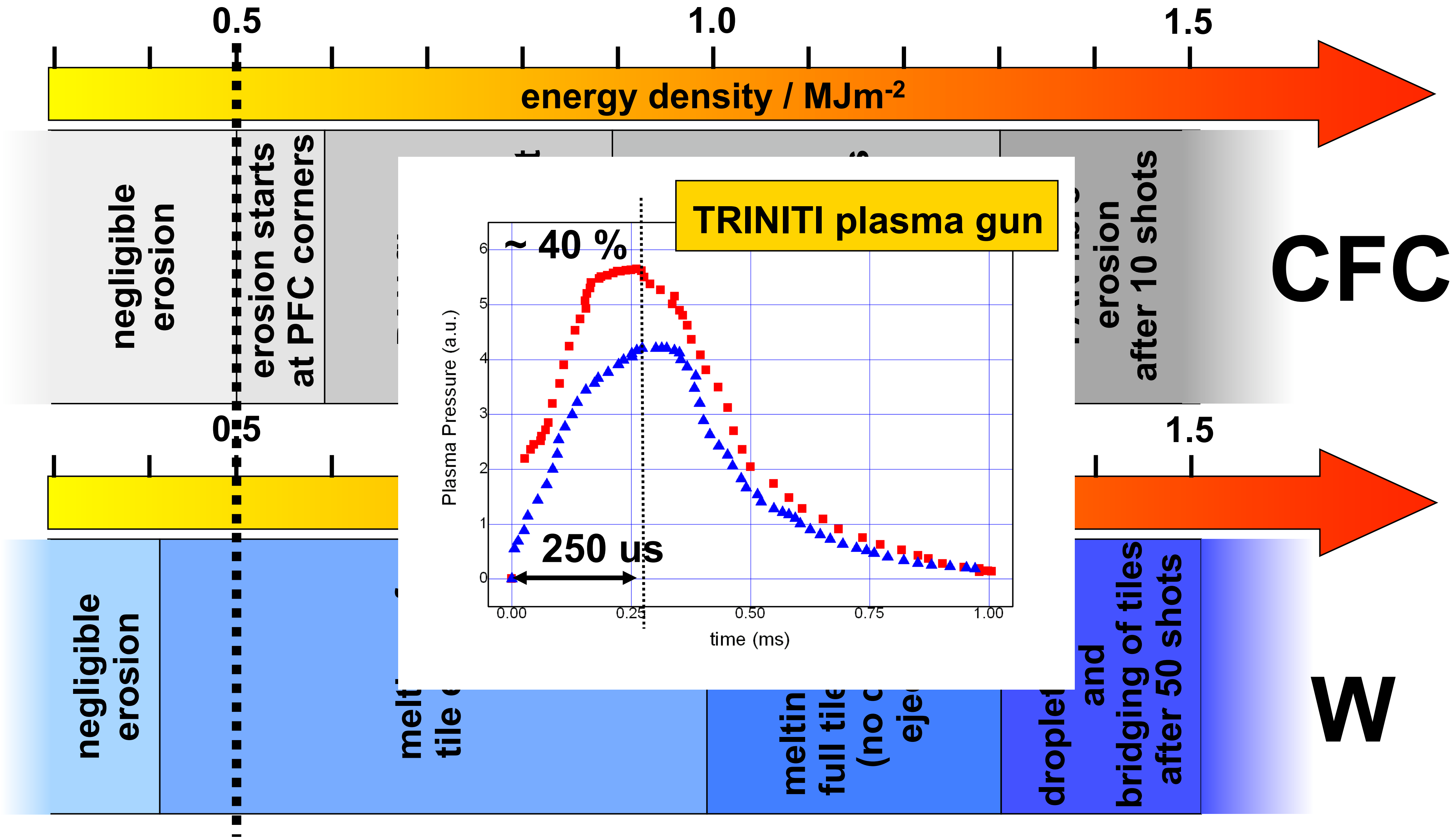

ITER adopted **0.5 MJ/m²** for the maximum allowed ELM energy load in 250 us

Max. permitted ELM size in ITER

Combining the above estimates for the ELM wetted area, in-out energy asymmetry and PFC transient energy limits one finds:

$\Delta W_{ELM} = Q_{ELM} \times S_{in} \times (1 + P_{out}/P_{in}) = 0.5\ MJ/m^2 \times 1.2\ m^2 \times 1.5 \sim 0.9\ MJ$

Assuming W ~ 400 MJ, $W_{ped}/W \sim 1/3$, then $\Delta W_{ELM} / W_{ped} < 1\ \%$

This requires a decrease in the 'natural' ELM size by a factor of ~ 20 !

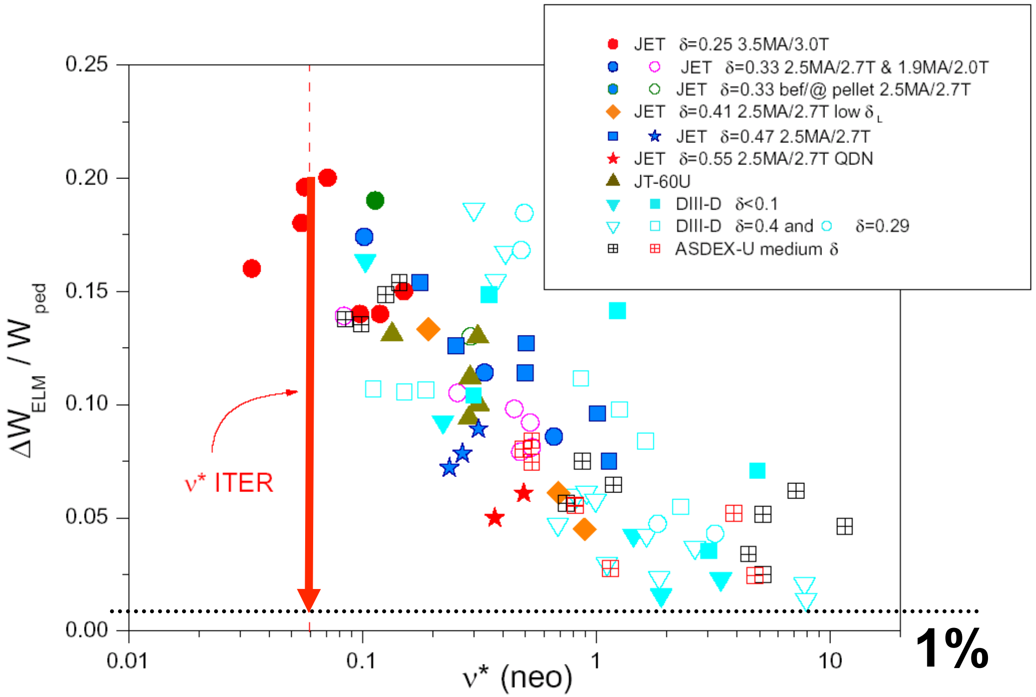

Some caveats:

Difference in temporal pulse shape and absolute plasma pressure between plasma gun and ELM

Not all ELMs are equal. Amplitude and temporal PDFs are intermittent. Large ELMs cause most damage.

Conclusions I

ELM divertor heat loads

- Heat load broadly consistent with free streaming of ions from mid-pedestal location
  - Scaling with sound speed confirmed by JET-AUG similarity experiment
  - Inner:outer energy asymmetry consistent with initial Mach number of pedestal ions
- ELM filaments observed on both AUG and JET
  - Temperature striations on divertor plates consistent with pre-ELM magnetic field
- Quasi-toroidal mode number increases with time
  - Suggests break up of filaments into ~ 2 – 3 smaller structures

ELM limiter heat loads

- ELM filaments observed at JET on both outer limiters and upper dump plate
  - mode number decreases with ELM size, and ~2-3 times larger than on divertor tiles
- Most recent analysis of ELM heat loads on JET indicate that radial Mach number increases as $(\Delta W/W_{ped})^{0.4}$, roughly in line with interchange scaling
- The parallel loss model, validated on JET measurements, used to predict fraction of ELM energy to the main chamber in ITER ($r - r_{sep} > 5$ cm) as
  - 25% for natural (unmitigated) ELMs (20 MJ, $\Delta W/W_{ped} \sim 13.3\%$)
  - 4% for small (mitigated) ELMs (1 MJ, $\Delta W/W_{ped} \sim 0.66\%$)

Impurity seeding: no ELM buffering

Only a small fraction (~10-20 %) of the ELM energy radiated during the ELM

Consistent with multi-fluid edge/SOL simulations, which indicate that ELM energy buffering occurs only for very small ELMs (below 20 kJ on JET).

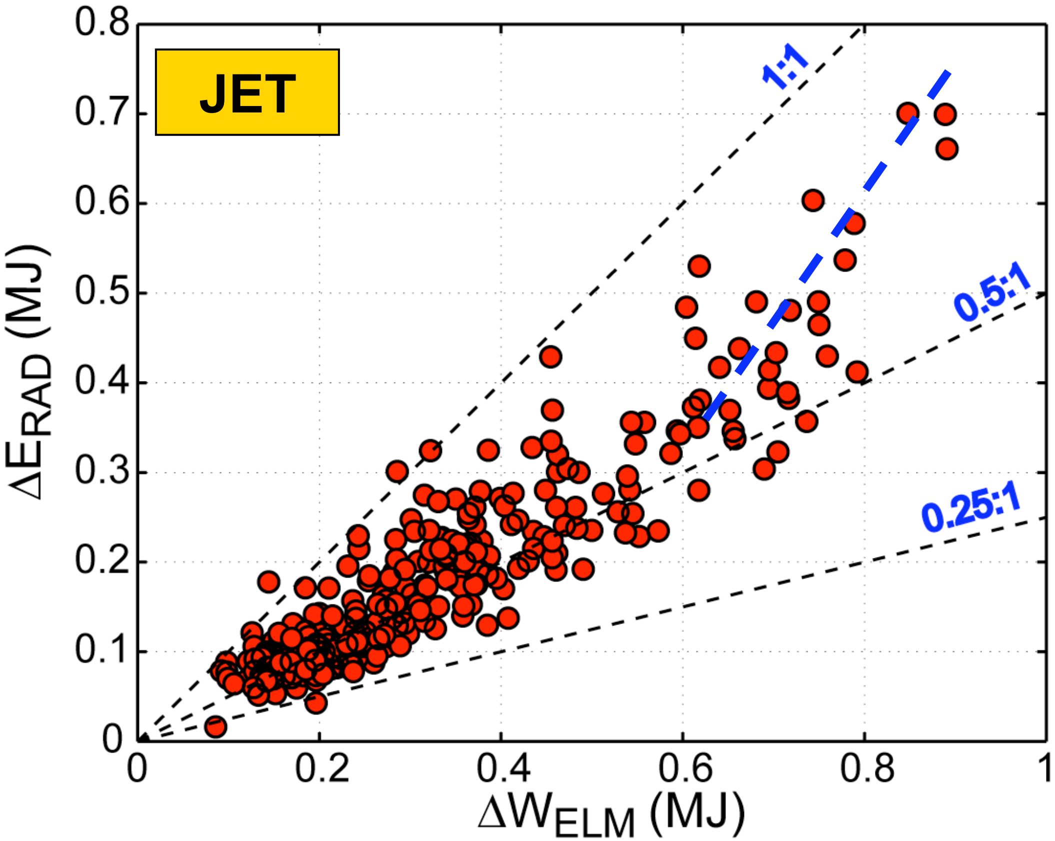

However, impurities released from the targets by the ELM, lead to large post-ELM radiation (comparable to the ELM energy itself) !!!

~ 20 %

~ 10 %

For sufficient large ELMs, the cooling of the X-point can result in a back transition to L-mode (loss of ETB)

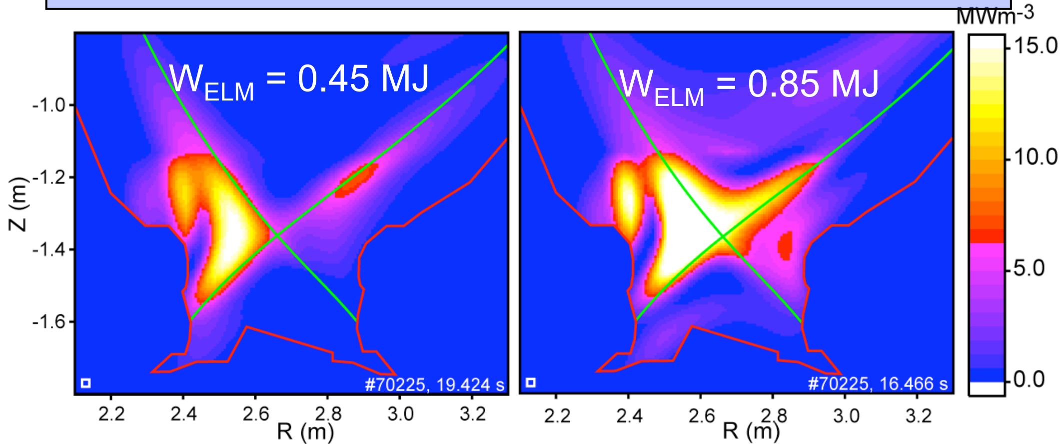

ELM induced impurity inflows

Inter-ELM W influx from outer divertor is strongly reduced as outer divertor plasma is cooled, consistent with the physical sputtering threshold

With the outer divertor detached, the average W influx is dominated by ELMs !

Transient W influx increases with ELM energy

In all cases, dominated by impurity sputtering

Argon seeding increases W erosion during ELMs, decreases erosion between ELMs

AUG

Optimum seeding rate (smallest W influx) is determined by competition between erosion by Ar ions and cooling by Ar radiation !!!

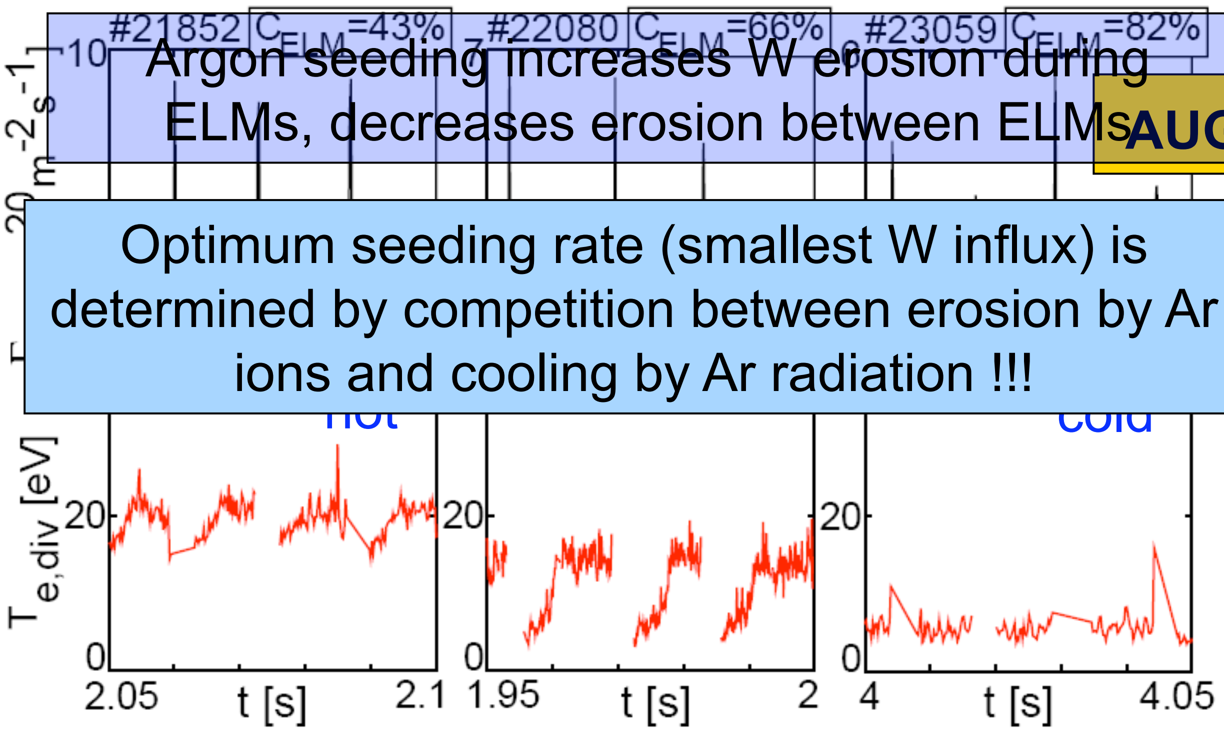

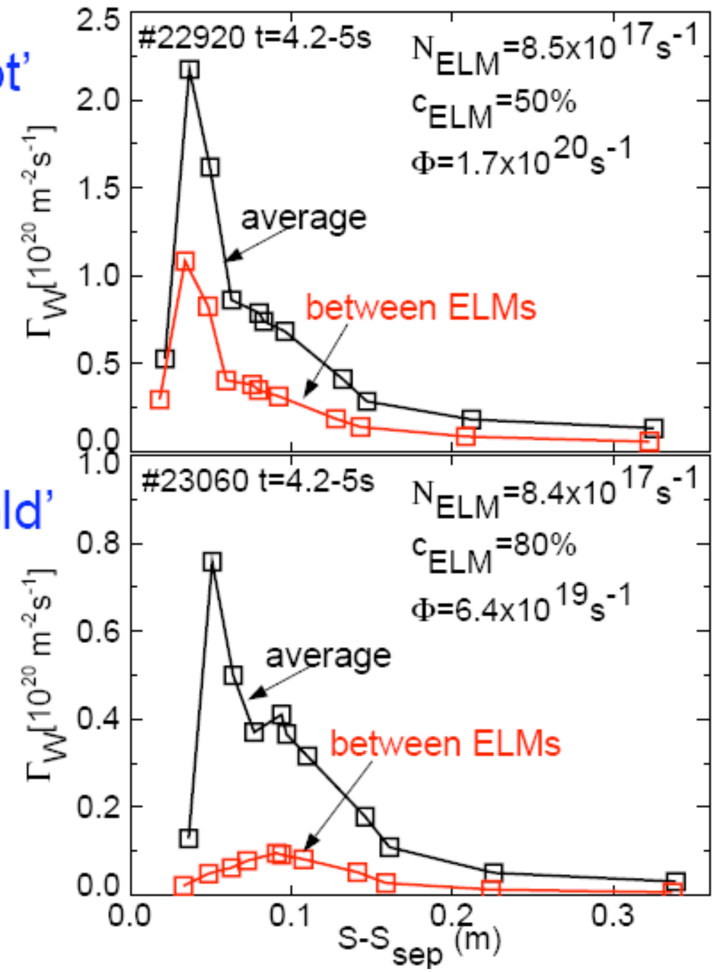

ELM control: Type-III ELMs

ELM frequency can be increased substantially (> factor of 10), by cooling the pedestal and thus replacing Type-I, by Type-III, ELMs

At present, the only scenario compatible with the all ITER exhaust requirements:

Q_{DT} = 10, can be recovered by increasing the current by ~13 % (to 17 MA)

f_{rad} ~ 75%, f_{GW} ~ 0.85, q_{95} ~ 3, Z_{eff} < 2, divertor detachment, $\Delta W/W_{ped}$ < 1%

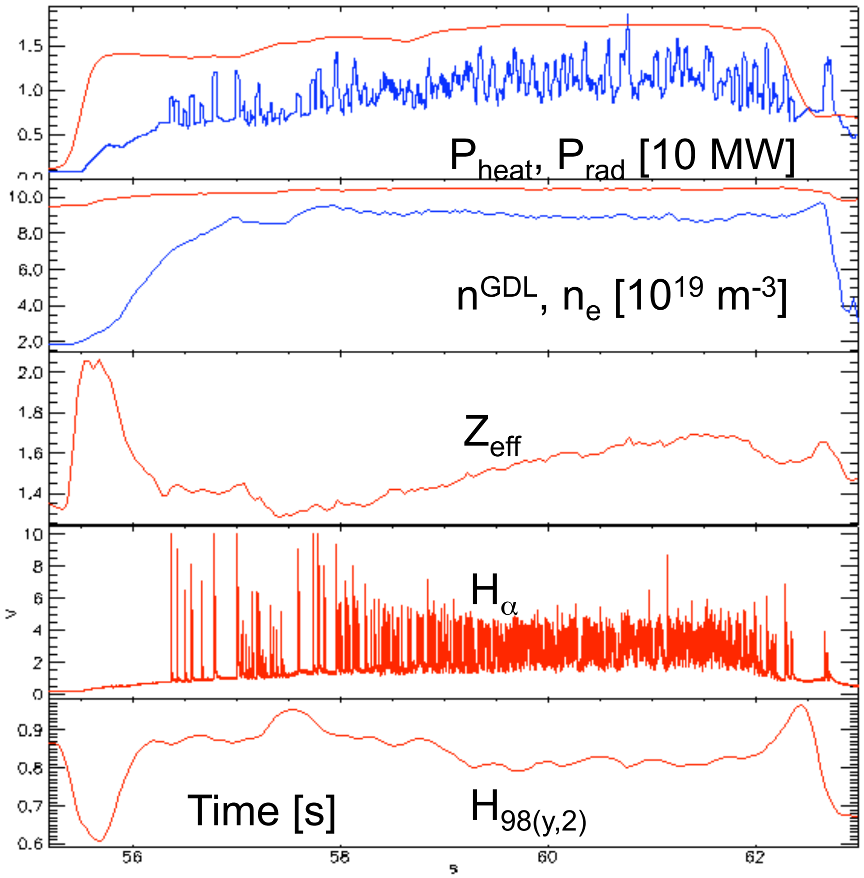

However, pedestal pressure reduced by ~ 50%, energy confinement (H98) by ~ 15-20%, so that Q_{DT} reduced by ~ 50% (Q_{DT} ~ 5 at 15 MA).

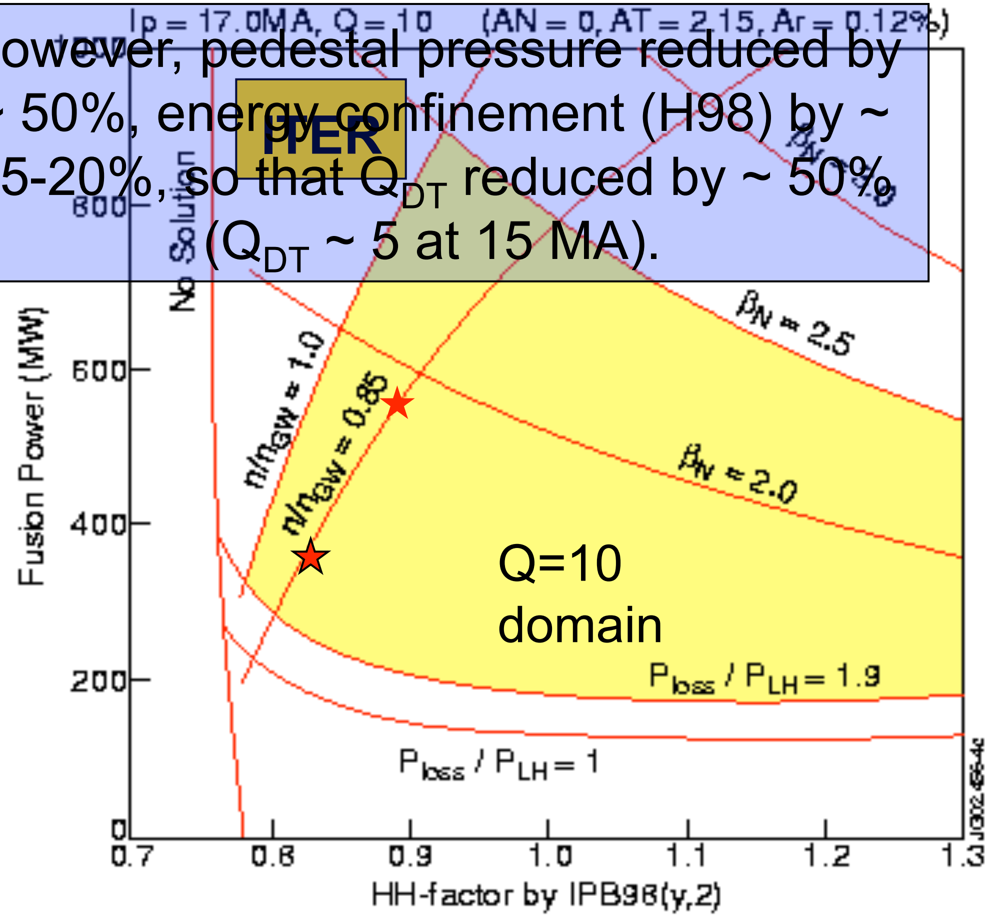

ELM control: pellets

Type-I ELM frequency can be increased by injection of small fuel ice pellets, provided that pellet frequency > 1.5 times the natural ELM frequency

Pellet provides a perturbation, eg. related to penetration depth, which leads to an MHD instability. It triggers a Type-I ELM at any point in the ELM cycle !

In AUG, stored energy and energy confinement (H_{98}) reduced by ~ 10-20% , due to increased convective losses. Pellets are too big !!!

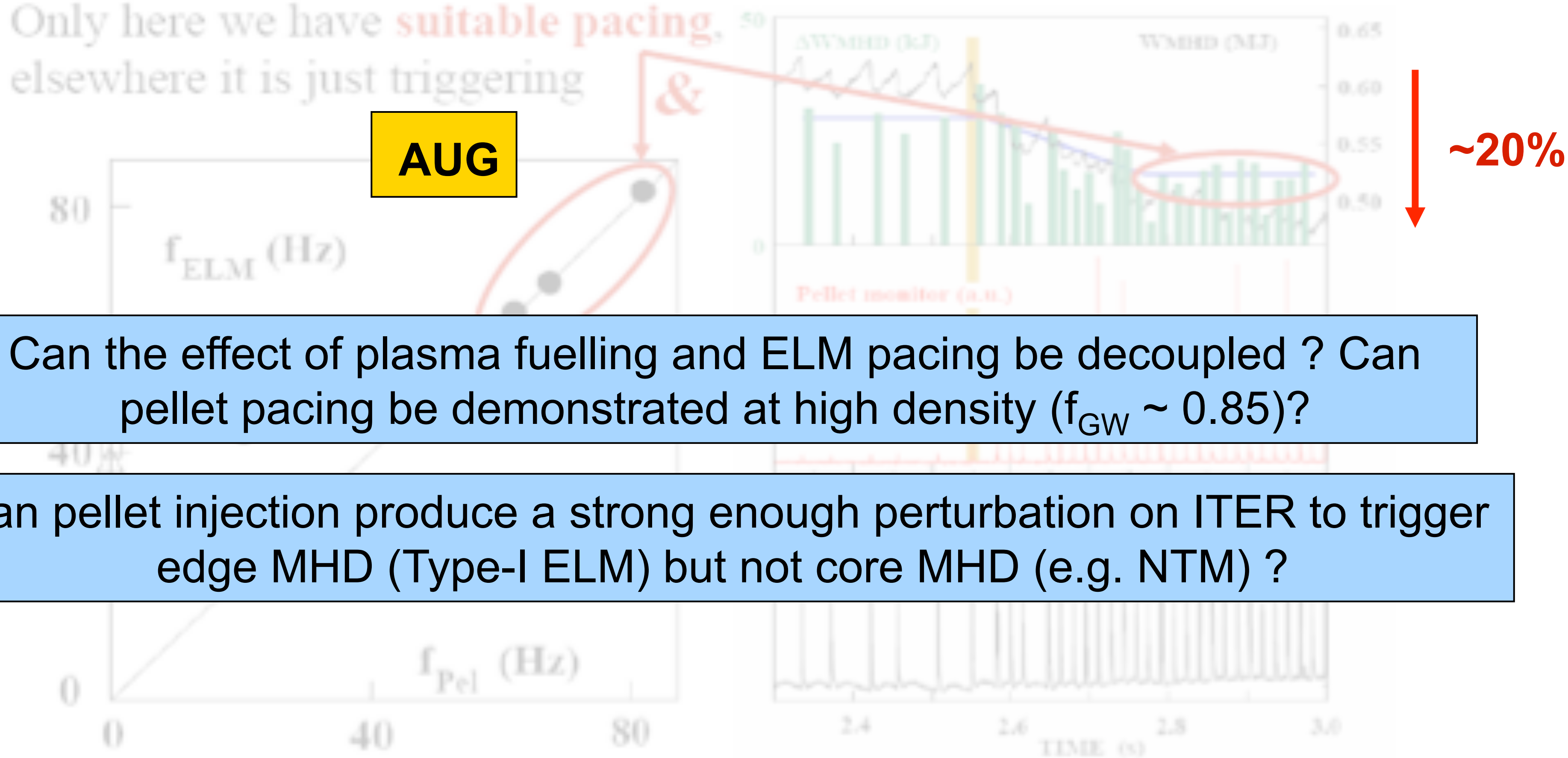

Can the effect of plasma fuelling and ELM pacing be decoupled ? Can pellet pacing be demonstrated at high density (f_{GW} ~ 0.85)?

Can pellet injection produce a strong enough perturbation on ITER to trigger edge MHD (Type-I ELM) but not core MHD (e.g. NTM) ?

ELM control: RMPs

Type-I ELMs can be suppressed entirely by resonant magnetic perturbations

Edge plasma density is reduced due to magnetic field ergodization, which increases parallel convection to the divertor

This effect, known as 'magnetic pump-out', is well documented with ergodic divertors, e.g. Tore-Supra. It represents edge plasma rarefaction, in the absence of cooling !

Pedestal density and pressure reduced by ~ 15-30%; energy confinement (H_{98})~ const

In ITER, 'magnetic pump-out' must be compensated by additional pellet fuelling to ensure f_{GW} ~ 0.85. Can ELMs still be suppressed in this case? If so, what is the reduction of p_{ped}, H98 due convective losses?

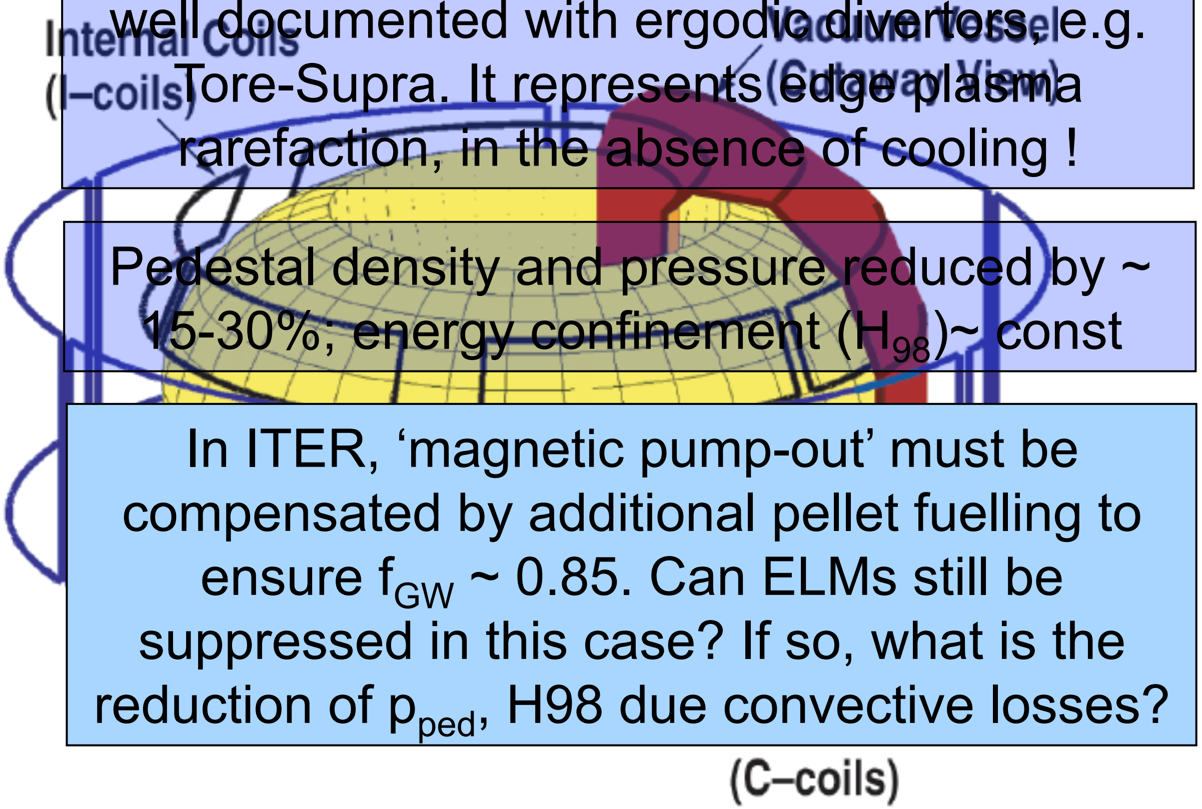

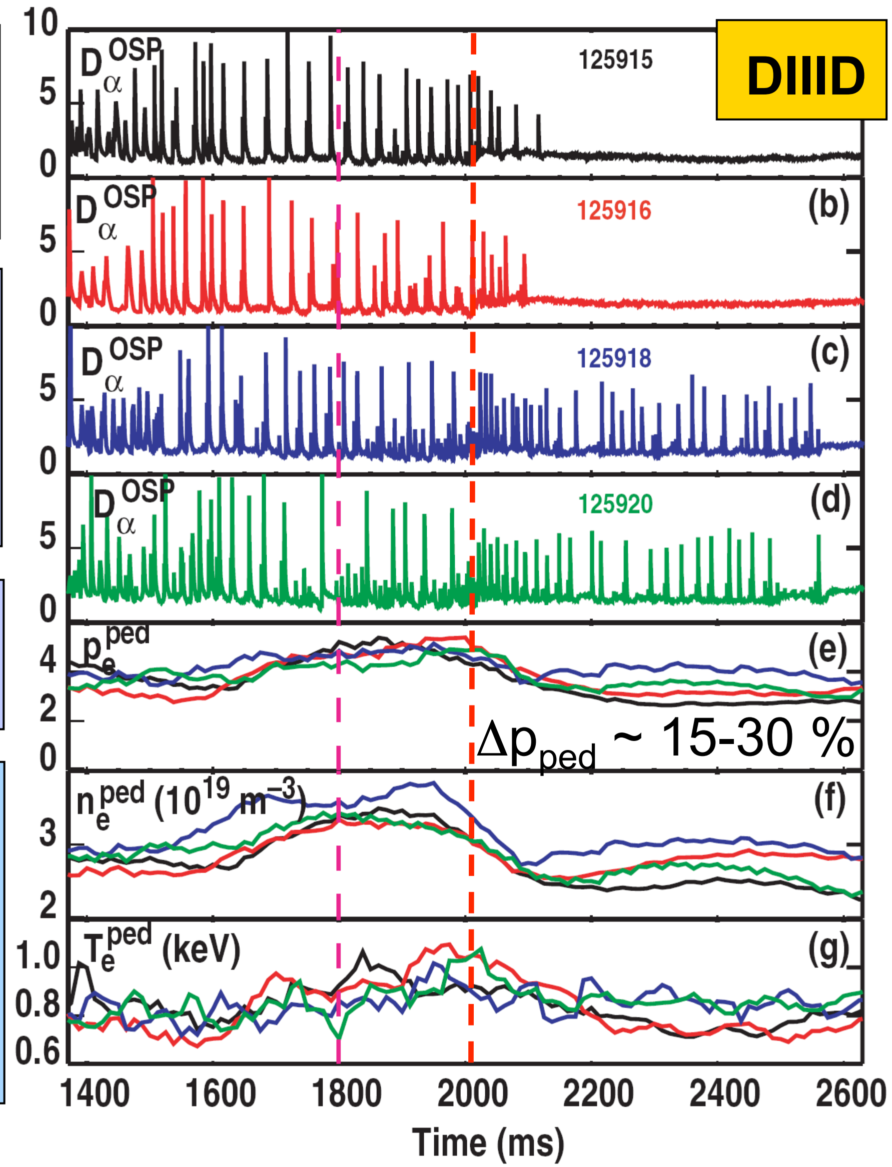

ELM control: n=1 to n=16 TF

ELM frequency can also be increased by both low n (1,2) and high n (16) toroidal field perturbations, generated with external coils. The former with error field correction coils (EFCCs), the latter due to toroidal field (TF) ripple.

In both cases, the pedestal density reduced due to 'magnetic pump-out'

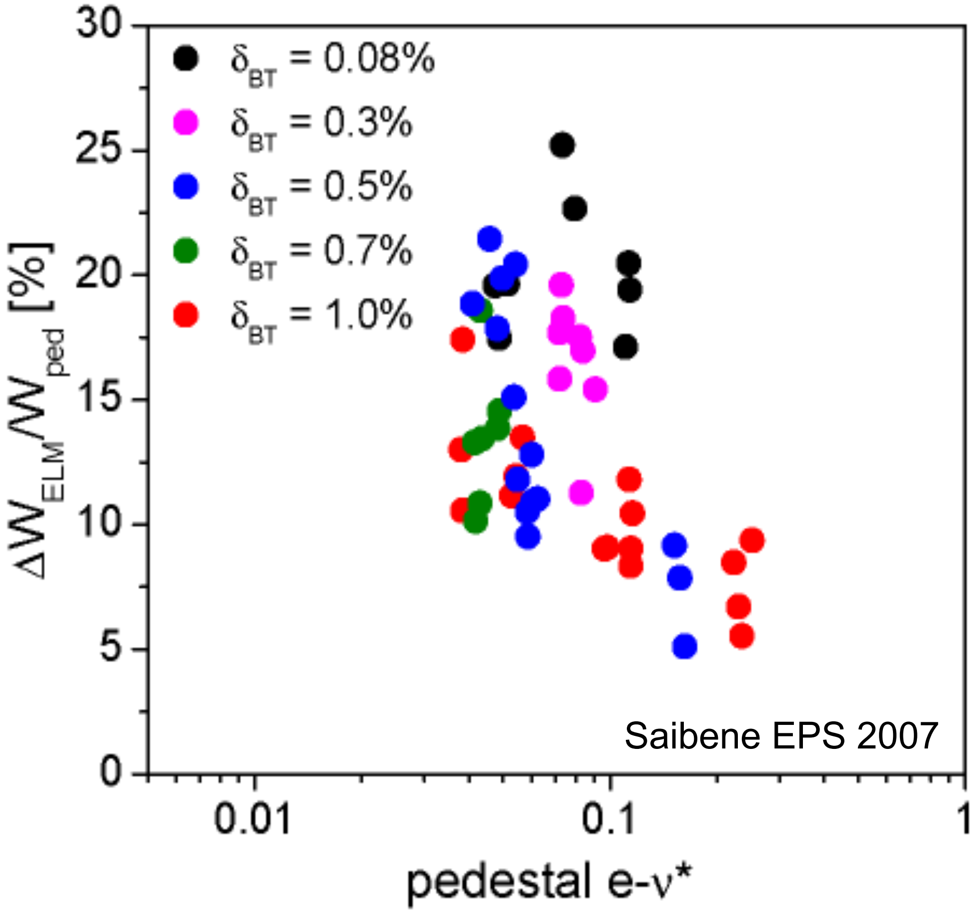

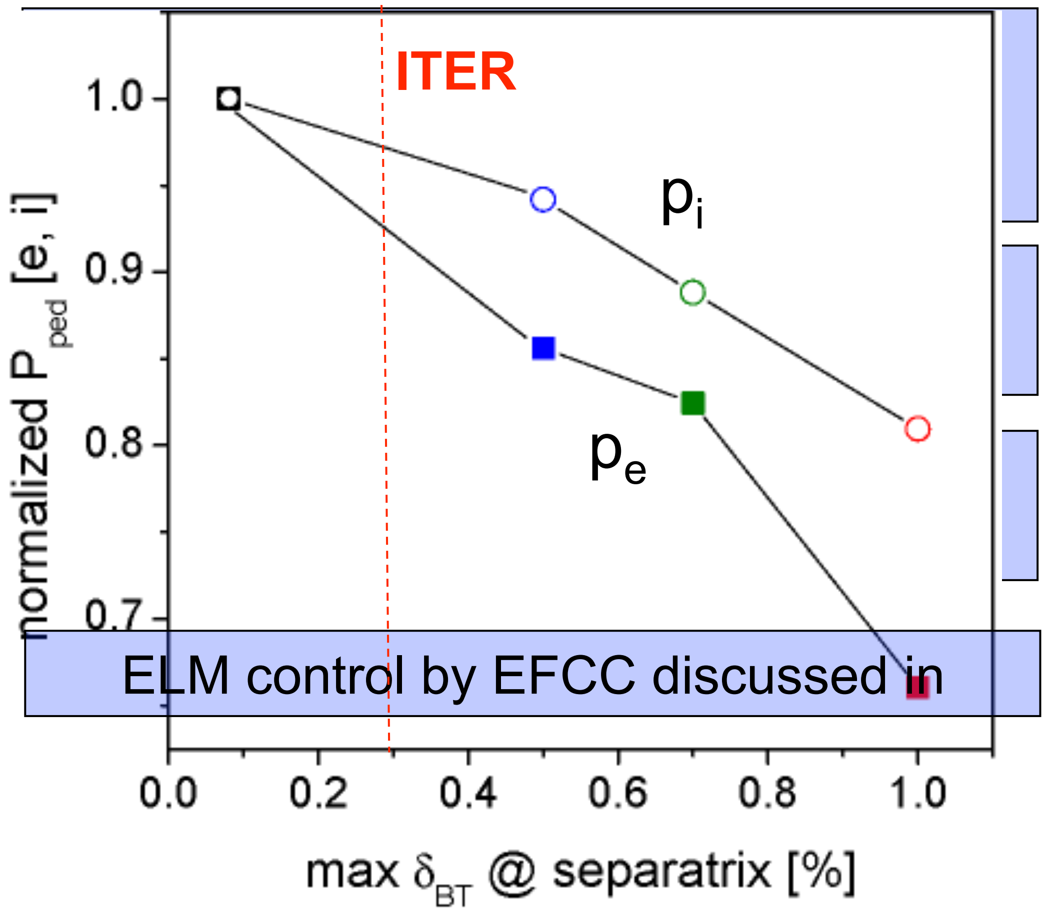

ELM control by EFCC discussed in

ELM control: summary

Consider the best results achieved so far

* = technique not optimized

Method (machine)	Increase in f_{ELM} vs Type-I	Density (f_{GW}) confinement	Energy (H98) confinement	Issues & problems
Type-III (JET)	x 30	~ 0.85 (-0%)	~ 0.85 (-15%)	Energy confinement
Pellets (AUG)	x 2*	~ 0.5*	~ 0.8*	Decoupling from fuelling
RMPs (DIIID)	Complete suppression	~ 0.25*	~ 1* (-15-30% in p_{ped})	Density confinement
RMPs (DIIID)	x 20	~ 0.6*	~ 0.9* (~0 % in p_{ped})	Energy confinement
EFCC (JET)	x 10	~ 0.78* (-10%)	~ 0.85* (-15%)	Density confinement
TF-ripple (JET, JT60U)	x 2	~ 0.8 (-5%)	~ 0.85 (-15%)	Density and energy conf.
Vertical kicks (JET, TCV)	x 15	~ 0.5*	~ 0.85* (-15%)	Magnetic shielding

Conclusions II

Compatibility between plasma and PFCs is not a binary signifier! Best measured as the impact on reactor performance, e.g. fusion gain, Q.

On the basis of our present knowledge (experiment) and understanding (theory), it appears that this impact, $\Delta Q/Q_0$, is negligible in existing tokamaks with C walls, but could be significant (~ 30-50% or more) for ITER and DEMO with metal walls

The dominant contribution to $\Delta Q/Q_0$ is the transient heat load limit and hence the requirement of small ELMs ($\Delta W/W_{ped}$ < 1%), which entails a reduction of the pedestal pressure by ~30-50% and H_{98} by ~ 10-15%

Although active ELM control by pellet injection and magnetic perturbations hold much promise, it remains to be seen whether these methods offer a smaller $\Delta Q/Q_0$ then the more conventional method of Type-III ELMy H-mode

Since high density (f_{GW}~ 0.85) and high radiation (f_{rad} ~ 0.75) are necessary in ITER to ensure detached divertor operation and reduce core plasma dilution, and the exact criteria governing the Type-I to Type-III transition are not fully understood, one may yet find that the transition to Type-III ELMs becomes unavoidable…

Quo Vadis ?

Teoria

Praxis

time ITER H-phase D-phase

Integrated core-edge-SOL

Use validated codes to predict impurity levels in hydrogen phase in ITER

Impurity seeding experiments in full metal machines, e.g. JET ILW, AUG W

Edge-SOL turbulence modelling: link to transport models

Hydrogen experiments in existing devices

Predict hydrogen phase in ITER

Use hydrogen phase of ITER to validate edge-SOL codes under Ohmic conditions

ELM control experiments

Kinetic ELM simulations

Use validated codes to predict ITER exhaust under Ohmic and L-mode conditions in deuterium plasmas

The End♪

Edge localized modes (ELMs)

Difference between ELM and pre-ELM infra-red images

JET

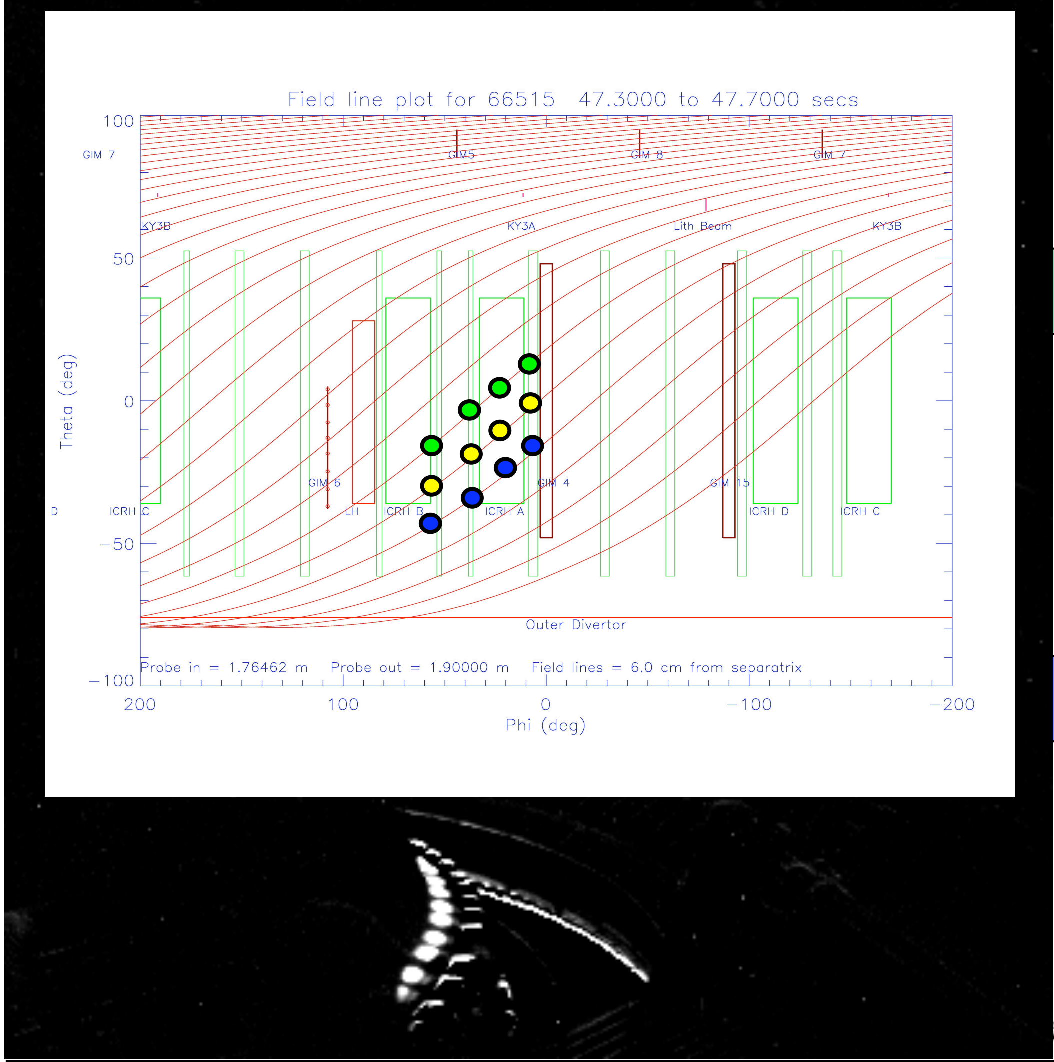

Growth stage:

Linear instability (e.g. ideal/resistive MHD mode) forms ~ 10-20 flute-like ripples in pedestal quantities

Transport stage:

These develop into ~10-20 filaments during the non-linear phase of the instability (beginning of transport)

Exhaust stage:

Filaments move outward, driven by interchange (curvature + pressure), while draining to the divertor targets

enski W *et al* 2006 *Plasma Phys. Control. Fusion* **48** 109

Parallel loss model of ELM exhaust

Consider the radial motion of the pedestal plasma subject to parallel losses.

Low ν*: plasma cools faster than it dilutes: mainly conductive losses.

Describe as a plasma filament, moving with some effective radial velocity.

High ν*: cooling and dilution comparable: mainly convective losses.

Evolution of density and temperature of the filament using a fluid model

Explains why small ELMs (high ν*) are mainly convective

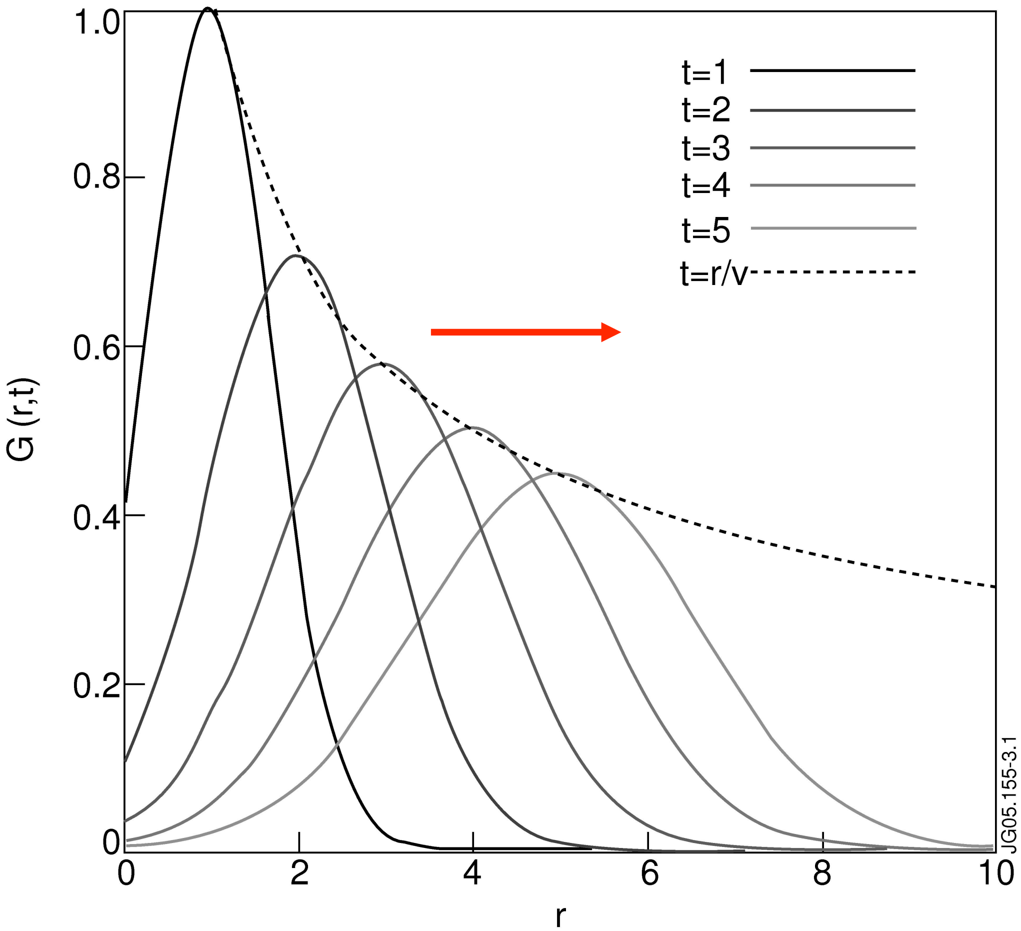

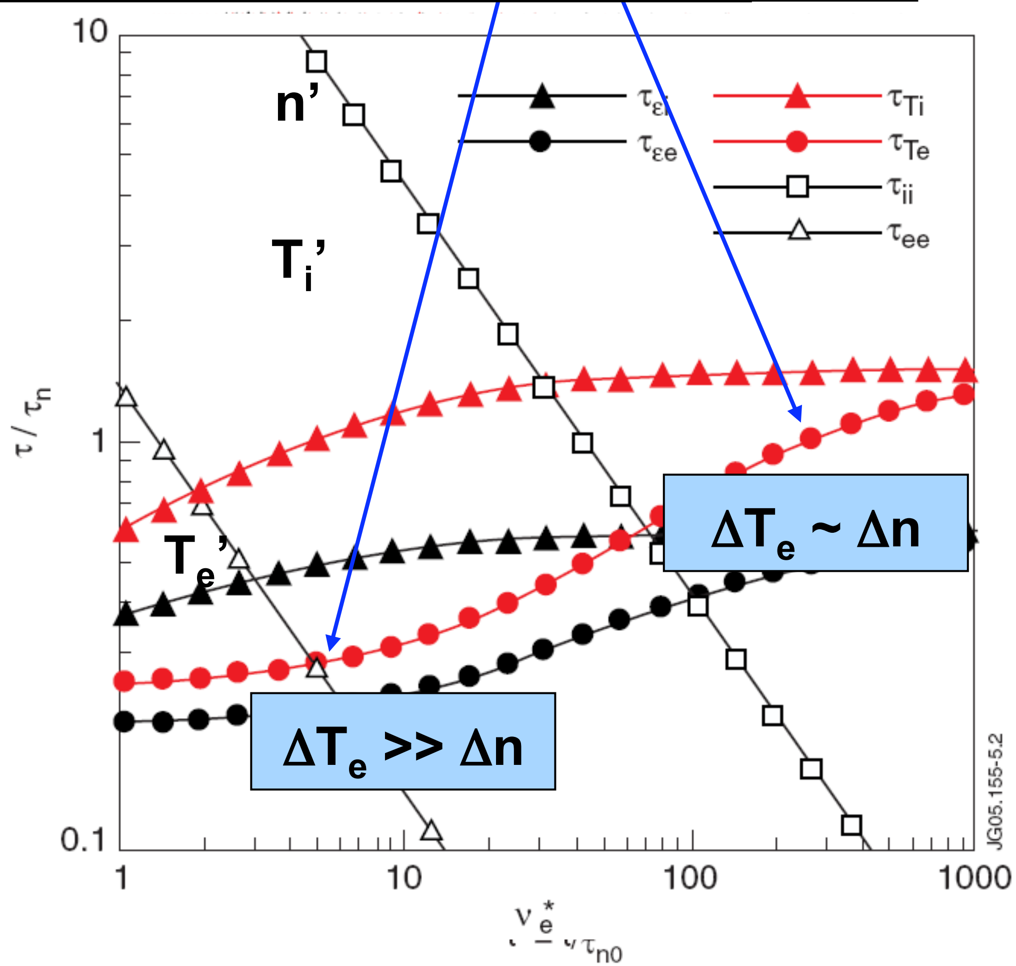

Fraction of ELM energy to the wall

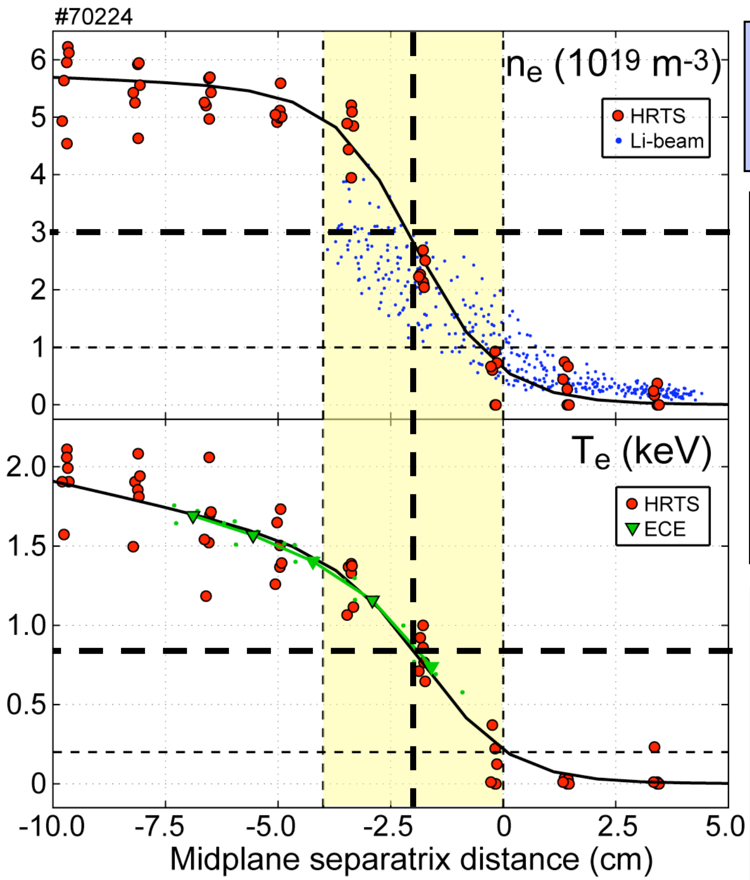

Consider a typical Type-I ELM on JET

Use mid-pedestal values of n, Te, Ti and effective radial velocity of 600 m/s measured using limiter probes

This yields an estimate of 10 % of ELM energy to wall, in agreement with the infra-red measured value.

IR measurements indicate that smaller ELMs deposit a smaller fraction of energy on the wall

Also observed as the energy missing from the divertor

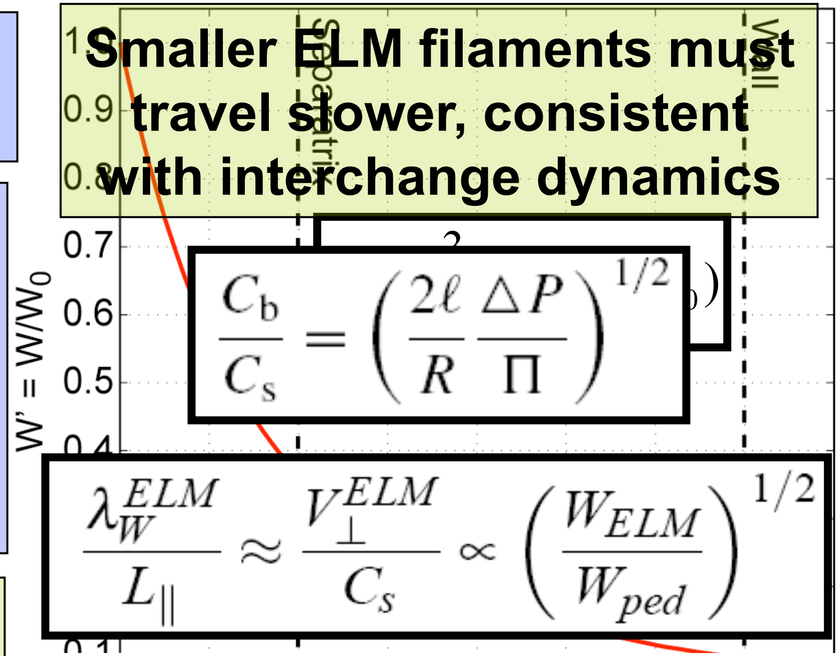

Smaller ELM filaments must travel slower, consistent with interchange dynamics

$$\frac{C_b}{C_s} = \left(\frac{2\ell}{R}\frac{\Delta P}{\Pi}\right)^{1/2}$$

$$\frac{\lambda_W^{ELM}}{L_\parallel} \approx \frac{V_\perp^{ELM}}{C_s} \propto \left(\frac{W_{ELM}}{W_{ped}}\right)^{1/2}$$

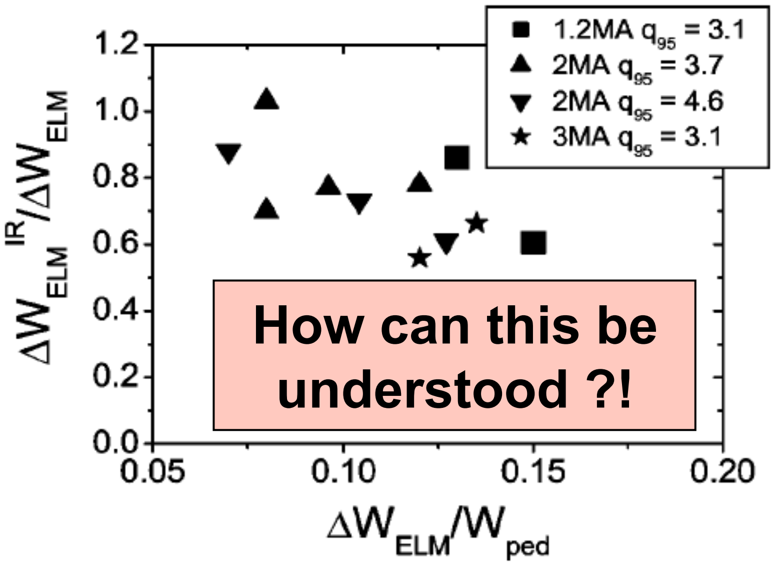

How can this be understood ?!

ELM-wall & limiter interaction on ITER

Same prescription as used to match JET data (**Type-I ELMs, ΔW/W = 5 %**)

~ 8 % of ELM energy onto **main wall** at 5 cm (omp)

~ 1.5 % of ELM energy onto **limiter** at 15 cm (omp)

ITER 2nd separatrix

movable limiter

Normalised ELM filament quantities

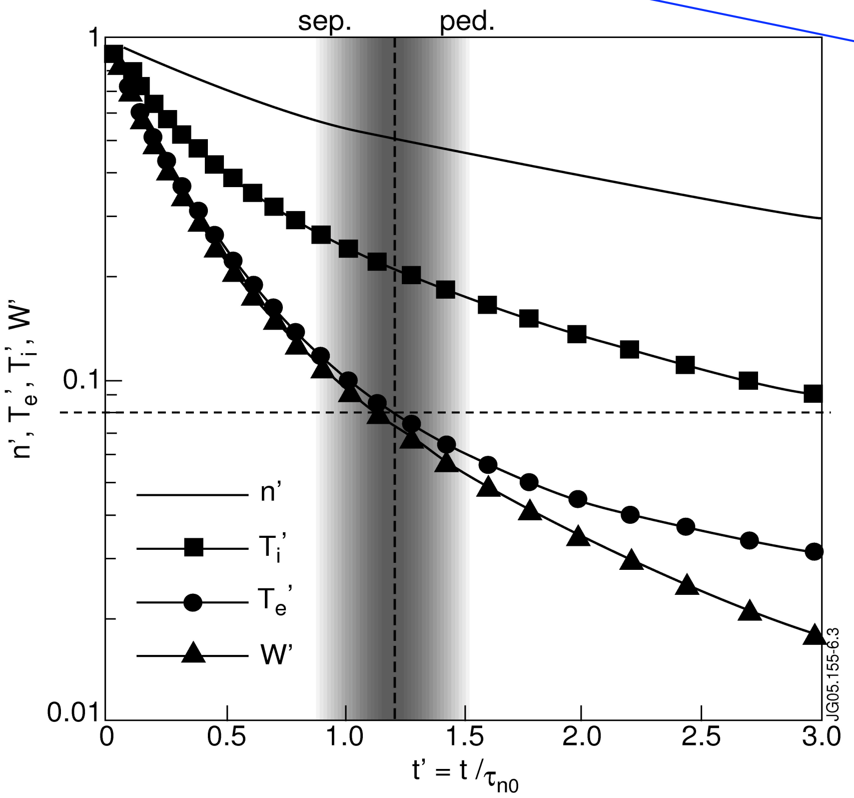

Normalised time since start of parallel losses

*W.Fundamenski et al., Plasma Phys. Control..Fusion, **48** (2006) 109*

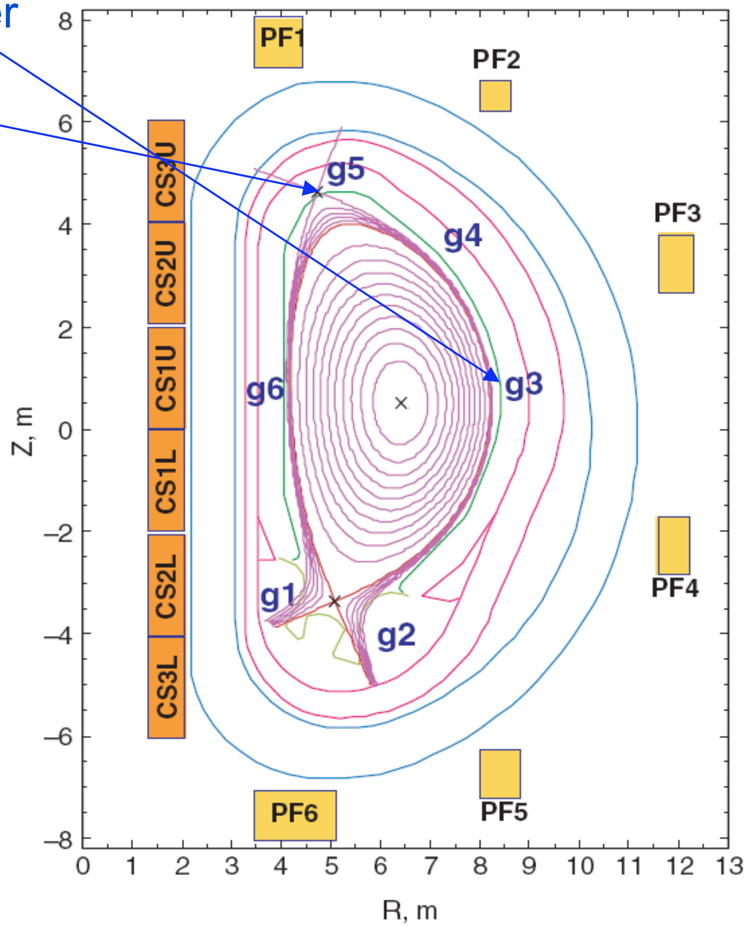

*R.Aymar et al., PPCF **44** (2002) 519*

Conclusions

- JET data indicates that bigger (more intense) ELMs deposit a larger fraction of their energy on the main chamber wall, which suggests that the radial Mach number increases with ELM size
- Two-field interchange model used to study size & amplitude scaling
- It was found that over a wide range of conditions, the radial Mach number is expected to increase as the square root of both ELM size and amplitude.

$$\frac{V}{C_s} \sim \left(\frac{2\ell}{R}\frac{\triangle\theta}{\Theta}\right)^{1/2}.$$

- This implies that radial e-folding length of ELM filament energy also increases

$$\lambda_W \approx V_\perp \tau_\| \approx \frac{V_\perp L_\|}{C_s} \qquad \Rightarrow \qquad \frac{\lambda_W^{ELM}}{L_\|} \approx \frac{V_\perp^{ELM}}{C_s} \propto \left(\frac{W_{ELM}}{W_{ped}}\right)^{1/2}$$

- Model predictions in fair agreement with JET data
- Preliminary predictions for ITER indicate the added benefit of reducing the ELM size: for small ELMs, $\Delta W/W_{ped} < 5\%$, less than 2% of ELM energy deposited on the wall (near 2nd separatrix at upper baffle); contact with limiters is negligible.

ITER-like ELMy H-mode equilibria

- Type-I ELM-filaments clearly observed with Δr ~ 2 cm-omp (top)
- No Type-III ELM-filaments, despite proximity to upper dump plate (~1.5 cm)